

ABSTRACT

Title of Document: DENITRIFICATION, N₂O EMISSIONS, AND NUTRIENT EXPORT IN MARYLAND COASTAL PLAIN STREAMS

John Robert Gardner, Master of Science, 2014

Directed By: Professor Thomas Fisher
University of Maryland Center for Environmental Science-Horn Point Laboratory

Small streams are hotspots for denitrification, emissions of a potent greenhouse gas nitrous oxide (N₂O), and are also highly connected to their watersheds via groundwater flowpaths. In-stream, reach scale denitrification and N₂O production as well as biogenic nitrogen gases delivered by groundwater were investigated in one small agriculturally impacted watershed. Groundwater was an important source of biogenic N₂, but most N₂O was produced in-stream and emissions were relatively high.

In addition, agricultural streams significantly contribute to nutrient loading and degradation of downstream aquatic ecosystems. Export and transport mechanisms of nitrogen and phosphorus were investigated during base and stormflow in three watersheds with varying amounts of agricultural and forested land use. Quickflow, which is associated with storms, transported most of the phosphorus and ammonium in the agricultural watersheds, but quickflow had little impact on nutrient concentrations and export in the forested watershed.

DENITRIFICATION, N₂O EMISSIONS, AND NUTRIENT EXPORT IN
MARYLAND COASTAL PLAIN STREAMS

By

John Robert Gardner

Thesis submitted to the Faculty of the Graduate School of the
University of Maryland, College Park, in partial fulfillment
of the requirements for the degree of
Master of Science
2014

Advisory Committee:
Professor Thomas Fisher, Chair
Professor Keith Eshleman
Dr. Thomas Jordan
Assistant Professor Karen Knee

© Copyright by
John Robert Gardner
2014

Table of Contents

List of Tables	iv
List of Figures	v
Chapter 1: Estimating in-stream production and groundwater delivery of N ₂ and N ₂ O using open channel methods	1
Abstract	1
Introduction	2
Methods	7
<i>Study Sites</i>	7
<i>Groundwater Sampling</i>	10
<i>Surface water Sampling</i>	13
<i>Laboratory Analysis</i>	14
<i>Gas Transfer Velocity</i>	15
<i>Argon Modeling</i>	19
<i>Estimation of N₂ and N₂O production</i>	19
<i>N₂O Emissions</i>	22
<i>Uncertainty Analysis</i>	22
Results	24
<i>Groundwater Data</i>	24
<i>Surface Water</i>	26
<i>Gas Transfer Velocity</i>	30
<i>N₂ and N₂O Production</i>	34
Discussion	36
<i>²²²</i> Rn and Gas Exchange Velocity	36
<i>Argon Modeling</i>	39
<i>N₂ Production</i>	40
<i>Controls of N₂ Production</i>	43
<i>N₂O Emissions</i>	46
<i>Controls of N₂O Emissions</i>	47
<i>Groundwater and N₂O Emissions</i>	48
<i>N₂O Emission Factors</i>	52
Conclusions	55
References	58
Chapter 2: Storm and baseflow nutrient export from agricultural and forested watersheds on the coastal plain of Maryland, USA	68
Abstract	68
Introduction	69
Methods	73
<i>Study Sites</i>	73
<i>Monitoring</i>	74

<i>Laboratory Analysis</i>	75
<i>Data Analysis and Calculations</i>	76
Results.....	80
<i>Hydrology</i>	80
<i>Baseflow Chemistry</i>	89
<i>Stormflow Chemistry</i>	94
<i>Annual Nutrient Export</i>	97
Discussion	103
<i>Hydrology</i>	103
<i>Phosphorus Sources and Transport Mechanisms</i>	108
<i>Nitrate Sources and Transport Mechanisms</i>	111
<i>Ammonium Sources and Transport Mechanisms</i>	116
<i>Annual Base and Stormflow Export</i>	118
Conclusions.....	120
References.....	122
Overall Bibliography	129

List of Tables

Table 1. Details for all regressions from Chapter 1.....	12
Table 2. Estimates of error for variables used in uncertainty analysis.	23
Table 3. Discharge and average chemistry in study reaches	28
Table 4. Comparison of k_{600} estimated from Ar and ^{222}Rn	33
Table 5. Uncertainty analysis of gas exchange velocity	33
Table 6. Total, in-stream, and groundwater N_2 and N_2O production rates	35
Table 7. Uncertainty analysis of N_2 and N_2O production.....	50
Table 8. Watershed characteristics for MH, BC, and SF.....	72
Table 9. Correlations between precipitation stations.....	76
Table 10. Annual water budgets for MH, BC, and SF.....	81
Table 11. Details from all regressions from Chapter 2.....	87
Table 12. Comparing base and stormflow concentrations.....	93
Table 13. Hydrologic characteristics of sampled storms.....	95
Table 14. Nutrient export for the MH, BC, and SF watersheds.....	102

List of Figures

Figure 1. Map of Choptank Basin and location of study sites.....	9
Figure 2. Patterns in surface water ^{222}Rn activity	17
Figure 3. Conceptual model of stream reach ^{222}Rn mass balance.	18
Figure 4. Examples of Ar modeling in stream water	20
Figure 5. Temporal patterns of groundwater NO_3^- and $\text{xN}_2\text{-N}$	26
Figure 6. Relationship between NO_3^- and $\text{N}_2\text{O-N}$ concentrations for surface and groundwater	27
Figure 7. Relationship between the groundwater flux per reach and the mean groundwater ^{222}Rn activity.....	27
Figure 8. Relationship between hydraulic head and groundwater ^{222}Rn activity.	28
Figure 9. Summary of surface water data during typical open channel study	31
Figure 10. Equilibrium and measured concentrations of $\text{N}_2\text{-N}$ and $\text{N}_2\text{O-N}$ concentrations at MH forested site	32
Figure 11. Relationship between stream and groundwater NO_3^-	32
Figure 12. Relationships between antecedent stream depth (ASD) and temperature with N_2O emissions, total N_2 production, and in-stream N_2 production	36
Figure 13. Regressions of N_2O versus N_2 production in-stream and groundwater. ...	51
Figure 14. NO_3^- , $\text{xN}_2\text{-N}$, and O_2 concentrations in groundwater.....	53
Figure 15. Relationship between storm size and event volume weighted mean of PO_4^{3-} , TP, and NH_4^+	80
Figure 16. SARR output from the Marshy Hope watershed.....	83
Figure 17. SARR output from the Baltimore Corner watershed	84

Figure 18. SARR output from the South Forge watershed	85
Figure 19. Relationships between quickflow and precipitation.....	86
Figure 20. Relationship of quickflow with peak flow and event base flow index	88
Figure 21. Temporal variation in baseflow concentration at MH and SF	90
Figure 22. Relationship between temperature and baseflow NH ₄ ⁺ concentration.....	91
Figure 23. Relationships of NO ₃ ⁻ with conductivity and discharge.....	92
Figure 24. Boxplots of baseflow and volume weighted stormflow concentrations....	93
Figure 25. Chemographs during the Hurricane Sandy in the MH watershed.....	96
Figure 26. Chemographs during the June 2013 storm in the BC watershed.	96
Figure 27. Chemographs during the June 2013 storm in the SF watershed.	97
Figure 28. Concentration-discharge plots at MH.....	98
Figure 29. Concentration-discharge plots at BC.....	99
Figure 30. Concentration-discharge plots at SF.....	100
Figure 31. Annual nutrient export separated by quickflow and baseflow.	101
Figure 32. Relationship between % annual discharge and % annual export of TP and TN from individual storm events in the BC watershed.	102
Figure 33. Interannual variation in TN and TP export at MH	104
Figure 34. Interannual variation in TN and TP export at SF	105
Figure 35. Relationship between event volume-weighted mean TP concentration and antecedent precipitation index	111

Chapter 1: Estimating in-stream production and groundwater delivery of N₂ and N₂O using open channel methods

Abstract

Small streams are hotspots for denitrification and potentially N₂O emissions and are also highly connected to their watersheds via groundwater flowpaths. Open channel methods were used to estimate reach scale N₂ and N₂O production occurring *in-situ* as well as the rate of biogenic N gas input from groundwater in a small agriculturally impacted watershed. Groundwater was an important source of biogenic N₂ (1.1-6.9 mmol N m⁻² hr⁻¹), accounting for 38-100% of the total N₂ production in streams with the remaining portion due to *in-situ* production (0-7.1 mmol N m⁻² hr⁻¹). In contrast, N₂O was largely produced *in-situ*, and groundwater inputs contributed on average 13% of the N₂O flux to the atmosphere which ranged from 14 to 211 µmol N m⁻² hr⁻¹. Antecedent stream stage and temperature were significantly related to total N₂ production ($r^2 = 0.81$ and 0.42 respectively) and N₂O emissions ($r^2 = 0.60$ and 0.85 respectively), representing controls over days (hot moments) and seasonal time scales. N₂O emission factors (EF5-g) for streams (mean = 0.29%) agreed with the current IPCC value of 0.25%; however, EF5-g estimated from emerging groundwater was lower (mean = 0.057%).

Introduction

Anthropogenic nitrogen (N) inputs have negatively impacted aquatic ecosystems around the world (Diaz and Rosenberg 2008), altered biogeochemical cycles, and contributed to global climate change (Vitousek et al. 1997). Increasing N loads to coastal systems have also enhanced phytoplankton production, a process described as eutrophication (Nixon 1995). This can lead to decreasing oxygen concentrations in bottom waters, or hypoxia, from the decomposition of organic matter with cascading ecological consequences (Diaz 2001; Kemp et al. 2005). N inputs have also stimulated diffuse emissions of nitrous oxide (N_2O), which is now the dominant ozone depleter (Ravishankara et al. 2009) and a greenhouse gas with 289 times the global warming potential of carbon dioxide (Shine et al. 2005).

The Chesapeake Bay, to which the watersheds in this study drain, has suffered from hypoxic bottom waters, declining fisheries, and loss of submerged aquatic vegetation as a result of N and phosphorus (P) inputs contributing to eutrophication (Kemp et al. 2005). A majority of nutrient inputs in the Chesapeake are agricultural in origin (Fisher and Oppenheimer 1991). It is critical to understand and quantify the fate and transport of N through these agricultural watersheds within the Chesapeake Bay region to develop management strategies that reduce the human impact on water and air quality.

Denitrification, or microbially-mediated anaerobic reduction of nitrate (NO_3^-) to N_2 gas, is an essential process to protect water quality, yet it remains the least understood transformation in the aquatic and terrestrial N cycle (Groffman et al. 2006; Kulkarni et al. 2009). It is likely the reason why watershed nitrogen budgets are

often unbalanced (i.e. inputs > outputs). This is known as “missing nitrogen”, defined as the difference between anthropogenic N inputs and riverine N export from a watershed. The missing N often accounts for a majority (~75%) of N inputs to large watersheds (Howarth et al. 1996; Jordan and Weller 1996; Van Breeman et al. 2002). Stream networks impacted by anthropogenic N inputs could provide a discrete location within a watershed (relative to the larger terrestrial area) to find missing nitrogen in the form of biogenic N gases, since streams are hotspots for denitrification (Duff and Triska 1990; Garcia-Ruiz et al. 1998). Gaining headwater streams are also highly connected to their catchments delivering additional NO_3^- and biogenic N gases via groundwater flowpaths, where presumably little N gas loss to the atmosphere occurs.

Denitrification can also negatively impact the environment through N_2O production if the process is inhibited prior to complete reduction to N_2 . N_2O is also a byproduct of nitrification, the aerobic oxidation of ammonium (NH_4^+) to NO_3^- . The largest source of N_2O to the atmosphere is a result of these natural microbial processes occurring in terrestrial and aquatic systems impacted by agricultural N inputs (Mosier et al. 1998; Foster et al. 2007). Yet denitrification represents one of the more important permanent nitrogen removal pathways and is a critical process for protecting water quality despite producing residual N_2O .

Among aquatic ecosystems, rivers have high areal rates of denitrification as well as spatial and temporal heterogeneity (Groffman et al. 2006; Pina-Ochoa and Alvarez-Cobelas 2006). This creates large uncertainties in N losses from streams and rivers (Seitzinger et al. 2006), despite a wealth of information on small-scale

denitrification controls (i.e. availability of NO_3^- , electron donors, O_2 , and presence of microbial denitrifiers) that was largely derived from laboratory studies (Anderson 1977; Knowles 1982; Seitzinger 1988; Garcia-Ruiz 1998). Reach scale, *in-situ* studies are needed to elucidate controls and constrain variability at scales relevant to watershed management and modeling.

Until recently, N_2O fluxes from lotic environments have received less attention compared to terrestrial systems despite evidence from modelling (Seitzinger and Kroeze 1998) and empirical studies (Baulch et al. 2010; Beaulieu et al. 2011) suggesting that streams and rivers could be a significant N_2O source. There is much uncertainty around the magnitude of global N_2O emissions from aquatic systems due to the potentially high, but variable, rates of denitrification and nitrification. The International Panel on Climate Change (IPCC) estimated 35% of anthropogenic N_2O emissions are from groundwater, streams, and rivers (Mosier et al. 1998). These sources are known as indirect emissions that are a result of microbial transformations of leached N, and N_2O fluxes are estimated using emission factors. The emission factor for streams and groundwater (EF5-g) is 0.25%, which is the estimated proportion of leached N inputs that escape to the atmosphere as N_2O . There is some controversy around emissions factors, and several studies have demonstrated that global models overestimate N_2O emissions when compared to measurements over local areas (Harrison and Matson 2003; Clough 2007).

Streams are integrators of watershed biogeochemistry. Sampling a stream at a given point integrates the heterogeneity of upstream groundwater flow paths as well as in-stream processes. In the context of this paper, denitrification and other

biogeochemical processes occur across the watershed in the stream, aquifer, vadose zone, and converge in the stream network where water masses containing different amounts of biogenic denitrification products, N₂ and N₂O, mix and exchange with the atmosphere. Sampling emerging groundwater at discrete locations in a stream network typically reveals the complexity and variability of groundwater flow paths and chemistry (Werner et al. 2010), making it difficult to assess the importance of biogenic gases in groundwater. Utilizing a reach scale approach, such as the open channel method, integrates this variability and may provide insight into groundwater as well as in-stream processes.

The open channel method for estimating in-stream denitrification (Laursen and Seitzinger 2002; McCutchan et al. 2003) has provided a relatively precise and cost effective means for measuring reach scale, *in-situ* denitrification in a variety of riverine systems (Yan et al. 2004; Harrison et al 2005; Pribyl et al. 2005; Smith et al. 2008). It has been noted such methods could help identify whole stream controls of denitrification and broaden our understanding by overcoming the small scale spatial heterogeneity. Laursen and Seitzinger (2002) developed a multi-station method that applies a Lagrangian sampling design to estimate denitrification within a moving parcel of water while accounting for atmospheric exchange. McCutchan et al. (2003) presented a one-station approach with a single sampling location that directly calculates denitrification correcting for atmospheric exchange and groundwater inputs. Both methods are mathematically identical and involve a whole stream N₂ mass balance to estimate water column accumulation of N₂ that is a result of biological processes.

Since the open channel method involves a mass balance, it cannot separate specific processes, such as annamox from denitrification with regards to N₂ production, and nitrification from denitrification with regards to N₂O production. Also, the calculated N₂ production rates represent net denitrification (N₂ production – N fixation). However, N₂ production is believed to be a good approximation for denitrification in systems with high reactive N concentrations that would inhibit N fixation (Laursen and Seitzinger 2002).

Groundwater inputs are typically subtracted away when applying the open channel method in order to isolate in-stream processes, but we included groundwater inputs to estimate the flux of biogenic N₂ and N₂O from emerging groundwater. We also evaluated a recently proposed ²²²Rn based method (Knee et al. in prep) for estimating gas exchange velocity (k).

Gas exchange across the air-water interface is an important rate controlling parameter in biogeochemical budgets and metabolism studies of aquatic systems (Marzolf et al. 1994; McCutchan et al. 1998; Laursen and Seitzinger 2005). Open channel methods depend upon accurate measurements of k , which is often estimated using injections of inert gases (propane and SF₆), making it the most laborious parameter to determine. There is a need for alternative methods of empirically estimating k in streams. Radon (²²²Rn) has long been used as a tracer for groundwater (Ellins et al. 1990; Genereaux et al. 1993) and to estimate k in the open ocean in combination with radium isotopes (Peng et al. 1979; Smethie et al. 1985). Yet, there are few examples of deriving k directly from ²²²Rn in streams (Wanninkhof 1990) despite being a promising tracer: inert, radioactive, short half-life (~3.8 days),

naturally high concentrations in groundwater, and negligible atmospheric background.

The objectives of this study are to 1) quantify biogenic N₂ and N₂O accumulation in streams from in-stream and groundwater sources, 2) evaluate a recently developed method for estimating gas transfer velocity (k) using ²²²Rn (Knee et al. in prep), and 3) examine reach scale controls of N₂ production and N₂O emissions in one small stream network. Specific hypotheses that were tested include 1) small agricultural streams are hot spots for accumulation of biogenic N₂ and N₂O due to both *in-situ* production and groundwater delivery, and 2) hydrology is an important control of N₂ and N₂O production in agricultural streams.

Methods

Study Sites

The study sites are located in the Choptank River and Nanticoke River Basins which drain into the Chesapeake Bay from the Delmarva Peninsula. This area lies within the Atlantic coastal plain physiographic region and is characterized by flat topography (<30 m asl). The hydrogeomorphology ranges from poorly drained uplands with shallow streams to well-drained, sandy soils with incised stream channels (Hamilton et al. 1993). Land use in the Choptank Basin is dominated by agriculture (62%), followed by forest (26%) and a small urban component (5%) (Norton and Fisher 2000; Fisher et al. 2006). The climate is humid temperate with an average annual rainfall of 112 cm evenly distributed throughout the year, and the

stream hydrology is largely driven by seasonal variation in evapotranspiration (Lee et al. 2000).

Specifically, this study was focused on Baltimore Corner (BC) watershed located within the upper Choptank Basin (Figure 1). BC is a small watershed (4.8 km^2) containing 25.6% agricultural, 59.6% forest, and 13.1% fallow, and 1.7 % impervious structures. The stream network has been largely channelized to drain adjacent lands in production under a corn-wheat-soybean rotation. Soils are generally well drained sandy loams with 67.6% of the watershed classified as partially hydric but only 1% as hydric. Stream sediments are largely composed of sand with localized accumulation of organic matter and fine sediments. BC1, BC2 and BC3 are the three branches in the BC watershed and are named in order of greatest to least discharge. These reaches are relatively similar in channel morphology and chemistry. However, BC2 differs from the others in its lower NO_3^- concentration, abundant emergent vegetation during summer months, higher dissolved organic carbon (DOC) concentration, and generally wider channel. The portion of the reach that was sampled measured 364, 109, and 227 meters in length for BC1, BC2, and BC3 respectively, but BC2 was expanded to 320 meters for one study.

Additional studies were conducted in stream reaches near the watershed outlet of two vastly different sites in terms of land use and as well as stream morphology compared to the BC streams. Marshy Hope (MH) is a small (1.36 km^2) 99% forested watershed in Nanticoke River Basin with very low N and P concentrations (Figure 1). South Forge (8.49 km^2) lies within the Choptank Basin and is dominated by agriculture: 66.5% agriculture, 28.2% forest, and 5.3% urban structures (Figure 1).

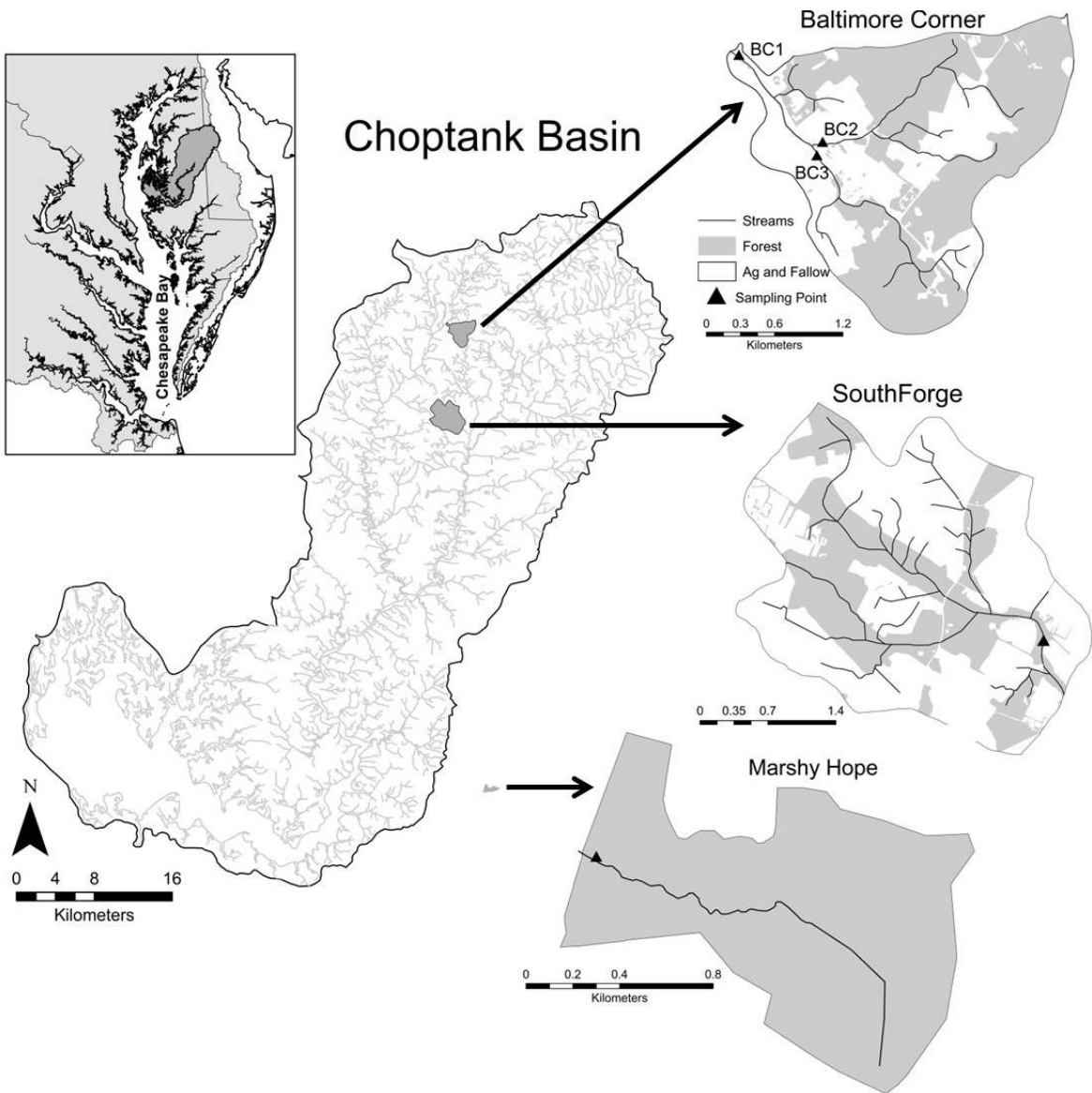


Figure 1. Map study Choptank Basin and location of study sites within the Basin. The downstream sampling points are represented by black triangles. Within the small study watersheds gray indicates forest cover and white agriculture/fallow area.

The main channel of the SF stream network is not channelized and has an intact floodplain containing mature forest. Most of the SF stream network (55%) is buffered, and the remaining un-buffered portion is largely ephemeral ditches.

Eleven open channel studies were conducted in the BC watershed using the one station approach (McCutchan et al. 2003). Each study was completed in six to eight hours during daylight, and repeated seasonally from September 2012-July-2013 in the three main stream reaches. One study in each of the MF and SF reaches was conducted fall 2012. By reducing the effort from the typical 12-24 (McCutchan et al. 2003; Laursen and Seitzinger 2002) to a 6 hour study period, the goal was to allow for more spatial-temporal coverage within a stream network. However, this approach sacrifices the ability to investigate diel variability in production, and rates are only representative of daytime when in-stream N₂ production is generally greater and N₂O emissions may be lower (Laursen and Seitzinger 2004; Harrison et al. 2005).

Groundwater Sampling

Groundwater discharge into the stream reach was estimated by the difference in streamflow between the upstream and downstream sampling points. The piston velocity (V_{gw} , m s⁻¹) was then calculated by dividing groundwater discharge by surface area measured from 10-12 cross sections multiplied by the reach length as follows; where Q_{ds} and Q_{us} represents the down and upstream discharge (m³ s⁻¹), and SA is the reach surface area (m²).

$$V_{gw} = (Q_{ds} - Q_{us})/SA \quad (\text{Eq. 1})$$

Streamflow was determined using a constant injection of a conservative tracer. A solution of sodium bromide (NaBr) was injected at a rate of 23 mL min⁻¹ using a peristaltic pump at an upstream location and allowed to mix over 50 meters of stream length. At the upstream and downstream points, water was sampled in 60 mL plastic bottles every 15 minutes for Br⁻ and other anions (Cl⁻, F⁻, NO₂⁻, NO₃⁻, PO₄³⁻,

SO_4^{2-}). Stream flow (Q , L s^{-1}) was calculated at both points using the injection rate (r , L s^{-1}), stock solution concentration (Br_{stock} , mg L^{-1}), and steady state Br^- concentration (Br_{post} , mg L^{-1}) minus background (Br_{pre} , mg L^{-1}).

$$Q = \text{Br}_{stock} r / (\text{Br}_{post} - \text{Br}_{pre}) \quad (\text{Eq. 2})$$

Streamflow was also estimated by measuring cross sectional area and velocity (Flo-Mate, Marsh-McBirney, Loveland, CO). Discharge calculated from the area-velocity and conservative tracer methods agreed well at the downstream site ($r^2=0.91$, $P < 0.001$; see Table 1 for description of all regressions).

Groundwater was sampled from 3-5 in-stream polyvinyl-chloride (PVC) piezometers (5 cm inner diameter) with a 20 cm screen length at a depth of 40-60 cm below the streambed. Hydraulic head was measured using a water level detector (Solinst model 101M, Georgetown, Canada) or meter stick. Piezometers were pumped dry with a peristaltic pump (Solinst model 410, Georgetown, Canada) and allowed to recharge immediately prior to sampling for dissolved gases. A small submersible pump (Whale Water Systems Inc., Manchester Center, VT) with positive pressure was used for sampling to reduce potential stripping of dissolved gases by negative pressure while pumping.

Dissolved gas samples were overflowed several volumes prior to covering with septa and caps. N_2 , O_2 , and argon (Ar) were sampled in quadruplicate in 27 mL glass tubes, N_2O was sampled in duplicate, ^{222}Rn was sampled in duplicate or triplicate in 250-mL glass bottles with septa, and one additional sample was taken for anion analysis. Dissolved organic carbon (DOC) was also sampled in 250 mL amber glass jars but only once during summer 2013 from each piezometer and stream.

Table 1. Details for all regressions including x and y variables, equation, r^2 , P-value and sample size (n).

Sites	x	y	Equation	r^2	P	n
BC, SF, MH	Discharge using Br^- ($\text{m}^3 \text{s}^{-1}$) reach averaged	Discharge Area- Velocity ($\text{m}^3 \text{s}^{-1}$)	$y=0.807x + 0.0001$	0.91	<0.001	12
BC	^{222}Rn in groundwater (Bq m^{-3}) reach averaged	groundwater flux per reach ($\text{m}^3 \text{hr}^{-1}$)	$y=0.0028x - 8.2$	0.7	0.0014	11
BC, SF, MH	^{222}Rn in groundwater (Bq m^{-3})	groundwater flux per reach ($\text{m}^3 \text{hr}^{-1}$)	$y=5\text{X}10^{-4}x - 7\text{X}10^{-4}$	0.37	0.0014	13
BC	hydraulic head (cm)	^{222}Rn in groundwater (Bq m^{-3})	$y=197x + 4361$	0.32	0.0002	40
BC	groundwater NO_3^- ($\mu\text{mol L}^{-1}$)	groundwater N_2O ($\mu\text{mol L}^{-1}$)	$y=0.0013x + 0.0941$	0.58	<0.0001	40
BC	stream NO_3^- ($\mu\text{mol L}^{-1}$)	stream N_2O ($\mu\text{mol L}^{-1}$)	$y= 0.0012x + 0.19$	0.6	0.003	11
BC	groundwater NO_3^- ($\mu\text{mol L}^{-1}$)	stream NO_3^- ($\mu\text{mol L}^{-1}$)	$y=0.731x + 2.927$	0.7	0.001	11
BC	stream temp (°C)	P_{T} of N_2 ($\text{mmol m}^{-2} \text{hr}^{-1}$)	$y=0.36x + 0.36$	0.42	0.03	11
BC	stream temp (°C)	P_{st} of N_2 ($\text{mmol m}^{-2} \text{hr}^{-1}$)	$y=0.30x - 3.05$	0.50	0.015	11
BC	stream temp (°C)	P_{gw} of N_2 ($\text{mmol m}^{-2} \text{hr}^{-1}$)	$y=0.07x - 3.4$	0.10	0.35	11
BC	ASD (cm)	P_{T} of N_2 ($\text{mmol m}^{-2} \text{hr}^{-1}$)	$y=0.22x - 1.7$	0.82	0.0001	11
BC	ASD (cm)	P_{st} of N_2 ($\text{mmol m}^{-2} \text{hr}^{-1}$)	$y=0.14x - 3.5$	0.60	0.005	11
BC	ASD (cm)	P_{gw} of N_2 ($\text{mmol m}^{-2} \text{hr}^{-1}$)	$y=0.08x + 1.7$	0.70	0.0014	11
BC	stream temp (°C)	N_2O emissions ($\mu\text{mol m}^{-2} \text{hr}^{-1}$)	$y=e^{0.2114x}$	0.85	<0.0001	11
BC	ASD (cm)	N_2O emissions ($\mu\text{mol m}^{-2} \text{hr}^{-1}$)	$y= 3.35x - 51.9$	0.6	0.0052	11
BC, SF,MH	P_{st} of N_2 ($\text{mmol m}^{-2} \text{hr}^{-1}$)	P_{st} of N_2O ($\text{mmol m}^{-2} \text{hr}^{-1}$)	$y= 0.022x + 0.028$	0.80	<0.0001	13
BC, SF,MH	P_{gw} of N_2 ($\text{mmol m}^{-2} \text{hr}^{-1}$)	P_{gw} of N_2O ($\text{mmol m}^{-2} \text{hr}^{-1}$)	$y= 0.0015x - 0.0016$	0.58	0.0024	13

Surface water Sampling

A YSI multiprobe instrument (Model 556 MPS, Xylem Inc., Yellow Springs, OH) was placed at mid-depth in the stream thalweg to measure stream temperature, pH, specific conductivity, salinity, dissolved oxygen (DO) concentration, and DO % saturation every minute. Barometric pressure was measured on-site every 10 minutes or less using a pressure transducer (Model 3001, Solinst Gold Levelogger, Canada). Air temperature data was downloaded from the closest Weather Underground station (Church Hill, MD ~16 km from BC watershed) that had high frequency (5 minute) data available for all study dates. In addition to monitoring during field studies, temperature and stage were continuously measured at 30 minute intervals using Solinst pressure transducers fixed to a cinderblock on the streambed near the downstream point of each reach. Rating curves have been developed to convert stage to discharge (Fisher et al. 2010).

Surface water samples for N₂, O₂, Ar (quadruplicate), and N₂O (duplicate) were collected every two hours at the downstream site. Vinyl tubing (2 mm inner diameter) was placed in a 27 mL glass tube that was inserted upside-down into the thalweg of the stream until the glass tube was completely submerged. The tubing provided a vent for air and was removed prior to covering the tubes with Teflon/silicon septa and caps underwater.

²²²Rn was measured every 10 minutes at the same sampling site by continuously pumping stream water with a submersible pump (Whale Water Systems Inc., Manchester Center, VT) through a RAD-AQUA attachment connected to a RAD7 radon-in-air monitor (Durridge, Billerica, MA). Stream water was sprayed into

the RAD-AQUA chamber, which was continuously monitored for temperature in order to convert ^{222}Rn in air to ^{222}Rn in water according the equations provided in the RAD7 manual.

Laboratory Analysis

Ground and surface water samples were held on ice or in a refrigerator (4 °C) until analysis, except for groundwater ^{222}Rn samples which were kept at ambient temperature and analyzed within 24 hours. Samples for dissolved gases N₂, O₂, and Ar were generally analyzed within 48 hours of collection at Horn Point Laboratory using a quadruple mass spectrometer with a membrane inlet (MIMS; Kana et al. 1994). One standard was prepared with deionized water in a glass flask and allowed to equilibrate overnight in a water bath under constant stirring. MIMS was calibrated to the mean stream temperature over the day in which the samples were collected. Standards were measured initially and every 40 samples. Ion currents from the standards bracketing each set of ~40 samples were used to correct for instrument drift. Corrections in N₂ and Ar due to O₂ scavenging were also applied based on empirical relationships between O₂ ion currents and the magnitude of scavenging (Fisher et al. 2010; Fox et al. 2014). Equilibrium concentrations for N₂ and Ar were estimated using temperature, barometric pressure, and solubility curves provided in Hamme and Emerson (2004) and for O₂ in Garcia and Gordon (1992).

Dissolved N₂O was measured using a Shimadzu Gas Chromatograph-14B (Shimadzu Corp, Kyoto, Japan) equipped with an electron capture detector within 24 hours of collection. Seven mL of water was injected into N₂-purged 12 mL Exetainers® (High Wycombe, UK) through the septum with a vent to maintain

atmospheric pressure. Exetainers® were shaken vigorously for 4 minutes and allowed to equilibrate at room temperature for at least 30 minutes prior to analysis. The dissolved concentration in water was calculated using water sample and headspace volumes as well as solubility data for the measured room temperature and pressure (Weiss and Price 1980). DOC was measured at Horn Point Laboratory Analytical Services using a Shimadzu TOC-5000A analyzer (Shimadzu Corp, Kyoto, Japan).

Analysis of anions and groundwater ^{222}Rn samples was conducted at the Smithsonian Environmental Research Center in Edgewater, Maryland. Grab samples were filtered through 45 μM pore-size membranes, and Br^- , Cl^- , F^- , NO_2^- , NO_3^- , PO_4^{3-} , SO_4^{2-} were measured using a Dionex ion chromatograph fitted with a KOH eluent generator, a conductivity detector, and an AS18 separatory column (Thermo Fisher Scientific, Waltham, Massachusetts, USA). Groundwater ^{222}Rn grab samples were analyzed using a RAD7 with a RAD-H₂O radon-in-water attachment (Durridge, Billerica, MA).

Gas Transfer Velocity

Gas transfer velocity (k) was estimated using two inert, noble gases, Ar and ^{222}Rn , with a one-station approach. As noted in Laursen and Seitzinger (2004), when measured Ar concentration in surface water deviates from equilibrium concentration k can be estimated by the rate of re-equilibration needed to predict observed Ar concentrations. The McCutchan et al. (2003) N₂ production equation was solved for reaeration coefficient (K, min^{-1}) and substituted with Ar data as follows;

$$K = \frac{\frac{C_t - C_o}{\Delta t}Z - (C_g - C_t)V_{gw}}{(C_{eq} - C_t)Z} \quad (\text{Eq. 3})$$

where K is the reaeration coefficient (min^{-1}), C_t is final concentration (mmol m^{-3}), C_0 the initial concentration (mmol m^{-3}), Z is the mean depth of the channel (m), C_g is measured concentration in groundwater (mmol m^{-3}), V_{gw} is the flux of groundwater per unit area (m min^{-1}), C_{eq} is the equilibrium concentration at time t (mmol m^{-3}), and Δt is the time interval (min). Reaeration coefficients were converted to a gas transfer velocity (k , m min^{-1}) by multiplying by depth and then converted to a common Schmidt number of 600 ($k600$, m min^{-1}) using the following equation (Wanninkhof 1992).

$$k600 = (600/Schmidt)^{-2/3} \times K \quad (\text{Eq. 4})$$

Schmidt numbers were calculated based on table 1 of Raymond et al. (2012), and an exponent of 2/3 was used for these low-gradient streams with little surface turbulence (Jahne et al. 1987). The gas transfer velocities were averaged to produce a daily mean $k600$ (m min^{-1}) for each study.

Gas transfer velocity using ^{222}Rn was calculated using three different methods. Method 1 applies equation (3) to ^{222}Rn data. Gas exchange velocity was estimated at 10 minute intervals (sampling frequency of surface water ^{222}Rn measurements) with assumptions of constant groundwater input and an equilibrium concentration of zero. Method 2 is identical to method 1 except that the stream ^{222}Rn data was smoothed first using local polynomial regression fitting (loess function; R 3.0.2). Figure 2 shows raw ^{222}Rn data with smoothed polynomial lines.

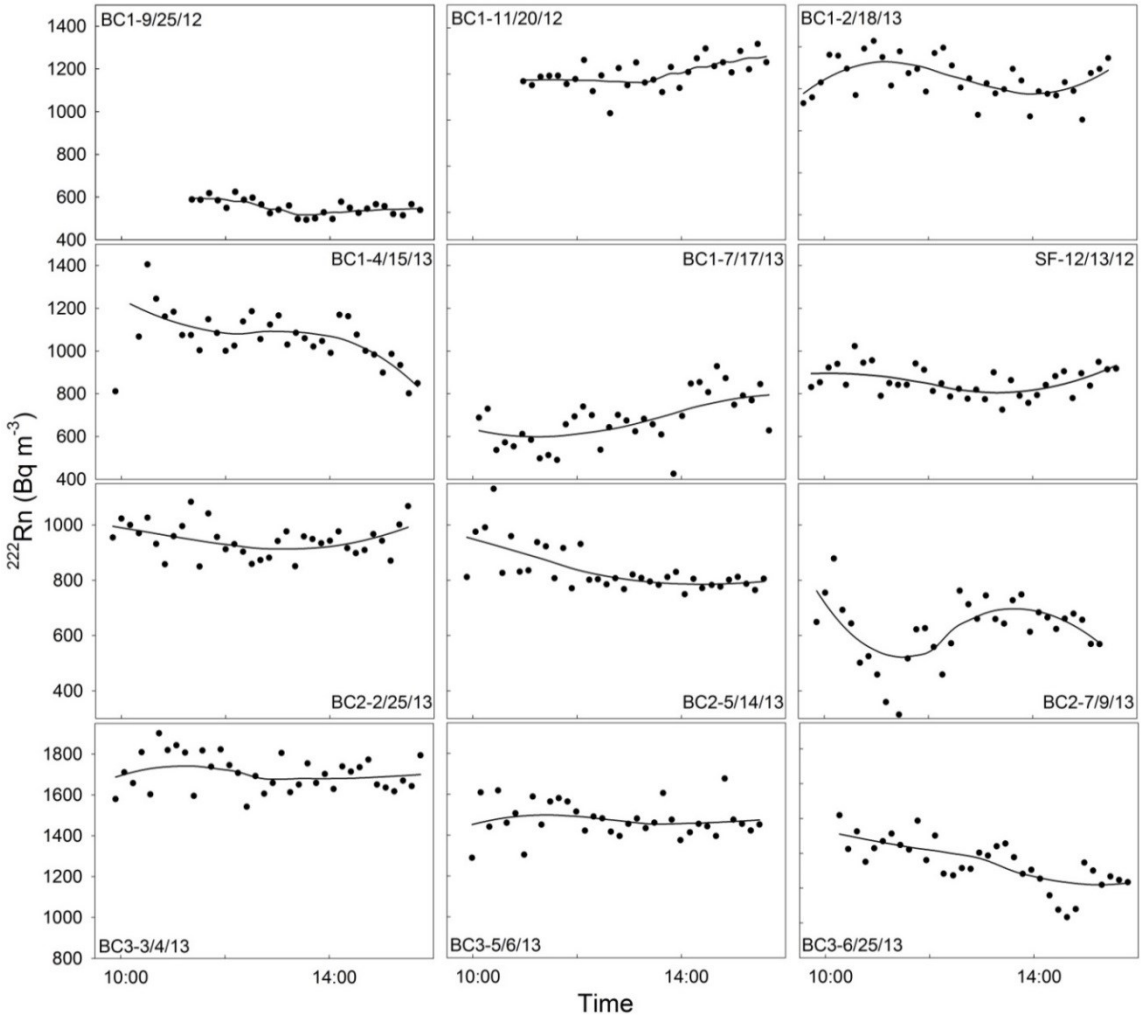


Figure 2. Patterns in surface water ^{222}Rn activity (sampled every 10 minutes) from all studies in the BC (11 studies) and SF (1 study) streams. Lines are local polynomial regression fits using a loess function in R.

Method 3 solves for k using a ^{222}Rn mass balance similar to Wanninkhof (1990) for a one meter long stream reach (Figure 3) assuming the ^{222}Rn flux out of the reach differs from the flux into the reach due only to groundwater inputs and loss to the atmosphere (i.e. $^{222}\text{Rn}_{\text{sw}}$ concentration in = concentration out) as follows,

$$k = \frac{[Rn_{\text{sw}}](Q_{us} - Q_{ds}) + [Rn_{\text{gw}}]Q_{gw}}{SA[Rn_{\text{sw}}]} \quad (\text{Eq. 5})$$

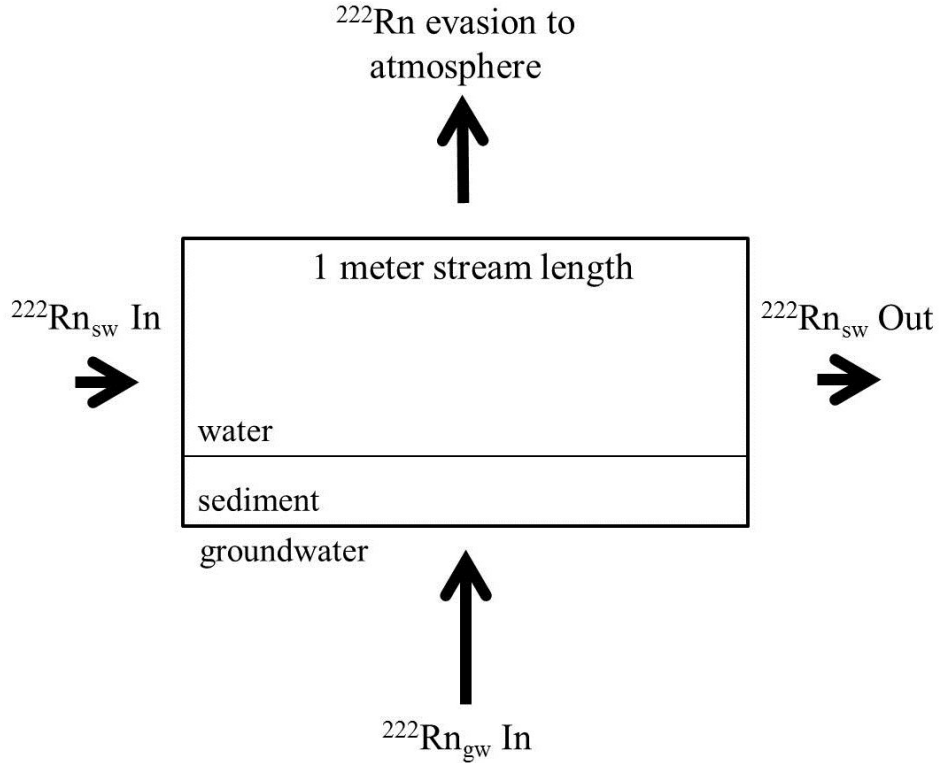


Figure 3. Conceptual model of stream reach ^{222}Rn mass balance at steady state based on model of Wanninkhof (1990) and Knee et al. (in prep). The surface water radon activity ($^{222}\text{Rn}_{\text{sw}}$) in equals the surface water activity out. This was used to estimate the rate of ^{222}Rn loss to atmosphere and thus gas exchange velocity.

where Rn_{sw} is the concentration in surface water (Bq m^{-3}); Rn_{gw} is the concentration in groundwater (Bq m^{-3}); Q_{us} and Q_{ds} are the upstream and downstream discharges respectively ($\text{m}^3 \text{s}^{-1}$); Q_{gw} is the flux of groundwater per meter of stream reach ($\text{m}^3 \text{s}^{-1} \text{ m}^{-1}$); SA is the stream surface area (m^2). $k600$ was calculated at 10 minute intervals and averaged over the sampling period. Radioactive decay was negligible since the travel time through the full reach length (0.01-0.17 days) was much less than ^{222}Rn half-life (3.8 days).

Argon Modeling

The concentration of Ar in surface water was modeled by solving equation (3) for C_t as follows.

$$C_t = \frac{C_{eq}KZ + C_g V_{gw} + C_o Z}{Z + KZ + V_{gw}} \quad (\text{Eq .6})$$

Modeled Ar was compared to measured Ar concentrations (Figure 4) and acted as a validation of the open channel model as noted by Laursen and Seitzinger (2002). Ar should behave conservatively, and therefore modeled concentrations should agree with measured concentrations if the terms are accurately quantified.

Estimation of N_2 and N_2O production

Biogenic N_2 and N_2O accumulation from both in-stream production (P_{st}), and production occurring within the watershed delivered to the stream via groundwater (P_{gw}), were calculated using the one station open-channel method (McCutchan et al. 2003). This approach is based on a stream N_2 (or N_2O) mass balance and assumes a well-mixed stream with a constant velocity and groundwater flux. P_T is the total biogenic N gas accumulation in the stream reach from in-stream and groundwater sources. P_T was estimated using recharge (i.e. physical) N gas concentrations in groundwater using Ar as a tracer for groundwater recharge temperature. P_{gw} was estimated by subtracting P_{st} from P_T . P_{gw} is thus constant over the sampling period; however, P_{st} varies as would be expected of in-stream processes. P_T and P_{st} were directly calculated between sampling intervals ($t= 2$ hours) as follows.

$$P_T = \frac{C_t - C_o}{\Delta t} Z - (C_g - C_t)V_{gw} - K(C_{eq} - C_t)Z \quad (\text{Eq. 7})$$

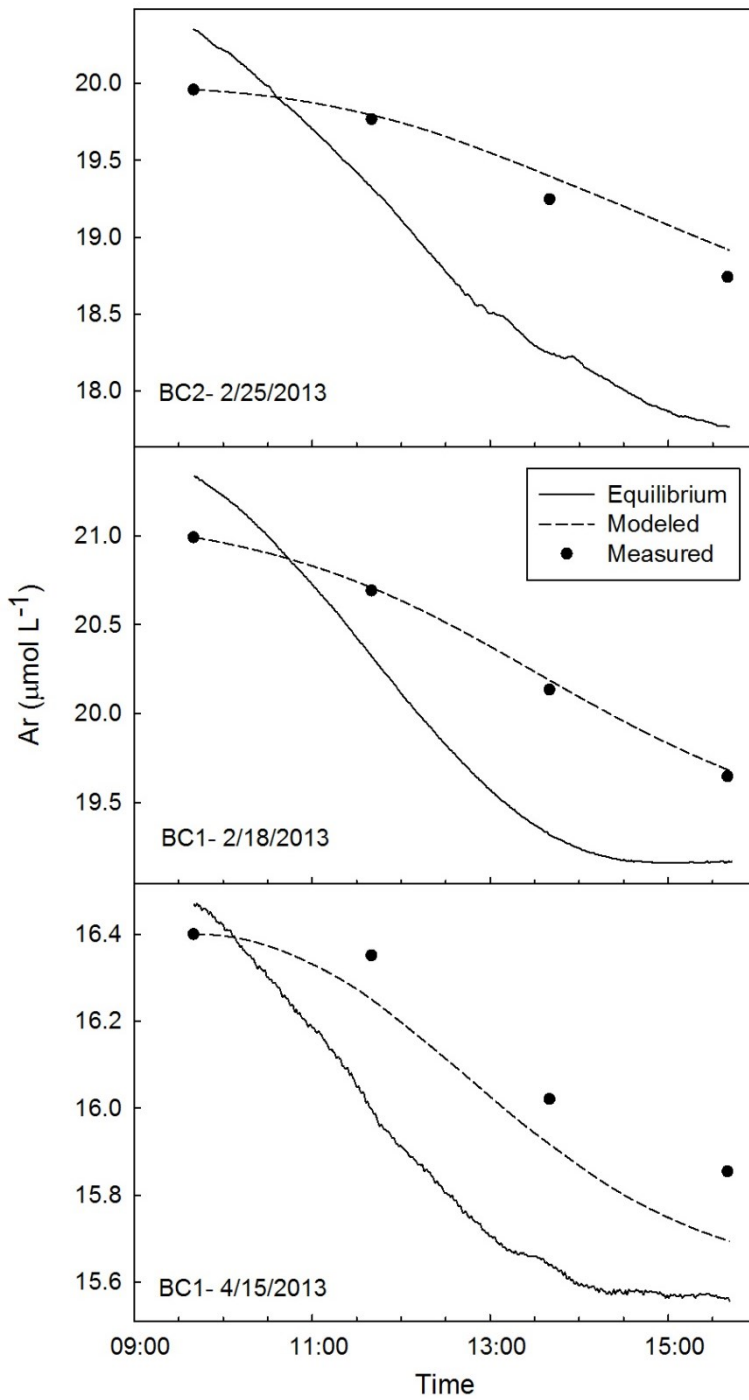


Figure 4. Examples of Ar modeling in stream water over a 6 hour period. The top panel is an example where the Ar was overestimated compared to measured. The middle panel shows good agreement. The bottom panel is data from the study with the poorest agreement between modeled and measured (2.4% difference at the last observation).

The only difference being C_g equals the recharge N_2 or N_2O concentration when estimating P_T , but C_g equals the measured concentration in groundwater when estimating P_{st} . The variables C_g , V_{gw} , and Z are assumed constant over the 6-8 sampling period (variables defined in Eq. 3). C_{eq} was re-calculated based on one-minute stream temperature data and corrected for air temperature, barometric pressure, and relative humidity (assumed constant 100% humidity at the air-water boundary layer). The daily mean $k600$ was converted to a reaeration coefficient for K_{N2} , K_{N2O} , or K_{Ar} and varied with Schmidt number scaling based on temperature data. Equation (7) was used to solve for N_2 and N_2O production with a time step equal to the frequency measurements ($\Delta t = 2$ hours). The mean of the 3-4 calculated values represent the spatially and temporally integrated 6-8 hour average production.

Measurements of groundwater Ar were essential to the calculation of P_T and separation of in-stream from groundwater contributions. Ar was used as a tracer for recharge temperature by back-calculating temperature from solubility curves (Colt 1984; Bohlke and Denver 1995; Fisher et al. 2010) provided in Hamme and Emerson (2004) according to the equation (8). Temperature and Ar concentration are in units of Celsius and $\mu\text{mol Kg}^{-1}$ respectively. Recharge N_2 and N_2O concentration were calculated using the reach averaged groundwater recharge temperature and the appropriate solubility equation (Weiss and Price 1980; Hamme and Emerson 2004). This represents the physical N_2 and N_2O gas present in groundwater. Measured N gases in excess of recharge concentrations in groundwater were assumed to be biogenic (Wilson et al. 1990).

$$T_{recharge} = 0.0099[Ar]^3 + 0.651[Ar]^2 - 16.086[Ar] + 144.62 \quad (\text{Eq. 8})$$

This technique assumes Ar behaves conservatively and was at atmospheric equilibrium during recharge (i.e. precipitation and infiltration into the aquifer). Argon recharge temperatures in the Choptank basin are typically slightly lower than groundwater temperatures since most recharge of the shallow aquifer occurs during cooler months (Fisher et al. 2010). Average recharge temperature of emerging groundwater was 15 °C, which was similar to previous estimates (9-14 °C) in upland shallow aquifers across the Delmarva Peninsula (Dunkle et al. 1993).

N₂O Emissions

N₂O emissions from streams were calculated using the air-water, two layer diffusive gas exchange model (Liss and Slater, 1974);

$$N_2O \text{ emissions} = k(C_m - C_{eq}) \quad (\text{Eq. 9})$$

where k is the gas exchange velocity (m hr^{-1}); C_m is the measured concentration (mmol m^{-3}); and C_{eq} is the equilibrium concentration.

Uncertainty Analysis

The uncertainty in k using the Ar and three ²²²Rn methods as well as P_T , P_{st} , and P_{gw} of N₂ and N₂O for each of the 13 studies was evaluated using a Monte Carlo approach similar to McCutchan et al. (2003). For k , terms in equations (3) and (5) were randomly sampled 1000 times from normal distributions described by measured means and empirical or literature derived standard deviations. An identical approach was applied to equation (7) to estimate uncertainty in production. Error in measured N₂ and Ar was assumed to be due to limits of precision and error in equilibrium concentrations due to measurement error of temperature, which would likely result in

the greatest deviation in concentration compared to uncertainty in pressure or solubility curves (Baulch et al. 2011). Error in groundwater inputs was assumed to be 10% of the measured value (McCutchan et al. 2003), and since we had few depth measurements, depth and surface area error were set at 2.5% which is in between values reported in McCutchan et al. (2003) and Smith et al. (2008). Uncertainty in groundwater concentrations of N₂, Ar, N₂O, and ²²²Rn was assumed to be due to spatial variation along the reach; therefore, the standard deviation of the 3-5 piezometer was used (Table 2). Output from the Monte Carlo simulations was used to estimate the standard deviation and 95% confidence interval for each method of calculating *k* and as well as N₂ and N₂O production.

Table 2. Estimates of error for variables used in uncertainty analysis of gas exchange velocity and N₂ and N₂O production.

Variable	SD
Z (m)	2.5% of value
SA (m ²)	2.5% of value
V _{gw} (m min ⁻¹)	10% of value
<i>k</i> ₆₀₀ (m hr ⁻¹)	35% of value*
T (°C)	-0.15
²²² Rn _{sw} (Bq m ⁻³)	12% of value*
²²² Rn _{gw} (Bq m ⁻³)	1769 (26% of value)*
Ar _{sw} (μmol L ⁻¹)	0.016 (0.1% of value)*
Ar _{gw} (μmol L ⁻¹)	0.91 (5.8% of value)*
N ₂ sw (μmol L ⁻¹)	0.8 (0.12% of value)*
N ₂ gw (μmol L ⁻¹)	35.8 (4.9% of value)*
recharge N ₂ gw (μmol L ⁻¹)	31.7 (5.3% of value)*
N ₂ O _{sw} (μmol L ⁻¹)	0.008 (4.7% of value)*
N ₂ O _{gw} (μmol L ⁻¹)	0.23 (124% of value)*
recharge N ₂ O _{gw} (μmol L ⁻¹)	0.001 (9.2% of value)*

*Varied depending on measurements from each study. Shown here are average error terms across all dates.

Results

Groundwater Data

Groundwater inputs over the study reaches (109-364 m) accounted for 2.3 to 23% of the surface water discharge within the study reach at the BC and MH watersheds. In SF, only 0.28% of the discharge was from groundwater over the reach length. Groundwater piston velocity was similar in magnitude across all sites and dates (0.13 to 0.72 m day⁻¹), except for SF (0.04 m day⁻¹), with lows occurring the summer and fall of 2012 following a drought. The lower piston velocity in the SF reach was consistent with the low hydraulic head measurements (-0.9 to 4.7 cm, mean=1.1) compared to 0-36 cm (mean=15) at BC, and 1.8-20 cm (mean=11) at MH. Groundwater flux per meter of stream length measured in the study reach (0.25-1.75 m³ day⁻¹ m⁻¹) was comparable to the estimated average groundwater flux in the upstream network found by dividing upstream discharge by upstream length (0.08-1.70 m³ day⁻¹ m⁻¹), indicating study reaches were representative. In addition, background groundwater (0.016-0.25 mg L⁻¹) and surface water (0.016-0.19 mg L⁻¹) Br- concentrations were comparable on each day, and correlated ($r^2 = 0.97$, $P < 0.001$), suggesting the sampled groundwater was representative of the average conditions contributing to surface water flow.

Most dissolved gases in groundwater were far from equilibrium concentrations and spatially variable. The average groundwater recharge temperature from all dates and sites was 15.02 °C (range of 8.52 to 22.09 °C). This agrees with previously sampled groundwater temperature variation measured with in-stream piezometers in the BC watershed. One measurement of 30 °C was likely a result of

gas stripping by ebullition because recharge temperatures greater than 20 °C are uncommon (Fisher et al. 2010). Therefore, N₂, Ar, and O₂ data from this piezometer were excluded from calculations and statistics. The average N₂-N concentration across all dates and sites was 1477 µM (range 1134-1766 µM), and excess N₂-N was 292 µM (range 33-591 µM). Most excess N₂-N concentrations were well above 100 µM, with the lowest occurring at the MH site. O₂ concentrations in groundwater were low (3.0-212 µM or 0.03-60.9% saturation) with a mean of 39.3 µM (11% saturation). N₂O-N was highly variable. Concentrations ranged from 0.001 to 2.1 µM (mean= 0.39, median = 0.07 µM), and 46% of measurements were marginally undersaturated.

Seasonal patterns in excess N₂, NO₃⁻, and ²²²Rn were observed in repeatedly sampled piezometers in the BC reaches. Excess N₂ followed a seasonal curve with peaks in February to March and lows in the summer. NO₃⁻ was more variable but generally the inverse of the excess N₂ pattern for a given piezometer with peaks occurring in the summer and lows in late winter (Figure 5). These data were variable as expected of groundwater chemistry. However, individual piezometers were relatively consistent in their range of excess N₂ and NO₃⁻ concentrations, being low or relatively high across all sampling dates, indicating consistent flow paths or sources during sampling. Groundwater NO₃⁻ and N₂O were significantly correlated ($r^2=0.58$, $P<0.0001$, Figure 6a). ²²²Rn activity in all piezometers followed the same pattern across dates, which was not a seasonal curve, but appears to be related to groundwater flux. In the BC watershed, the reach averaged groundwater ²²²Rn activity was positively related to the groundwater flux over the reach ($r^2=0.70$, $P=0.0014$, Figure 7). Additionally, aggregating all individual piezometer measurements in the BC

watershed, groundwater ^{222}Rn activity was weakly but positively correlated with hydraulic head ($r^2=0.32$ $P=0.01$, Figure 8).

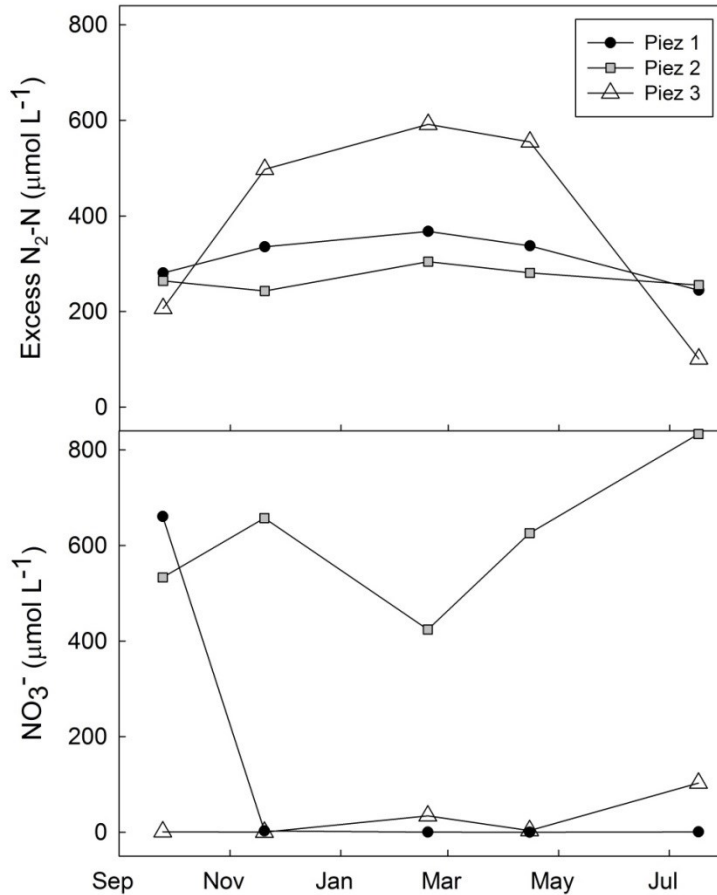


Figure 5. Temporal patterns of NO_3^- and $\text{xsN}_2\text{-N}$ from individual piezometers (1-3) in the BC1 reach. All piezometers followed the same seasonal $\text{xsN}_2\text{-N}$ pattern, peaking in early spring. Patterns were variable, but generally piezometers with high $\text{xsN}_2\text{-N}$ had lower NO_3^- concentrations.

Surface Water

Studies were conducted during baseflow but over a wide range of hydro-climatic conditions in the BC1 reach encompassing a summer drought (2012) and an anomalous wet summer (2013) with streamflow varying between 4.5 and 121.6 L s^{-1} . Only three studies were conducted in each of the BC2 and BC3 reaches with a lesser degree of hydro-climatic variability. Streamflow varied from 28.8 to 39.5 L s^{-1} in

BC2 and 12.3 to 15.7 L s⁻¹ in BC3. Streamflow at the SF and MH sites was 83.0 and 7.4 L s⁻¹ respectively. NO₃⁻ concentrations the BC1, BC3, and SF reaches were high (109-370 μM), lower in BC2 (21-46 μM), and very low in MH (0.59 μM) (Table 3). DOC was relatively high at all BC sites (BC1= 680, BC2=2044, BC3=531 μmol C L⁻¹). No DOC measurements were taken at MH or SF.

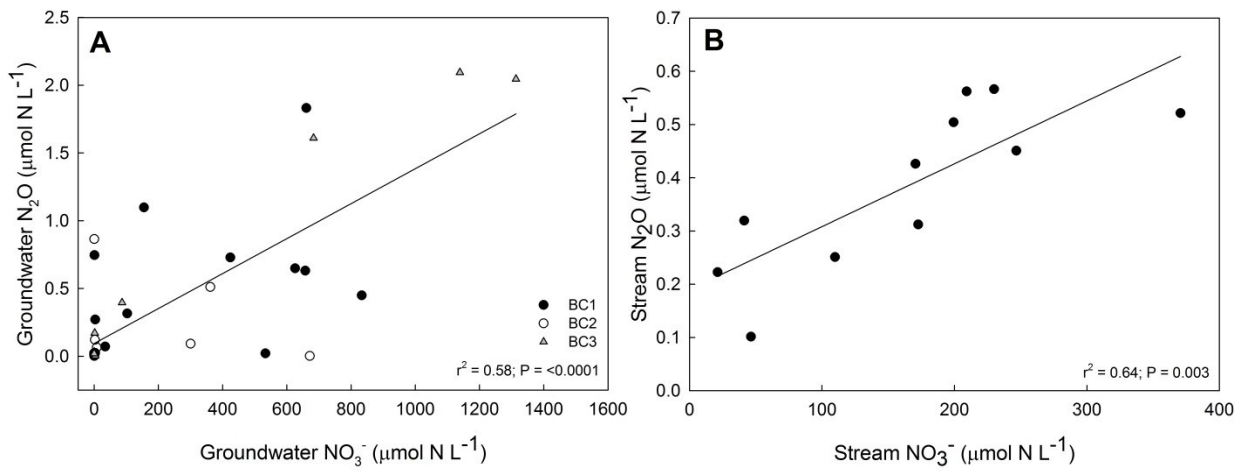


Figure 6. Linear regressions between NO₃⁻ and N₂O-N concentrations for groundwater (A) and surface water (B) using data from all BC reaches (1-3).

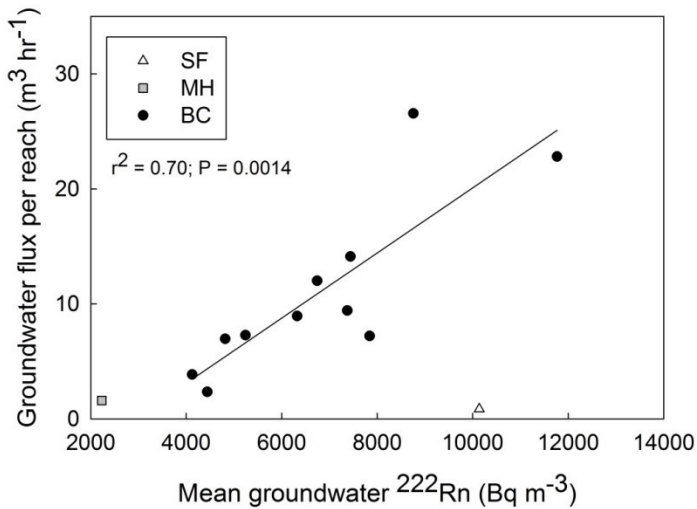


Figure 7. Linear regression between the groundwater flux per reach and the mean groundwater ²²²Rn activity sampled from 3-5 piezometers from all BC reaches. One data point from MH and SF reaches are also displayed but not included in the regression. When adding these two points the r^2 and P value decreased to 0.37 and 0.028 respectively.

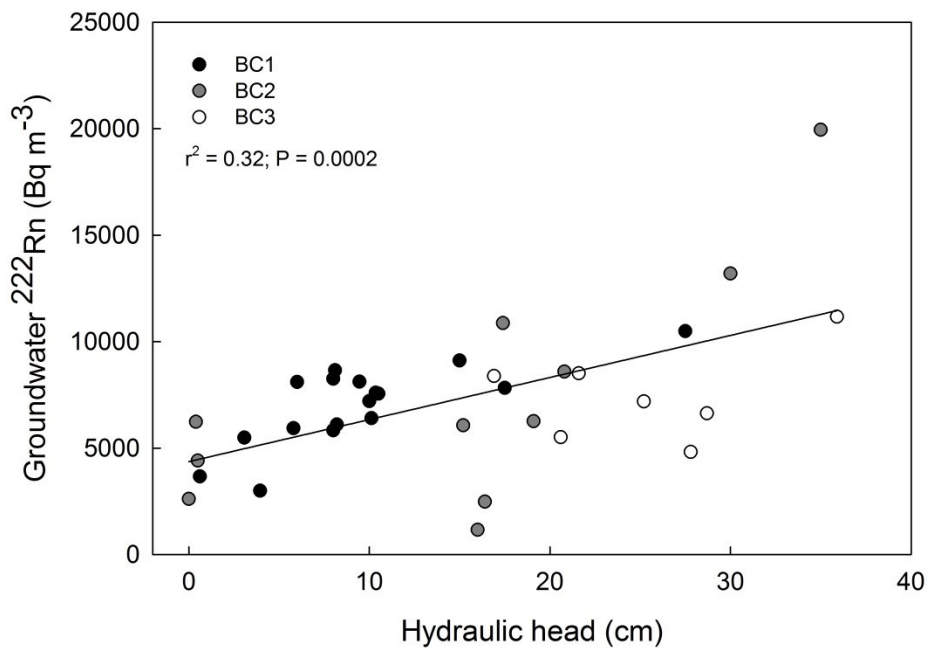


Figure 8. Relationship between hydraulic head and groundwater ^{222}Rn activity for all individual piezometers in the BC watershed.

Table 3. Discharge, average stream temperature, average nitrate concentration, and average percent saturation of nitrogen gas, nitrous oxide, and oxygen during each study.

Date	Site	Q (L s ⁻¹)	Stream Temp (C)	NO ₃ (μM)	N ₂ (% sat)	N ₂ O (% sat)	O ₂ (% sat)	DOC (mg L ⁻¹)
9/25/12	BC	4.49	15.6	371	104	2463	81.0	-
11/20/12	BC	46.0	11.2	199	106	2045	85.5	-
2/18/12	BC	68.3	4.44	173	105	978	98.8	-
4/15/13	BC	167	14.1	110	104	1124	80.5	-
7/17/13	BC	82.5	24.0	171	103	2585	73.7	8.87
2/25/12	BC2	49.8	6.45	46	105	344	100	-
5/14/13	BC2	61.8	17.4	21	104	1077	88.2	-
7/9/13	BC2	42.0	24.6	41	102	1982	51.4	16.7
3/4/12	BC3	24.5	7.13	247	107	3111	93.6	-
5/6/13	BC3	19.2	13.7	230	104	5004	82.3	-
6/25/13	BC3	28.4	23.0	209	106	6681	63.9	8.17
12/13/12	SF	81.3	7.74	317	103	616	83.4	
11/15/12	MH	9.71	10.3	0.59	100	89.2	66.7	

As expected, stream temperature was the dominant control of N₂ and Ar but not the other dissolved gas concentrations in streams. Figure 9 shows temperature and various dissolved gases (O₂, N₂, N₂O, ²²²Rn) for a typical study in the BC watershed. Mean temperature across all 6 hour study periods ranged from 4.4 to 24.6 °C with temperature fluctuations over the study period of 0.68 to 9.0 °C. Dissolved N₂ concentrations tracked theoretical equilibrium but were always supersaturated (Figure 9), except in the forested MH reach where N₂ varied around equilibrium (Figure 10). Ar also tracked equilibrium during all studies at all sites; however, Ar was often undersaturated in the morning and became supersaturated as stream temperature increased (Figure 4). In contrast, dissolved N₂O and O₂ did not track equilibrium (Figure 9). N₂O was always highly supersaturated (344-6681%) with little variability over 6 hours, except at the MH site (Figure 10) which was under-saturated (average of 89%). Stream O₂ saturation increased during all studies peaking in the afternoon, indicating *in-situ* photosynthetic production (Figure 9). The MH site was again the exception, and O₂ decreased suggesting little or no photosynthetic production. Within the BC watershed, there was a significant positive linear relationship between NO₃⁻ and N₂O concentration ($\mu\text{mol N L}^{-1}$) in stream water ($r^2= 0.64$, $P=0.003$, Figure 6b.). Stream water NO₃⁻ concentration was also linearly correlated with the average groundwater NO₃⁻ concentration from the 3-5 piezometers within each reach ($r^2=0.70$, $P=0.001$, Figure 11), indicating groundwater is the dominant NO₃⁻ source in the BC watershed.

Gas Transfer Velocity

Gas exchange velocities (k_{600}) calculated from ^{222}Rn (k_{Rn}) and Ar (k_{Ar}) were generally in agreement as were the three calculation methods used with ^{222}Rn data (Table 4). k_{Ar} was often lower than k_{Rn} but not consistently. The three k_{Rn} methods estimated k_{600} values that were within 0.04-23% of each other depending on the day (Table 4). There was no consistent directional bias amongst k_{Rn} methods. Using a paired t-test to compare all methods against each other across dates, there was not a statistical difference between any groups except for k_{Rn} method 1 being marginally higher than k_{Rn} method 3 ($P=0.049$). Although, when regressing k_{Rn} versus k_{Ar} , the slope (0.86) was significantly lower than 1. Output from the Monte Carlo simulations is displayed in Table 5. The means of the resulting distribution of Methods 2 and 3 agreed well with k_{600} values estimated from raw data. The standard deviations averaged 31% of the k_{600} value across all studies for method 2 and 3, and 95% confidence intervals were relatively small. Argon derived k values were generally more variable and uncertain.

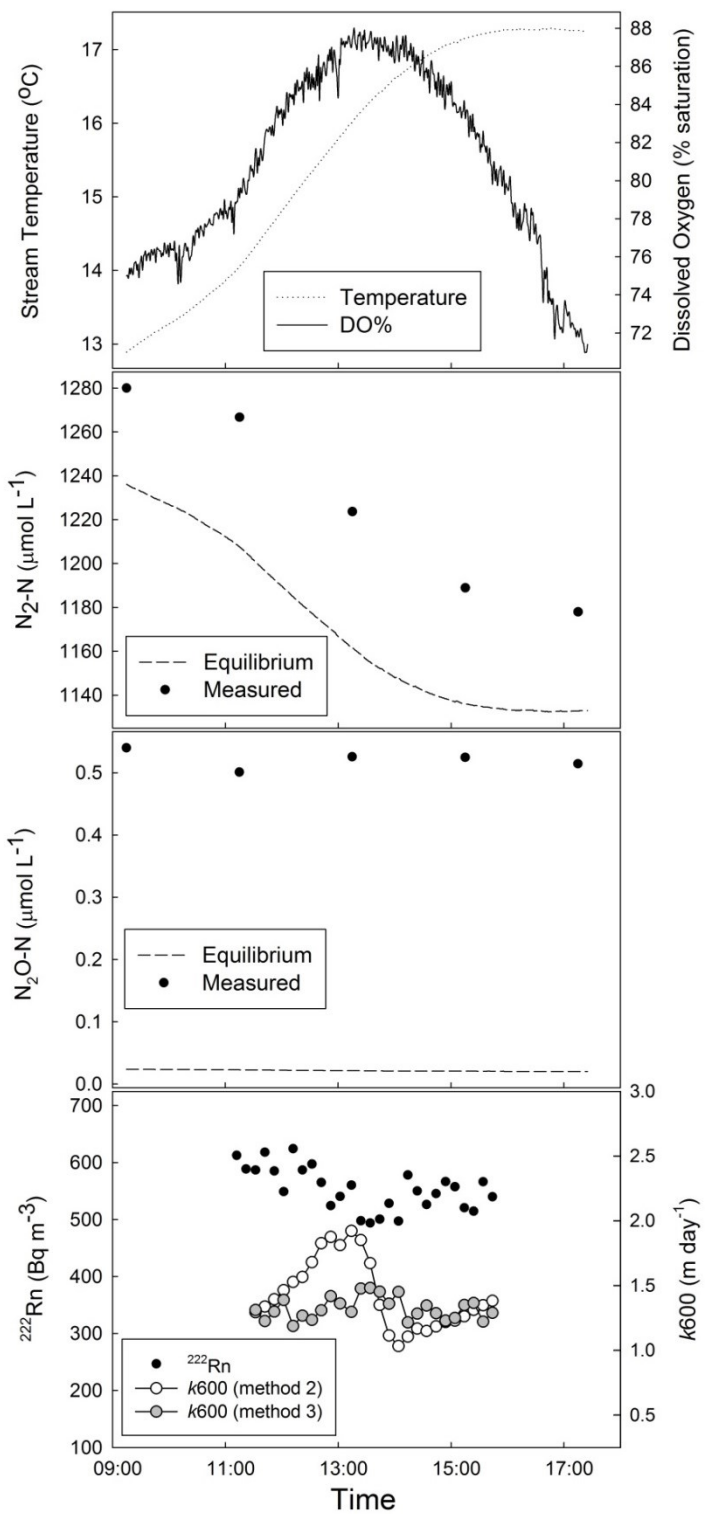


Figure 9. Summary of stream water data from a typical study in the BC watershed (BC1 9/25/2012) including temperature, dissolved oxygen, $\text{N}_2\text{-N}$ measured and equilibrium concentrations, $\text{N}_2\text{O}\text{-N}$ measured and equilibrium concentrations, ^{222}Rn activity, and k_{600} calculated from ^{222}Rn data using method 2 (smoothed data) and 3 (mass balance).

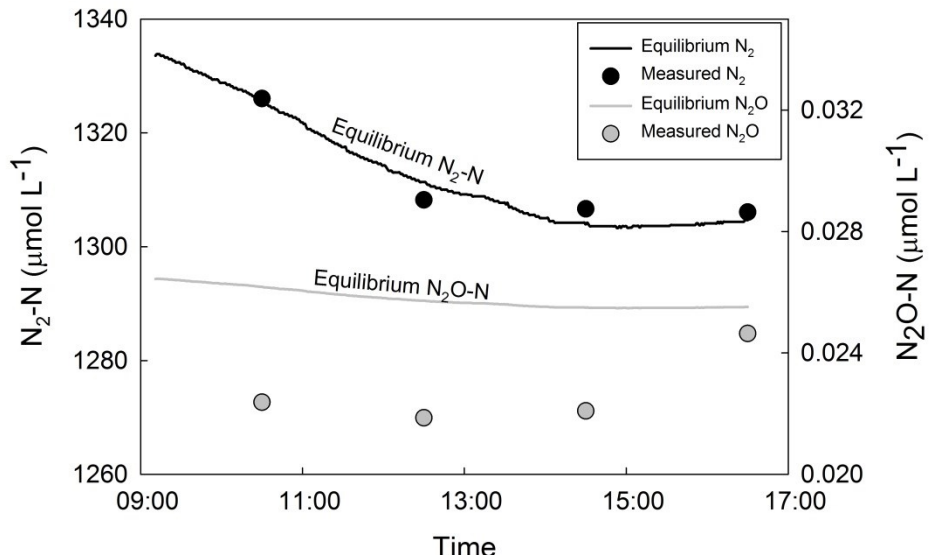


Figure 10. Equilibrium and measured concentrations of N₂-N and N₂O-N during one study at the Marshy Hope stream. N₂ varied around equilibrium. N₂O-N was undersaturated, but approaching equilibrium in the late afternoon.

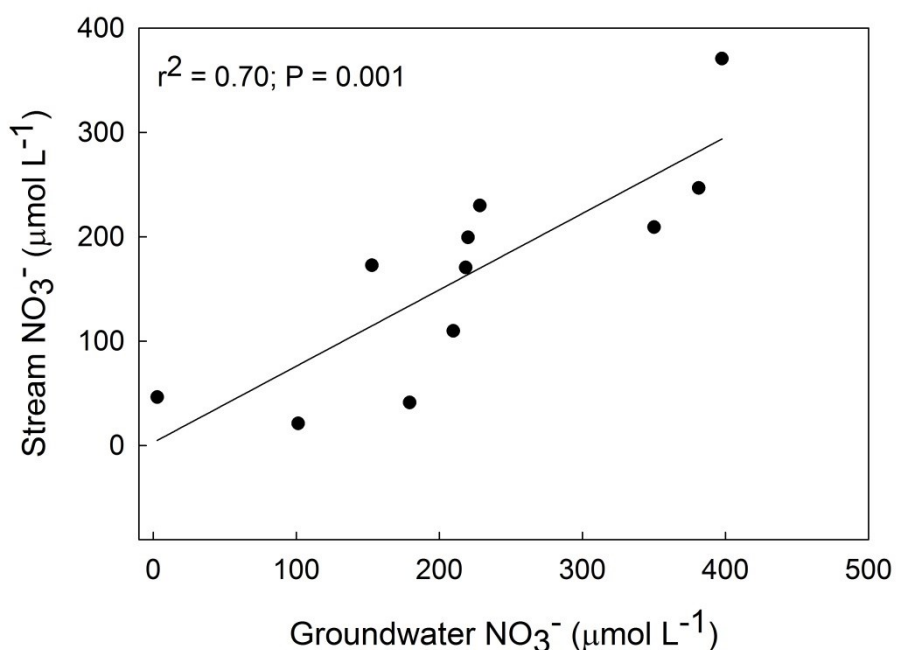


Figure 11. Linear regression between stream NO₃⁻ and reach averaged groundwater NO₃⁻ concentration from all BC reaches.

Table 4. Average daily k_{600} (m day^{-1}) estimated from Ar data and the three ^{222}Rn calculation methods as well as the percent difference.

Date	Ar method	Method 1 (raw ^{222}Rn)	Method 2 (smooth ^{222}Rn)	Method 3 (^{222}Rn balance)	% diff method 1 to 2	% diff method 1 to 3	% diff method 2 to 3
9/25/12	1.29	1.47	1.42	1.32	3.5	9.8	6.5
11/20/12	0.08	2.50	2.28	2.50	8.5	0.0	-9.4
2/18/12	1.95	2.27	2.12	2.43	6.5	-6.9	-14.3
4/15/13	2.92	4.56	4.44	3.54	2.7	22.4	20.3
7/17/13	10.7	10.9	9.49	10.1	13.1	7.5	-6.5
2/25/12	1.34	1.32	1.30	1.27	1.5	3.9	2.4
5/14/13	3.35	3.35	3.36	3.01	-0.3	10.2	10.5
7/9/13	12.9	11.4	10.71	10.8	6.3	5.6	-0.7
3/4/12	1.33	2.09	2.22	2.25	-6.0	-7.5	-1.4
5/6/13	1.07	1.31	1.29	1.33	1.7	-1.2	-2.9
6/25/13	1.97	3.11	2.83	2.60	9.1	16.5	8.1
12/13/12	0.67	1.09	0.88	0.95	19.3	12.4	-8.5
11/15/12	2.17	0.89	1.44	1.10	-61.3	-22.9	23.8

Table 5. Output from uncertainty analysis of gas exchange velocity including mean k, standard deviation in parentheses, and the 95% confidence interval

Date	Ar method	95% CI	Method 1 (raw ^{222}Rn)	95% CI	Method 2 (smooth ^{222}Rn)	95% CI	Method 3 (^{222}Rn balance)	95% CI
9/25/12	1.07 (0.14)	0.01	2.53 (0.82)	0.05	1.44 (0.55)	0.03	1.34 (0.50)	0.03
11/20/12	0.05 (0.75)	0.05	3.78 (0.87)	0.05	2.27 (0.49)	0.03	2.49 (0.37)	0.02
2/18/12	2.05 (1.13)	0.07	4.61 (1.29)	0.08	2.22 (0.57)	0.04	2.44 (0.41)	0.03
4/15/13	1.83 (1.42)	0.09	5.96 (1.13)	0.07	4.38 (0.84)	0.05	3.55 (0.75)	0.05
7/17/13	10.9 (6.87)	0.43	12.7 (2.01)	0.12	9.54 (1.64)	0.10	10.2 (1.46)	0.09
2/25/12	1.32 (0.27)	0.02	3.38 (1.40)	0.09	1.33 (0.97)	0.06	1.31 (0.92)	0.06
5/14/13	2.58 (0.65)	0.04	4.82 (1.52)	0.09	3.41 (1.29)	0.08	3.04 (1.24)	0.08
7/9/13	27.1 (105)	6.56	12.6 (10.9)	0.68	10.6 (4.98)	0.31	10.6 (5.0)	0.31
3/4/12	0.60 (0.44)	0.03	3.51 (0.89)	0.06	2.20 (0.52)	0.03	2.25 (0.39)	0.02
5/6/13	8.15 (244)	15.2	2.16 (0.67)	0.04	1.32 (0.52)	0.03	1.35 (0.49)	0.03
6/25/13	1.91 (0.36)	0.02	3.58 (0.66)	0.04	2.84 (0.58)	0.04	2.6 (0.51)	0.03
12/13/12	0.65 (0.62)	0.04	1.25 (0.49)	0.03	0.90 (0.47)	0.03	0.97 (0.46)	0.03
11/15/12	1.46 (0.79)	0.05	1.61 (0.37)	0.02	0.88 (0.32)	0.02	1.09 (0.30)	0.02

N₂ and N₂O Production

P_T (total production) of N₂ ranged from -0.59 to 13.96, P_{st} (in-stream) from -2.17 to 7.05, and P_{gw} (groundwater) from 0.38 to 6.91 mmol N m⁻² m hr⁻¹. P_{gw} of N₂ accounted for 38-100% of the total N₂ production. In five of the thirteen studies, negative P_{st} of N₂ was calculated suggesting N fixation. Due to high dissolved inorganic nitrogen (DIN), fixation is unlikely at these sites, and we provide alternative explanations in the discussion. However, all data is presented as calculated (Table 6). The one negative P_T rate is from a reach in the forested watershed confirming the open channel method is not suited to streams with low N concentrations and presumably denitrification rates. In BC reaches, P_T and P_{st} of N₂ were positively related to mean daily stream temperature ($r^2=0.42$, $P=0.03$ and $r^2=0.49$, $P=0.015$ respectively, Figure 12) as well as the mean stream stage during the week prior to the study ($r^2=0.81$, $P=0.0001$ and $r^2=0.60$, $P=0.005$ respectively, Figure 12), which will be referred to as the antecedent stream depth (ASD). Correlations with discharge were also found, but stream stage correlations were stronger, likely a result of direct monitoring of stage as opposed to discharge that depends on rating curves. No significant correlations were found between P_T or P_{st} and other physiochemical data such as NO₃⁻ concentration or streamflow during the study. P_{gw} of N₂ was also positively related to ASD ($r^2=0.69$, $P=0.0014$).

Table 6. Total, in-stream, and groundwater N₂ and N₂O production rates as well as N₂O emissions. All N₂ rates are in mmol N m⁻² hr⁻¹ and all N₂O rates are in μmol N m⁻² hr⁻¹.

Date	Site	Total N ₂	In-stream N ₂	Ground-water N ₂	Total N ₂ O	In-stream N ₂ O	Ground-water N ₂ O	N ₂ O emissions
9/25/12	BC	1.81	0.41	1.40	25.7	21.0	4.69	22.9
11/20/12	BC	6.43	2.45	3.98	44.0	41.8	2.17	34.7
2/18/12	BC	3.05	-1.24*	4.29**	16.8	14.3	2.55	13.8
4/15/13	BC	7.81	1.93	5.88	37.8	33.5	4.34	34.0
7/17/13	BC	14.0	7.05	6.91	231	220	10.8	211
2/25/12	BC2	1.07	-1.58*	2.65**	2.79	2.78	0.01	2.23
5/14/13	BC2	2.20	-1.51*	3.71**	25.5	24.6	0.90	24.3
7/9/13	BC2	8.15	4.77	3.38	173	171	1.94	169
3/4/12	BC3	5.53	0.76	4.77	26.3	17.5	8.80	21.2
5/6/13	BC3	3.02	-2.17*	5.20**	30.5	22.9	7.57	22.9
6/25/13	BC3	7.14	1.40	5.74	105	93.5	11.5	78.2
12/13/12	SF	1.09	0.71	0.38	5.69	5.68	0.01	3.93
11/15/12	MH	-0.59	-1.07*	0.48**	-0.015	-0.001	-0.014	-0.14

*negative N₂ Pst rates should be interpreted as unmeasurable with this method or zero

**If N₂ Pst is negative, N₂gw should be interpreted as equal to PT rather than greater than PT due to apparent in-stream N fixation

N₂O fluxes were highly variable over time. P_T, P_{st}, and emissions of N₂O to the atmosphere were similar in magnitude on each day for all sites, indicating most of the N₂O was produced in-stream and was rapidly lost to the atmosphere. The MH forested site was the only stream undersaturated with respect to N₂O, making it a small N₂O sink (-0.137 μmol N m⁻² hr⁻¹). P_T of N₂O in the BC and SF sites ranged from 2.8 to 230 μmol N m⁻² hr⁻¹ and averaged 55.7 across all dates and sites. Most (66.5-99.6%) of the total N₂O accumulation was a result of in-stream production (2.78 to 220 μmol N m⁻² hr⁻¹) with the remaining portion from groundwater (0.008 to 10.82 μmol N m⁻² hr⁻¹). Using data only from the three BC reaches, N₂O emissions were exponentially related to mean daily stream temperature ($r^2 = 0.85$, $P < 0.0001$, Figure 12) and linearly related to ASD ($r^2 = 0.60$, $P < 0.0052$, Figure 12).

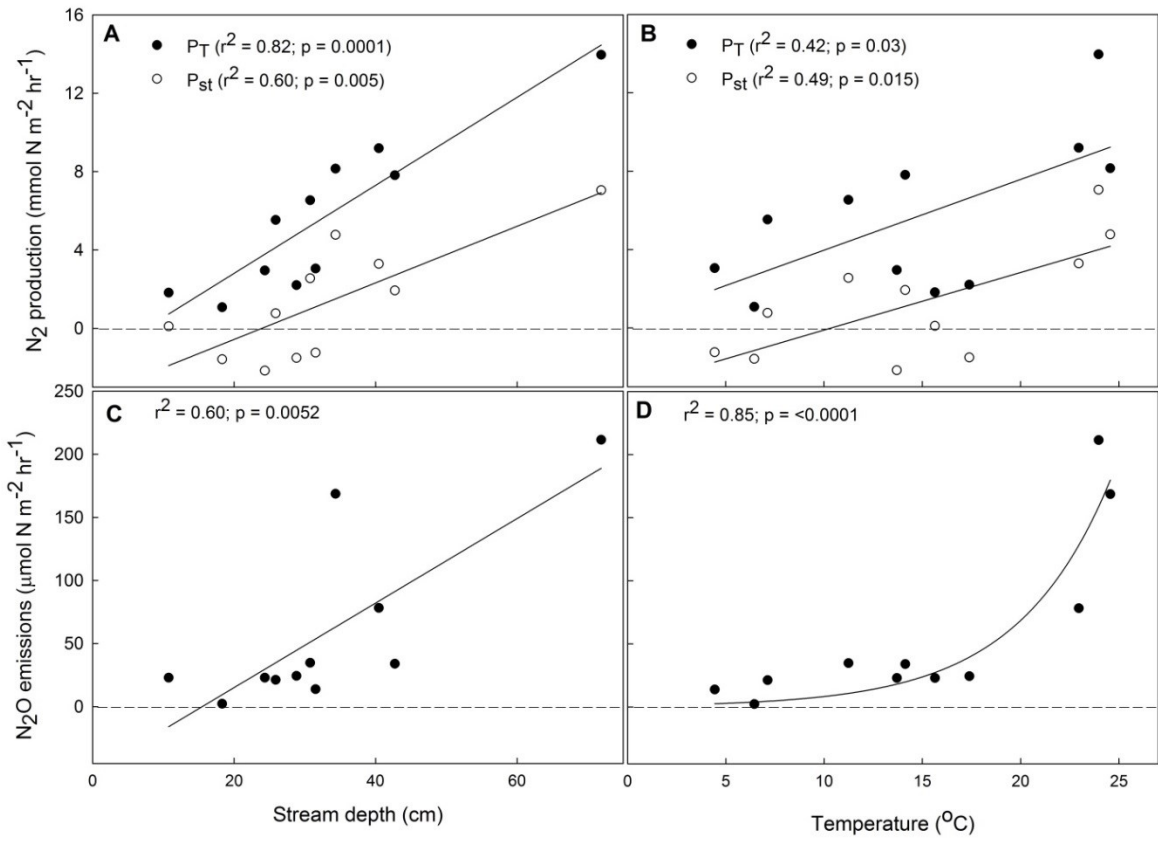


Figure 12. Relationships between antecedent stream depth (ASD), or the mean depth a week prior to each study, and temperature with N₂O emissions, total N₂ production (P_T), and in-stream N₂ production (P_{st}).

Discussion

²²²Rn and Gas Exchange Velocity

²²²Rn is a valuable tracer in hydrology and a promising method for estimating *k* in gaining streams. There are variety of applications for ²²²Rn including groundwater discharge into coastal waters (Cable et al. 1996; Burnett and Dulaiova 2003; Dulaiova et al. 2010), lakes (Dimova and Burnett 2011), and rivers (Ellins et al. 1990; Genereux et al. 1993; Lee and Hollyday 1993; Cook et al. 2003; Knee and

Jordan 2013). Specific applications include hyporheic residence time (Lamontage and Cook 2007), groundwater recharge dynamics (Savoy et al. 2011), and baseflow separation (Kies et al. 2005). ^{222}Rn has been sparsely used to calculate k in streams and radium (Ra) cannot be used since it is not soluble in freshwater, but there is a long history of $^{222}\text{Rn}/\text{Ra}$ isotope based k measurements in the open ocean (Peng et al. 1979; Smethie et al. 1985). Wanninkhof (1990) did use a combined ^{222}Rn and SF₆ method to simultaneously estimate groundwater discharge and k in a first order stream. The ^{222}Rn method first outlined in Knee et al. (in prep) and applied in this study is a relatively simple method in all aspects; field, lab, and calculations. However, this has only been tested in gaining head water streams which are likely the most appropriate systems.

The fact that several calculation methods yielded approximately the same mean daily k_{600} supports the validity of our k calculations and may make our methods applicable to a wider range of situations in the field. For example, method 3 (reach mass balance) does not rely on repeated measurements of stream ^{222}Rn and may be applied by taking grab samples instead of continuous monitoring. Gas exchange velocity estimated from this method did not vary greatly over time (Figure 9). Therefore, it may be feasible to rapidly estimate k for many streams with one stream sample, several groundwater samples, and knowledge of ground and surface water discharge. Method 1 (unsmoothed ^{222}Rn) is useful for its simplicity, but can only be used to estimate an average k_{600} with at least several hours of continuous surface water measurements. ^{222}Rn activity in streams is inherently noisy, which results in negative and positive k values when using an iterative open channel

calculation, but approximately the same average daily k_{600} as the other methods. Method 2 (smoothed ^{222}Rn) is useful because it eliminates noise and negative k values and may provide insight into the temporal variation in k . Stream ^{222}Rn activity generally decreased over the day (Figure 2). Decreasing ^{222}Rn activity could be due to variation in groundwater inputs or gas exchange velocity. If the rate of groundwater discharge and groundwater ^{222}Rn activity are truly constant over the 6-8 hour study period as this method assumes, then the variation in stream ^{222}Rn implies variability in k .

Evaluating whether variability in stream ^{222}Rn activity is a result of physical mechanisms of gas exchange, such as stream turbulence, velocity, temperature and wind speed, is beyond the scope of the study. But if such variability does exist, it would have implications for open channel studies. Typically, k is scaled by temperature using Schmidt number scaling (Wanninkhof 1992) or a temperature correction as in Thomann and Mueller (1987). Schmidt number scaling predicted an increase in k during the day as the streams warmed up, and this agreed with the general decrease in ^{222}Rn activity. However, during several studies ^{222}Rn increased (k decreased) or oscillated indicating there could be short-term variability in k and that it may not always scale with temperature (Figure 2).

^{222}Rn was a more reliable method of estimating k compared to Ar at our study sites. Although k estimated from the two tracers was not significantly different across all dates, k_{Ar} was generally lower, had large uncertainties, and on one occasion calculated a value orders of magnitude below than the lowest k_{Rn} measurement. The analytical error associated with Ar (+/- 0.1%) as well as the spatial variation in

groundwater Ar concentration (SD= 5.8% of value on average) was much lower than ^{222}Rn (SD=26% of value on average, Table 2); yet, the uncertainty in $k\text{Ar}$ (95% CI = +/- 1.73) was greater than $k\text{Rn}$ on average (95% CI = +/- 0.06-0.11, Table 5). Error in equilibrium Ar concentration due to temperature measurement error was not even considered in the uncertainty analysis. When this additional error term is accounted for, error in $k\text{Ar}$ is greatly inflated.

Estimating $k\text{Ar}$ involves measuring extremely small deviations in Ar from theoretical equilibrium, and therefore requires high analytical precision and accuracy in Ar measurements, temperature, pressure as well as relatively homogenous groundwater Ar concentrations if the study reach is highly gaining. Uncertainty in $k\text{Ar}$ was generally higher during days when Ar concentrations showed little deviation from equilibrium. This method is most applicable when Ar is highly supersaturated due to large diel temperature swings and/or groundwater flux is low. The ^{222}Rn method requires less analytical precision given the large difference between stream and groundwater ^{222}Rn activities, and the theoretical equilibrium is always zero eliminating temperature and pressure measurement error. Uncertainty is driven by analytical error and the spatial variability in groundwater ^{222}Rn concentrations, which can be assessed through sampling.

Argon Modeling

Generally, modeled Ar agreed with measured Ar concentrations (within 0-1.7%) providing confidence in the open channel model and measured terms. There was only one individual measurement beyond this range where modeled Ar was 2.4% lower than the measured concentration. We have no means of evaluating what is an

acceptable level of error since open channel modeling of Ar has not been quantitatively assessed, but this amount of error is comparable with data from Laursen and Seitzinger (2002). Modeled Ar fell both above (15.4% of studies) and below (30.8%) measured Ar, but a majority of the cases were a good fit (53.8%) (Figure 4). Studies that were not a great fit indicate error in the most uncertain terms: groundwater discharge, mean groundwater Ar concentration, and k .

Analytical precision in Ar is high (+/- 0.1%) using MIMS; however, we did introduce a slight bias by using one standard calibration at the mean stream temperature during each study. Therefore, there could be a trivial overestimation of Ar concentration for stream samples that were above the mean temperature and underestimation when below the mean temperature (Kana et al. 1994). Three point standard curves were developed for most of the MIMS runs, but not all, and data recalculated from standard curves showed there was a slight temperature bias that could help explain cases where modeled Ar fell below measured. Since we were not able to develop standard curves for all dates, we used the one-standard calibration to be consistent across all studies.

N₂ Production

The N₂ production results demonstrate that the open channel method can be applied in streams with high groundwater N₂ concentration and seepage rates. Furthermore, the delivery rate of biogenic N₂ from groundwater, as well as in-stream N₂ production, can be quantified simultaneously. In-stream denitrification rates were comparable with other open channel studies which have ranged from 0-15.9 mmol N m⁻² m hr⁻¹ (Baulch et al. 2010) compared to our range of 0-7.1 and mean of 2.9 mmol

$\text{N m}^{-2} \text{ m hr}^{-1}$, after omitting negative rates which are explained below. Despite being highly impacted, denitrification in the BC reaches was similar to rivers known to have high rates such as the South Platte in Colorado (Sjodin et al. 1997; Pribly et al. 2005).

However, our ability to detect P_{st} (in-stream production) of N_2 was often inhibited by the groundwater inputs and large diel temperature swings, resulting in apparent N fixation. The high excess, or biogenic, N_2 concentrations observed at the BC sites are typical of groundwater in agricultural areas within the Choptank Basin (Fisher et al. 2010; Fox et al. 2014). In addition to excess biogenic N_2 , groundwater introduces excess physical N_2 into the stream due to the seasonal asymmetry of groundwater recharge under cool conditions (Fisher et al. 2010). Diel stream temperature variation can also add excess physical N_2 gas due to the lag between theoretical equilibrium and actual re-equilibration of measured N_2 . This combination of high groundwater N_2 , high seepage rates, and diel temperature swings can at times overwhelm the ability of the open channel method to detect biogenic N_2 accumulation from in-stream sources.

Negative P_{st} of N_2 was calculated during the winter and spring under these conditions in 4 of the 12 studies in agricultural streams. These could be interpreted as N fixation, but are more likely zero or below the detection limit of open channel methods. Other studies have reported P_{st} of N_2 rates of 0 (Pribyl et al. 2005) or as low as $\sim 0.03 \text{ mmol m}^{-2} \text{ hr}^{-1}$ (McCutchan and Lewis 2008) during winter months in Colorado, but in reaches with less groundwater input.

Additional source of uncertainty that could affect in-stream and total N_2 production rates include error in groundwater discharge, ebullition, and excess air.

Groundwater flux could be overestimated due to incomplete recovery of Br⁻ at the downstream site (Payn et al. 2009), which would generally increase P_{st}. Methane ebullition can rapidly strip N₂ and other dissolved gases (e.g. Ar, O₂, and ²²²Rn) from pore water. The ebullitive flux of N₂ was estimated to be 6-16% of the total diffusive N₂ flux from one section of the South Platte River (Higgins et al. 2008). However, only one groundwater sample had evidence of ebullition during this study suggesting ebullition had little effect on estimated production rates. Excess air artificially increases dissolved gas concentrations in groundwater due to bubble dissolution under high hydrostatic pressure (Heaton and Vogel 1981). Noble gas sampling conducted prior to this study estimated that excess air was a small portion (~5%) of the excess N₂ signal within the BC watershed (Fisher and Hamme, in prep).

Our data support the hypothesis that agricultural streams are hot spots for biogenic N gases. N₂ and N₂O accumulated in the stream network as a result of instream and terrestrial biogeochemical processes occurring across the watershed, most likely the riparian zone. In the BC watershed, P_{gw} of N₂ accounted for 41 to 100% (mean 81%) of the P_T assuming P_{gw} = P_T when P_{st} is negative. The importance of P_{gw} in the BC watershed may be especially great as a result of the extensive channelization that drains groundwater by design. In contrast, the SF reach had comparatively low rate of groundwater discharge, low excess N₂, and the study reach was not channelized; however, P_{gw} still accounted for 38% of P_T during one study in December 2012. Emergence of groundwater enriched with biogenic N₂ may be an important unaccounted for loss term in watershed nitrogen budgets in headwater regions impacted by anthropogenic N inputs.

Controls of N₂ Production

Within the BC stream network, physical processes of temperature and stream stage fluctuations appear to be dominant controls of P_{st} and P_T of N₂. These streams have a constant supply of NO₃⁻ and DOC based on measured concentrations; however, denitrification can still be limited depending on the specific groundwater interactions within a patch of streambed. For example, denitrification could be inhibited by advection of high O₂ surface water through sediments or by the lack of DOC and NO₃⁻ delivery into low O₂ sediments (Hill et al. 2000; Pucket et al. 2008; Predick and Stanley 2010). In other words, the groundwater-surface water interactions are important for setting up the conditions necessary for denitrification (i.e. low O₂, high NO₃⁻, and high DOC). The BC reaches have similar physiochemical characteristics and are spatially proximate; therefore, it is not surprising that they would respond comparably to physical conditions.

Laboratory experiments have established that increasing the temperature can accelerate denitrification rates in soils and aquatic sediments under non limiting conditions (Standford et al. 1975; Hill 1983; Pfenning and McMahon 1996). Using the open channel method, McCutchan and Lewis (2008) found a positive relationship between temperature and P_{st} of N₂ in the South Platte River. The x-intercept of 10.3° C in the P_{st} of N₂ vs. temperature regression could be interpreted as a threshold temperature inhibiting in-stream denitrification (Figure 12). Saleh Lakha et al. (2009) showed that in pure bacterial cultures denitrification and denitrifying gene expression were slower at 10°C compared to higher temperatures. Optimal temperatures for denitrification in temperate marine systems were estimated at 26°C and 34°C during

winter and summer respectively by Canion et al. (2014). A more likely explanation is that the open channel method is unable to detect the presumably low P_{st} rates during the winter, or that this method is not suitable during high N₂ loading from groundwater as previously discussed. P_T was also significantly related to temperature; however, this was driven by the P_{st} component because P_{gw} and temperature were not significantly correlated ($r^2=0.19$ $p=0.18$). As expected, stream temperature should have no effect on biogenic N₂ delivered from groundwater.

The mechanism for the relationship between antecedent stream depth (ASD) and N₂ production is likely a function of groundwater-surface water interactions and the resulting biogeochemistry induced by stream stage fluctuations. O₂ dynamics in the hyporheic zone can be complicated by the mixing of multiple groundwater flow paths with varying O₂ signatures and high-O₂ surface water (Malard and Hervant 1999; O'connor et al 2012). During peak flow, hydraulic gradients can reverse (Gu et al. 2008), potentially injecting NO₃⁻, DOC, and O₂ rich surface water into stream sediments. During the recession limb, it has been observed that O₂ in stream sediments rapidly decreases as low O₂ groundwater becomes the dominant water source (Soulsby et al. 2009) in addition to increased heterotrophic metabolism stimulated by DOC. This combination of events creates ideal conditions for denitrification in stream sediments at some point along the recession limb of a storm hydrograph. A combined field and modeling study in the adjacent Virginia coastal plain, Gu et al. (2008) also concluded that storms could enhance NO₃⁻ removal due to the groundwater-surface water interactions described above.

Increasing P_{gw} of N_2 with antecedent stream depth (ASD) could simply be a function of higher groundwater discharge rates as a result of storm events occurring within the week prior to a given study, thus delivering more biogenic N_2 . Enhanced riparian denitrification could also contribute to the observed P_{gw} -ASD correlation. Several studies have shown that riparian denitrification can be stimulated during or immediately following storms (Ocampo et al. 2006, Gu et al. 2008; Gu et al. 2012; Roley et al. 2012). Ocampo et al. (2006) concluded control of NO_3^- can shift from hydrologic to biogeochemical control during an event on a hill slope where transport time is long relative to reaction time facilitating denitrification (i.e. low gradient slopes such as those on the coastal plain). Gu et al. (2012) also found stream stage fluctuations induced denitrification hot moments in the riparian zone. The authors called this the “Bank Storage Hot Moment” and through a modeling exercise discovered these hot moments were a significant sink for stream NO_3^- on an annual time scale. Riparian zones are well known to be hotspots for denitrification due to the typically high DOC and low O_2 environment (Lowrance et al. 1997; Hill et al. 2000; Vidon et al. 2010), and shifting hydraulic gradients can increase subsurface flow residence time in riparian areas enhancing the opportunity for denitrification. Furthermore, Roley et al. (2012) observed increased floodplain denitrification in response to inundation events in a two-stage agricultural ditch not unlike the BC and BC3 reaches. It is possible that in addition to in-stream denitrification, riparian denitrification was also enhanced at our study sites during baseflow recession when increased residence time of riparian water (Gu et al. 2008) coincided with high concentrations of NO_3^- and DOC under low oxygen conditions. This can be described

as a “baseflow recession hot moment” of biogenic N₂ accumulation in streams from *in-situ* and groundwater processes.

N₂O Emissions

N₂O production and emissions to the atmosphere from BC stream reaches were relatively high but comparable to the literature from both small and large riverine systems. Mean emission rates in streams and rivers impacted by anthropogenic inputs have ranged from 0.92 (Stow et al. 2005) to 43 $\mu\text{mol N m}^{-2} \text{ h}^{-1}$ (Harrison et al. 2005), with the maximum ranging from 4.6 to 175 $\mu\text{mol N m}^{-2} \text{ h}^{-1}$. Excluding the MH forested site, the mean N₂O emission rate at agricultural sites was 53.2 with a maximum of 211 $\mu\text{mol N m}^{-2} \text{ h}^{-1}$. Rates from the BC streams are higher than studies conducted downstream of wastewater treatment plants (Hemond and Duran 1989; McMahon and Dennehy 1999), but an order of magnitude lower than one study of agricultural streams in Japan that estimated a mean flux of 531 $\mu\text{mol N m}^{-2} \text{ h}^{-1}$ (Hasegawa et al. 2000). Beaulieu et al. (2008) reviewed the literature and concluded that mean rates $> 35.7 \mu\text{mol N m}^{-2} \text{ h}^{-1}$ ($500 \mu\text{g N m}^{-2} \text{ h}^{-1}$) are uncommon and often a result of a point source. Tile drains are present upstream of the BC3 reach. However, none were active during field sampling, and we are not aware of any direct waste water inputs. Yet, we measured N₂O emissions higher than 35.7 on average. In contrast, the MH forest stream was consuming N₂O. N₂O undersaturation has been episodically observed in various streams and rivers (Hemond and Duran 1989; Stow et al. 2005; Beaulieu et al. 2008). Baulch et al. (2011) reported one stream in Ontario, Canada that was a consistent net sink. Streams acting as an N₂O sink are generally associated with low NO₃⁻ concentration, and Baulch et al. (2011) found the

threshold NO_3^- concentration between source and occasional sink to be 2.7 μM . Undersaturation has also been associated with low flows and low O_2 concentration (Hemond and Duran, 1989; LaMontagne et al. 2003; Stow et al. 2005), which generally characterize the MH stream. If the N_2O emissions rates from the BC and MH sites are representative of headwater streams with high and low anthropogenic N inputs across the Delmarva Peninsula, then much of the region's streams have been transformed from a small sink or negligible term to a source of N_2O as land use has converted from forest to agriculture (Benitez and Fisher 2004).

Controls of N_2O Emissions

Like N_2 production, N_2O emissions were significantly related to temperature and ASD (Fig. 12c and d). Temperature was exponentially related to N_2O emissions in the BC reaches likely reflecting the effect temperature has on all terms in the flux equation (Eq. 9). Temperature increases N_2O concentration by enhancing rates of denitrification and nitrification, increases gas exchange velocity, as well as the N_2O concentration gradient by pushing down the temperature-dependent equilibrium concentration. By definition of the flux calculation, we would expect temperature to have a non-linear effect on N_2O emissions since multiplicative terms are increased. This may only be true in systems that are generally not limited by N or labile carbon so that N_2O is consistently produced through nitrification and denitrification depending on the redox conditions (low O_2 = denitrification, high O_2 = nitrification).

The relationship between ASD and N_2O emissions is weaker than ASD versus N_2 production, but is likely a result of a similar mechanism as described earlier. From a physical perspective, stream depth or discharge should impact N_2O emissions.

Wilcock et al. (2008) suggested stream hydraulics has a strong influence on N₂O emissions by affecting multiple variables in the flux equation. Gas exchange velocity often increases with stream flow and residence time of gases (and solutes) within the reach decreases. Therefore, during low flow gas exchange is minimal allowing more time for complete reduction of N₂O (and NO₃⁻), but emissions are amplified during high flows.

N₂O production is complicated by the competing factors regulating denitrification and nitrification and by variable N₂O yield from either process. Nitrification can be regulated by NH₄⁺, organic carbon, pH, temperature, and O₂ (Triska et al. 1990; Strauss et al. 2002; Stenstrom and Poduska 1980; Paul and Clark 1989), and its contribution to N₂O emissions in streams is relatively unknown. Often global models assume nitrification produces twice as much N₂O as denitrification (Mosier et al. 1998). This study was not designed to assess the role of nitrification and denitrification in N₂O emissions, but nitrification also may have been stimulated with stream stage fluctuations due to mobilization of NH₄⁺ during storms (Gardner and Fisher, in prep).

Groundwater and N₂O Emissions

Dissolved N₂O in groundwater was not an important source of N₂O emissions from streams in the BC watershed. Groundwater accounted for 0.19-41 % (13% on average) of N₂O emissions in the BC and SF reaches. This is likely an overestimate since we had to assume the N₂O measured in emerging groundwater was not reduced to N₂ prior to diffusing into the water column, and that all groundwater N₂O subsequently evaded into the atmosphere. There is some uncertainty in the P_{st} and P_{gw}

components of N₂O production attributed to the highly variable and under-sampled (3-5 piezometers per reach) groundwater N₂O concentrations. Despite variable groundwater concentrations, 95% confidence intervals of production rates were relatively narrow (Table 7). To produce the observed N₂O accumulation in surface water exclusively from a groundwater source, it would require a reach averaged groundwater N₂O concentration 1.5 to 60 fold greater than what was measured depending on the day (average of 12 fold greater). The average groundwater N₂O concentration across all studies required for groundwater to be the sole source was 1.82 µM, which was comparable with the highest recorded concentration in emerging groundwater of 2.1µM. The small contribution of dissolved N₂O in groundwater to emissions from streams was also supported by the relationship between in-stream N₂ and N₂O production compared to groundwater N₂ and N₂O production. Both were significantly correlated (Table 2). Linear regressions indicated that on average in-stream N₂O was 2.2% of N₂ production; however, groundwater N₂O was only 0.2% of N₂ production (Figure 13). In addition to greater N₂O production via in-stream nitrification, this may suggest denitrification leaks out more N₂O when it occurs in-stream sediments relative to the more consistently reducing groundwater environment.

Table 7. Means and 95% confidence intervals (CI) from the Monte Carlo uncertainty analysis of total, in-stream, and groundwater N₂ and N₂O production.

Date	N ₂ mmol N m ⁻² hr ⁻¹						N ₂ O μmol N m ⁻² hr ⁻¹					
	Total	CI	Stream	CI	Ground	CI	Total	CI	Stream	CI	Ground	CI
9/25/12	1.82	0.11	0.42	0.11	1.40	0.02	28.4	0.90	23.3	0.95	5.12	0.32
11/20/12	6.56	0.14	2.58	0.14	3.98	0.07	44.9	0.81	42.7	0.85	2.19	0.25
2/18/12	3.13	0.19	-1.22	0.19	4.35	0.09	16.9	0.51	14.5	0.55	2.36	0.25
4/15/13	7.84	0.17	1.98	0.17	5.86	0.10	38.0	0.56	33.7	0.62	4.39	0.29
7/17/13	13.9	0.34	6.92	0.28	6.96	0.26	228	2.45	217	2.53	11.1	0.80
2/25/12	1.30	0.24	-1.37	0.24	2.66	0.03	2.96	0.16	2.95	0.16	0.01	0.01
5/14/13	2.43	0.26	-1.30	0.26	3.73	0.08	26.18	0.74	25.3	0.74	0.94	0.05
7/9/13	7.70	0.79	4.43	0.79	3.27	0.10	168	9.83	165	9.83	2.55	0.33
3/4/12	5.53	0.17	0.81	0.18	4.72	0.07	26.4	0.58	17.4	1.06	8.96	0.87
5/6/13	2.98	0.09	-2.23	0.09	5.21	0.05	30.6	0.75	22.9	1.14	7.66	0.84
6/25/13	7.12	0.14	1.33	0.16	5.79	0.08	89.4	1.22	78.7	1.67	10.7	1.13
12/13/12	1.09	0.05	0.71	0.05	0.38	0.03	4.78	0.13	4.77	0.13	0.01	0.00
11/15/12	-0.62	0.03	-1.08	0.05	0.46	0.06	-0.05	0.01	0.06	0.01	-0.12	0.00

*negative stream N₂ rates should be interpreted as unmeasurable with this method or zero

**If in-stream production is negative, delivery from groundwater should be interpreted as equal to total production.

It is possible we did not representatively sample emerging groundwater and missed N₂O hotspots. Measured concentrations and variances did fall within the range of previous studies in groundwater below or near agricultural streams (Werner et al. 2010; Fox et al. 2014), but mean concentrations were on the lower end compared to uplands as has been noted in other studies where groundwater N₂O concentrations generally decrease from field to stream (Vilain et al. 2011; Fox et al. 2013).

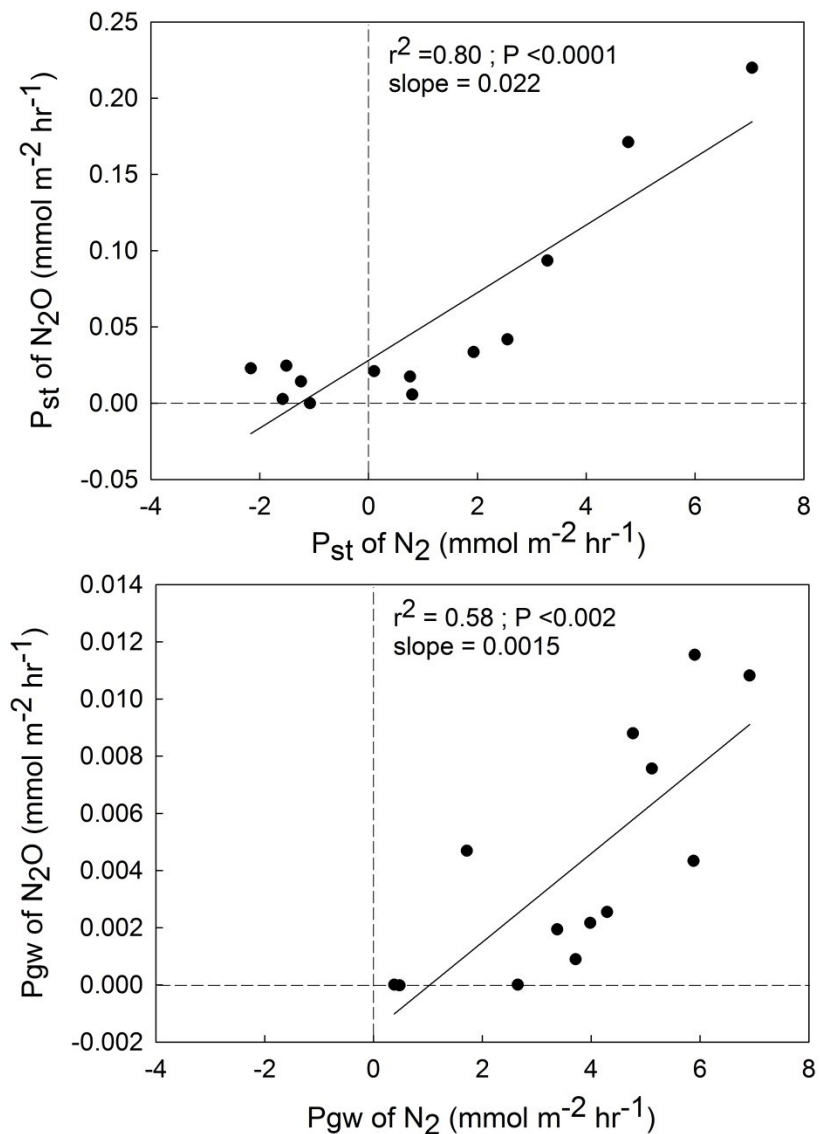


Figure 13. Linear regressions of N_2O versus N_2 production in-stream P_{st} (top) and groundwater P_{gw} (bottom). The slopes indicate the average ratio of $N_2O:N_2$ produced which is an order of magnitude higher in streams compared to groundwater.

The variability in groundwater chemistry was indicative of combined flowpaths and biogeochemical processing, and may suggest NO_3^- and N_2O sources. Groundwater samples high in NO_3^- and N_2O likely represented deeper flow paths that bypassed the riparian zone, maintained oxic conditions, encountered less opportunity for denitrification, thus the NO_3^- remains largely unreduced. In such flowpaths, the

N_2O source has been attributed to soil nitrification following flushing of N_2O into the aquifer. This process has been suggested by various studies (Ueda 1993; Hiscock 2003; Werner 2010; Vilain 2012) and is often supported by the linear relationship between groundwater NO_3^- and N_2O concentrations as was observed in this study (Figure 6a). Lower O_2 samples with high excess N_2 and low NO_3^- likely passed through reducing conditions associated with riparian areas or saturated depressions within the watershed. O_2 concentrations were highly variable, but there was a significant difference ($P<0.05$) in mean O_2 when separating the data into low and high NO_3^- groups as defined by the 50 μM threshold for denitrification (Seitzinger 1988; Golterman et al. 2004). Interestingly, mean O_2 from the high and low NO_3^- groups were 61 and 27 μM respectively, a range that straddles the O_2 threshold for denitrification of 31 μM (Pina-Ochoa and Alvarez-Cobelas, 2006). Most of the samples did not fit cleanly into the reducing versus less reducing flowpath paradigm since emerging groundwater often reflects a combination of flowpaths (Figure 14). As a result, there were no significant correlations among all data between O_2 , $\text{xsN}_2\text{-N}$, and NO_3^- . Excess $\text{N}_2\text{-N}$ sampled from in-stream piezometers was almost uniformly high (mean=305 μM ; SD=118) in the BC watershed suggesting denitrification was occurring to some degree in nearly all groundwater flowpaths.

N_2O Emission Factors

Indirect emission factors from streams and groundwater (i.e.EF5-g) are used to estimate global emissions of N_2O as a result of leached N, largely in the form of NO_3^- . There has been some controversy in the EF5-g value which has been reduced from 1.5% to the current value of 0.25%, which represents to proportion of leached N

that is emitted to the atmosphere as N₂O. Indirect emission factors from rivers (EF5-r), estuaries (EF5-e), and streams and groundwater (EF5-g) currently have the same value (0.25%), and it is assumed that N₂O in streams is derived from groundwater. The IPCC methodology estimates EF5-g from the ratio of dissolved N₂O to NO₃⁻.

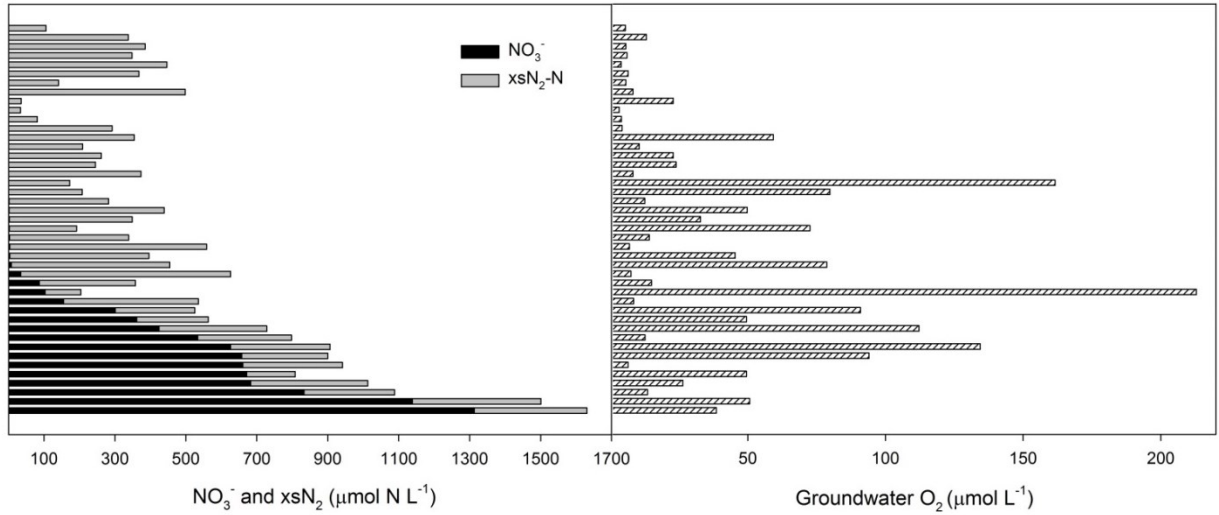


Figure 14. NO₃⁻, xsN₂-N, and O₂ concentrations in groundwater sampled from in-stream piezometers in the BC watershed. Each bar represents one individual piezometer sample.

We compared this simple ratio to an alternative method for streams and groundwater. In streams, Beaulieu et al. (2008) estimated emission factors using the N₂O-N concentration in excess of atmospheric equilibrium (xsN₂O-N) divided by NO₃⁻. For groundwater, Well et al. (2005) included excess N gases in the denominator to represent the reactivity of NO₃⁻ along groundwater flow paths as follows.

$$EF5g = \frac{xsN_2O \cdot N}{xsN_2O \cdot N + xsN_2 \cdot N + NO_3 \cdot N} \quad (\text{Eq. 10})$$

Alternative methods for estimating emission factors (EF5-g) from streams (Beaulieu et al. 2008) and groundwater (Well et al. 2005) may provide more realistic

values compared to a simple N₂O-N:NO₃⁻ ratio. For streams, the simple ratio and equilibrium corrected ratio (Beaulieu et al. 2008) estimated average emission factors similar to the current EF5-g (0.25%), which were 0.32% and 0.29% respectively. The Beaulieu et al. (2008) method only slightly decreased the EF5-g in streams that have high N concentrations, but this correction becomes very important in low NO₃⁻ streams. For example, in the MH stream the EF5-g according to the simple ratio was 3.86%, but after adjusting it for atmospheric equilibrium it was -0.46%, which better represented the fact that MH was a N₂O sink. Estimates of EF5-g from streams have varied widely in time and space (Beaulieu et al. 2008) as they have in this study (-0.45 to 0.95%, using the equilibrium corrected method), but there seems to be growing support for the current value of 0.25%.

In groundwater the simple ratio estimated unreasonably high EF5-g values (mean = 13.6%, range = 0.002-390%). This method does not incorporate reactions along flow paths. A more logical approach of Well et al. (2005) better reflects the definition of an emission factor by taking into account total N inputs in the denominator assuming that excess N₂-N and N₂O-N are a result of reduced NO₃⁻ inputs. However, it still must be assumed that this N₂O eventually evades into the atmosphere. Using this approach, our results suggested a lower EF5-g for groundwater (mean = 0.057%, range = -0.059 to 0.59%) compared to streams and with a more constrained range relative to the IPCC method. Emission factors in groundwater are often variable, and this range is comparable to that (0.043-0.44%) reported by Weyman et al. (2008) using the same method. It is not surprising that the average EF5-g from emerging groundwater is lower than 0.25% considering this

water has nearly completed its groundwater residence time thus was more likely to undergo reduction. Vilain et al. (2012) found higher emission factors, which agreed with the 0.25% value, for upland areas compared to low lands.

Weyman et al. (2009) demonstrated that groundwater N₂O contributes negligibly to the flux of N₂O to the atmosphere from surface soils, and we found that groundwater N₂O makes up a small portion of N₂O emissions (13% on average) from highly gaining agricultural streams. N₂O was largely produced in-stream yet the IPCC's estimate of global N₂O emissions is predicated on the assumption that groundwater is the dominant N₂O source in small streams and that in-stream production is the dominant N₂O source for large rivers. The probability that N₂O in groundwater will reach the atmosphere may be low, given that it is often found in deeper flow paths, has a long tortuous pathway to the surface, is reactive in anoxic environments and may be largely reduced prior to emerging in surface water. These results and concepts suggest that 1) small streams and large rivers could be grouped together, instead of streams and groundwater, under the current EF5-r of 0.25%, and 2) EF5-g could represent just groundwater with a lower value than 0.25%, but this would require wider assessment to justify another decrease in the groundwater emissions factor.

Conclusions

- This study demonstrated the one-station open channel method can be reduced to 6 hours and used to simultaneously quantify biogenic N₂ and N₂O production from in-stream and groundwater sources. Biogenic N₂ from groundwater accounted for 38-100% of the total N₂ production in

agricultural headwater streams and could be an important term loss term of watershed N budgets in coastal plain headwater areas. In-stream denitrification rates during summer months were comparable to some of the highest previously reported rates (Laursen and Seitzinger 2004). However, in-stream denitrification was undetectable with this method during late winter months largely due to increased N₂ loading from groundwater.

- Antecedent stream depth and temperature were significant controls of N₂ and N₂O production in the BC stream reaches. Antecedent stream depth is a control over small time scales that reflects hot moments occurring in stream sediments and riparian zones during baseflow recession induced by high flow events (Gu et al. 2012). Warmer temperatures accelerate microbial processes controlling rates over a seasonal time scale.
- N₂O was largely produced in-stream while groundwater influx was not an important source. N₂O emissions were relatively high in the agricultural streams, but with strong seasonality. One study conducted in a low nutrient stream draining a forested watershed suggested this reach was a N₂O sink.
- Our data supported the emission factor of 0.25% for streams (EFg-5); however, it suggests streams and rivers could be grouped together and groundwater could have its own emission factor (EFg-5) that is lower than 0.25%. (i.e. ~0.06%). Also, alternative methods for calculating EF5-g (i.e.

Beaulieu et al. 2008 and Well et al. 2005), may provide more realistic values compared to a N₂O-N to NO₃⁻ ratio.

- ²²²Rn may provide a relatively simple and reliable method of empirically estimating gas exchange velocity in gaining streams.
- This study leads to many questions regarding N₂ and N₂O production in stream networks as well as gas exchange velocity. Is biogenic N₂ from emerging groundwater an important loss term in N budgets from watersheds of various sizes and properties? How do in-stream, groundwater, and total N₂ production scale across the stream network and are they related to watershed and/or channel properties? How can the open channel, or other reach scale methods, be improved to facilitate such studies? What is the role of emerging groundwater to the emissions of N₂O, or other biogenic greenhouse gases (CH₄ and CO₂), from streams and rivers? Is the short-term temporal variability in stream ²²²Rn activity driven by mechanisms of gas exchange or other factors?
- More reach scale studies are needed to identify controls of N₂ and N₂O production and emissions and to enable scaling over larger areas. Advancements in open channel methods as well as techniques for measuring and scaling gas exchange velocity in lotic systems could greatly assist such efforts.

References

- Andersen JM (1977) Rates of denitrification of undisturbed sediment from six lakes as a function of nitrate concentration, oxygen and temperature. *Archives Hydrobiology* 80:147-159.
- Baulch HM, Schiff SL, Maranger R, Dillon PJ (2011) Nitrogen enrichment and the emission of nitrous oxide from streams. *Global Biogeochemical Cycles* GB004047.
- Baulch HM, Venkiteswaran JJ, Dillon PJ, Maranger R (2010) Revisiting the application of open-channel estimates of denitrification. *Limnology and Oceanography: Methods* 8:4–6.
- Beaulieu JJ, Arango CP, Hamilton SK, Tank JL (2008) The production and emission of nitrous oxide from headwater streams in the Midwestern United States. *Global Change Biology* 14:878–894.
- Beaulieu JJ, Tank JL, Hamilton SK, et al. (2011) Nitrous oxide emission from denitrification in stream and river networks. *Proceedings of the National Academy of Sciences of the United States of America* 108:214–9.
- Benitez JA, Fisher TR (2004) Historical land-cover conversion (1665-1820) in the Choptank watershed, eastern United States. *Ecosystems* 7:219–232.
- Bohlke JK, Denver JM (1995) Combined use of groundwater dating, chemical, and isotopic analyses to resolve the history and fate of nitrate contamination in two agricultural watersheds, Atlantic coastal plain, Maryland. *Water Resources Research* 31:2319–2339.
- Burnett WC, Dulaiova H (2003) Estimating the dynamics of groundwater input into the coastal zone via continuous radon-222 measurements. *Journal of Environmental Radioactivity* 69:21–35.
- Cable JE, Bugna GC, Burnett WC, Chanton JP (2014) Application of ^{222}Rn of and CH^4 for assessment of groundwater discharge to the coastal ocean. *Limnology and Oceanography* 41:1347–1353.
- Canion A, Kostka JE, Gihring TM, et al. (2014) Temperature response of denitrification and anammox reveals the adaptation of microbial communities to in situ temperatures in permeable marine sediments that span 50° in latitude. *Biogeosciences* 11:309–320.

Colt J (1984) Computation of dissolved gas concentrations in water as functions of temperature, salinity, and pressure. Special publication No. 14 of the American Fisheries Society.

Cook PG, Favreau G, Dighton JC, Tickell S (2003) Determining natural groundwater influx to a tropical river using radon, chlorofluorocarbons and ionic environmental tracers. *Journal of Hydrology* 277:74–88.

Davidson EA, Seitzinger S (2006) The enigma of progress in denitrification research. *Ecological applications: a publication of the Ecological Society of America* 16:2057–63.

Diaz RJ (2001) Overview of hypoxia around the world. *Journal of Environmental Quality* 30:275–81.

Diaz RJ, Rosenberg R (2008) Spreading Dead Zones and Consequences for Marine Ecosystems. *Science* 321:926–929.

Dimova NT, Burnett WC (2011) Evaluation of groundwater discharge into small lakes based on the temporal distribution of radon-222. *Limnology and Oceanography* 56:486–494.

Duff H, Triska F (1990) Denitrification in sediments from the hyporheic zone adjacent to a forested stream. *Canadian Journal of Fisheries and Aquatic Sciences* 47:1140–1147.

Dulaiova H, Camilli R, Henderson PB, Charette MA (2010) Coupled radon, methane and nitrate sensors for large-scale assessment of groundwater discharge and non-point source pollution to coastal waters. *Journal of environmental radioactivity* 101:553–63.

Dunkle SA, Plummer LN, Busenberg E, Phillips PJ, Denver JM, Hamilton PA, Michel RL, and Coplen TB (1993) Chlorofluorocarbons (CCl_3F and CCl_2F_2) as dating tools and hydrologic tracers in shallow groundwater of the Delmarva Peninsula, Atlantic Coastal Plain, United States. *Water Resources Research*. 29: 3837–3860.

Ellins KK, Roman-Mas A, Lee R (1990) Using ^{222}Rn to examine groundwater/surface discharge interaction in the rio Grande de Mantai, Puerto Rico. *Journal of Hydrology* 115:319–341.

Fisher DC, Oppenheimer M (1991) Atmospheric nitrogen deposition and the Chesapeake Bay. *Ambio* 20:102–108.

Fisher TR, Benitez JA, Lee K-Y, Sutton AJ (2006a) History of land cover change and biogeochemical impacts in the Choptank River basin in the mid Atlantic region of the US. *International Journal of Remote Sensing* 27:3683–3703.

Fisher TR, Gustafson AB, Koskelo AI, et al. (2010) The Choptank Basin in transition: intensifying agriculture, slow urbanization, and estuarine eutrophication. In *Coastal Lagoons: Systems of Natural and Anthropogenic Change* 137–168.

Fisher TR, Hagy III JD, Boynton WR, Williamns MR (2006b) Cultural eutrophication in the Choptank and Patuxent estuaries of Chesapeake Bay. *Limnology and Oceanography* 51:435–447.

Forster P, Ramaswamy V, Artaxo P, Berntsen T, Betts R, Fahey DW, Haywood J, Lean J, Lowe DC, Myhre G, Nganga J, Prinn R, Raga G, Schulz M, Van Dorland R (2007) Changes in Atmospheric Constituents and in Radiative Forcing. In: *Climate Change 2007. The Physical Science Basis. Contribution of Working Group I to the Fourth Assessment Report of the Intergovernmental Panel on Climate Change* [Solomon, S., D. Qin, M. Manning, Z. Chen, M. Marquis, K.B. Averyt, M.Tignor and H.L. Miller (eds.)]. Cambridge University Press, Cambridge, United Kingdom and New York, NY, USA.

Fox RJ, Fisher TR, Gustafson AB, et al. (2014) Searching for the missing nitrogen: biogenic nitrogen gases in groundwater and streams. *The Journal of Agricultural Science*.

Garcia HE, Gordon LI (1992) Oxygen solubility in seawater: Better fitting equations. *Limnology and Oceanography* 37:1307–1312.

Garcia-Ruiz R, Pattinson SN, Whitton BA (1998) Denitrification in river sediments: relationship between process rate and properties of water and sediment. *Freshwater Biology* 39:467–476.

Genereux DP, Hemond HF, Mulholland PJ (1993) Use of radon-222 and calcium as tracers in a three-end-member mixing model for streamflow generation on the West Fork of Walker Branch Watershed. *Journal of Hydrology* 142:167–211.

Golterman HL (2004) *The Chemistry of Phosphate and Nitrogen Compounds in Sediments*. Kluwer Academic Publishers , Dorsrecht.

Groffman PM, Altabet MA, Böhlke JK, et al. (2006) Methods for measuring denitrification: diverse approaches to a difficult problem. *Ecological Applications* 16:2091–2122.

Gu C, Anderson W, Maggi F (2012) Riparian biogeochemical hot moments induced by stream fluctuations. Water Resources Research WR011720.

Gu C, Hornberger GM, Herman JS, Mills AL (2008) Influence of stream-groundwater interactions in the streambed sediments on NO_3^- flux to a low-relief coastal stream. Water Resources Research WR006739

Hamilton PA, Denver JM, Phillips PJ, and Shedlock RJ (1993) Water-quality assessment of the Delmarva Peninsula, Delaware, Maryland, and Virginia: Effects of agricultural activities on, and distribution of, nitrate and other inorganic constituents in the surficial aquifer. USGS Open File Report 93-40.

Hamme RC, Emerson SR (2004) The solubility of neon, nitrogen and argon in distilled water and seawater. Deep Sea Research Part I 51:1517–1528.

Harrison J, Matson P (2003) Patterns and controls of nitrous oxide emissions from waters draining a subtropical agricultural valley. Global Biogeochemical Cycles 17:1080.

Harrison JA, Matson PA, Fendorf SE (2005) Effects of a diel oxygen cycle on nitrogen transformations and greenhouse gas emissions in a eutrophied subtropical stream. Aquatic Sciences 67:308–315.

Hasegawa K, Hanaki K, Matsuo T, Hidaka S (2000) Nitrous oxide from the agricultural water system contaminated with high nitrogen. Chemosphere - Global Change Science 2:335–345.

Heaton TH., Vogel JC (1981) “Excess air” in groundwater. Journal of Hydrology 50:201–216.

Hemond HF, Duran AP (1989) Fluxes of N_2O at the sediment-water and water-atmosphere boundaries of a nitrogen-rich river. Water Resources Research 25:839–846.

Higgins TM, McCutchan JH, Lewis WM (2008) Nitrogen ebullition in a Colorado plains river. Biogeochemistry 89:367–377.

Hill AR (1983) Denitrification: its importance in a river draining an intensively cropped watershed. Agriculture, Ecosystems & Environment. 10:47-62.

Hill AR, Devito KJ, Campagnolo S, Sanmugadas K (2000) Subsurface denitrification in a forest riparian zone : Interactions between hydrology and supplies of nitrate and organic carbon. Biogeochemistry 51:193–223.

- Howarth RW, Elmgren R, Caraco N, et al. (1996) Regional nitrogen budgets and riverine N & P fluxes for the drainages to the North Atlantic Ocean: Natural and human influences. *Biogeochemistry* 35:75–139.
- Jahne B, Heinz G, Dietrich W (1987) Measurement of the diffusion coefficients of sparingly soluble gases in water. *Journal of Geophysical Research* 92:10767–10776.
- Jordan TE, Weller DE (1996) Human contributions to terrestrial nitrogen flux. *Bioscience* 46:655–664.
- Kana TM, Darkangelo C, Hunt MD, et al. (1994) Membrane inlet mass spectrometer for rapid environmental water samples. *Analytical Chemistry* 66:4166–4170.
- Kemp WM, Boynton WR, Adolf JE, et al. (2005) Eutrophication of Chesapeake Bay: historical trends and ecological interactions. *Marine Ecology Progress Series* 303:1–29.
- Kies A, Hofmann H, Tosheva Z, et al. (2005) Using ^{222}Rn for hydrograph separation in a micro basin (Luxembourg). *Annals of Geophysics* 48:101–107.
- Knee KL, Jordan TE (2013) Spatial distribution of dissolved radon in the Choptank River and its tributaries: Implications for groundwater discharge and nitrate inputs. *Estuaries and Coasts* 36:1237–1252.
- Knowles R (1982) Denitrification. *Microbiology Reviews*. 46:43-70.
- Kroeze C, Seitzinger SP (1998) Nitrogen inputs to rivers, estuaries and continental shelves and related nitrous oxide emissions in 1990 and 2050: a global model. *Nutrient Cycling in Agroecosystems* 52:195–212.
- Kroeze C, Seitzinger SP, Domingues R (2001) Future trends in worldwide river nitrogen transport and related nitrous oxide emissions: a scenario analysis. *The Scientific World Journal* 1:328–35.
- Kulkarni M V, Groffman PM, Yavitt JB (2008) Solving the global nitrogen problem: it's a gas! *Frontiers in Ecology and the Environment* 6:199–206.
- LaMontagne MG, Duran R, Valiela I (2003) Nitrous oxide sources and sinks in coastal aquifers and coupled estuarine receiving waters. *The Science of the total environment* 309:139–49.
- Lamontagne S, Cook PG (2007) Estimation of hyporheic water residence time in situ using ^{222}Rn disequilibrium. *Limnology and Oceanography: Methods* 5:407–416.

- Laursen A, Seitzinger S (2005) Limitations to measuring riverine denitrification at the whole reach scale: effects of channel geometry, wind velocity, sampling interval, and temperature inputs of N₂-enriched groundwater. *Hydrobiologia* 545:225–236.
- Laursen AE, Seitzinger SP (2002) Measurement of denitrification in rivers: an integrated, whole reach approach. *Hydrobiologia* 67–81.
- Laursen AE, Seitzinger SP (2004) Diurnal patterns of denitrification, oxygen consumption and nitrous oxide production in rivers measured at the whole-reach scale. *Freshwater Biology* 49:1448–1458.
- Lee K, Fisher TR, Jordan TE, et al. (2000) Modeling the hydrochemistry of the Choptank River Basin using GWLF and Arc/Info:1. Model calibration and validation. *Biogeochemistry* 49:143–173.
- Lee RW and Hollyday EF (1993) Use of radon measurements in Carters Creek, Maury County, Tennessee, to determine location and magnitude of ground-water seepage, in *Field Studies of Radon in Rocks, Soils, and Water*, edited by L. C. S. Gundersen and R. B. Wanty. 237–242, C. K. Smoley, Boca Raton, Fl.
- Liss PS and Slater PG (1974) Flux of gases across the air-sea interface. *Nature*. 247:181–184.
- Lowrance R, Altier L, Newbold J, et al. (1997) Water Quality Functions of Riparian Forest Buffers in Chesapeake Bay Watersheds. *Environmental management* 21:687–712.
- Malard F, Hervant F (1999) Oxygen supply and the adaptations of animals in groundwater. *Freshwater Biology* 41:1–30.
- Marzolf ER, Mulholland PJ, and Steinman AD (1994) Improvements to the diurnal upstream-downstream dissolved-oxygen change technique for determining whole-stream metabolism in small streams. *Canadian Journal of Fisheries and Aquatic Science*.51:1591–1599.
- McCutchan JH, Lewis WM (2008) Spatial and temporal patterns of denitrification in an effluent-dominated plains river. *Verh Internat Verein Limnol.* 30:323–328.
- McCutchan JH, Saunders JF, Pribyl AL, Lewis WM (2003) Open-channel estimation of denitrification. *Limnology and Oceanography: Methods* 1:74–81.
- McCutchan JH, Lewis WM, Saunders JF (1998) Uncertainty in the estimation of stream metabolism from open-channel oxygen concentrations. *Journal North American Benthological Society* 17:155–164.

McMahon PB, Dennehy KF (1999) N₂O emissions from a nitrogen-enriched river. Environmental science & technology 33:21–25.

Mosier A, Kroeze C, Nevison C, et al. (1998) Closing the global N₂O budget: nitrous oxide emissions through the agricultural nitrogen cycle inventory methodology. Nutrient Cycling in Agroecosystems 52:225–248.

Nixon SW (1995) Coastal marine eutrophication: A definition, social causes, and future concerns. Ophelia 41:199–219.

Norton MM, Fisher TR (2000) The effects of forest on stream water quality in two coastal plain watersheds of the Chesapeake Bay. Ecological Engineering 14:337–362.

O'Connor BL, Harvey JW, McPhillips LE (2012) Thresholds of flow-induced bed disturbances and their effects on stream metabolism in an agricultural river. Water Resources Research 48:W08504.

Ocampo CJ, Oldham CE, Sivapalan M (2006) Nitrate attenuation in agricultural catchments: Shifting balances between transport and reaction. Water Resources Research WR003773.

Paul EA and Clark FE (1989) Soil microbiology and biochemistry. Academic Press. New York.

Payn RA, Gooseff MN, McGlynn BL, et al. (2009) Channel water balance and exchange with subsurface flow along a mountain headwater stream in Montana, United States. Water Resources Research WR007644.

Peng TH, Broecker WS, Mathieu GG, et al. (1979) Radon evasion rates in the atlantic and pacific oceans as determined during the geosecs program. Journal of Geophysical Research 84:2471–2486.

Pfenning KS, McMahon PB (1996) Effect of nitrate, organic carbon, and temperature on potential denitrification rates in nitrate-rich riverbed sediments. Journal of Hydrology 187:283–295.

Piña-Ochoa E, Álvarez-Cobelas M (2006) Denitrification in aquatic environments: A Cross-system analysis. Biogeochemistry 81:111–130.

Pribyl AL, Mccutchan JH, Lewis WM, Saunders JF (2005) Whole-system estimation of denitrification in a plains river: A comparison of two methods. Biogeochemistry 73:439–455.

Puckett LJ, Zamora C, Essaid H, Wilson JT, Johnson HM, Brayton M, and Vogel JR (2008) Transport and Fate of Nitrate at the Ground-Water/Surface-Water Interface.

Ravishankara AR, Daniel JS, Portmann RW (2009) Nitrous oxide (N_2O): the dominant ozone-depleting substance emitted in the 21st century. *Science* 326:123–125.

Raymond PA, Zappa CJ, Butman D, et al. (2012) Scaling the gas transfer velocity and hydraulic geometry in streams and small rivers. *Limnology & Oceanography: Fluids & Environments* 2:41–53.

Roley SS, Tank JL, Williams MA (2012) Hydrologic connectivity increases denitrification in the hyporheic zone and restored floodplains of an agricultural stream. *Journal of Geophysical Research JG001950*.

Saleh-Lakha S, Shannon KE, Henderson SL, et al. (2009) Effect of pH and temperature on denitrification gene expression and activity in *Pseudomonas mandelii*. *Applied and environmental microbiology* 75:3903–3911.

Savoy L, Surbeck H, Hunkeler D (2011) Radon and CO_2 as natural tracers to investigate the recharge dynamics of karst aquifers. *Journal of Hydrology* 406:148–157.

Seitzinger S, Harrison JA, Böhlke JK, et al. (2006) Denitrification across landscapes and waterscapes: a synthesis. *Ecological Applications* 16:2064–2090.

Seitzinger SP (1988) Denitrification in freshwater and coastal marine ecosystems: Ecological and geochemical significance. *Limnology* 33:702–724.

Shine KP, Fuglestvedt JS, Hailemariam K, Stuber N (2005) Alternatives to the global warming potential for comparing climate impacts of emissions of greenhouse gases. *Climate Change* 68:281–302.

Sjodin AL, Lewis WM, Saunders JF (1997) Denitrification as a component of the nitrogen budget for a large plains river. *Biogeochemistry* 39:327–342.

Smethie WMJ, Takahashi T, Chipman DW, Ledwell JR (1985) Gas exchange and CO_2 flux in the tropical Atlantic ocean determined from ^{222}Rn and pCO_2 measurements. *Journal of Geophysical Research* 90:7005–7022.

Smith TE, Laursen AE, Deacon JR (2008) Nitrogen attenuation in the Connecticut River, northeastern USA; a comparison of mass balance and N_2 production modeling approaches. *Biogeochemistry* 87:311–323.

- Soulsby C, Malcolm IA, Tetzlaff D, Youngson AF (2009) Seasonal and inter-annual variability in the hyporheic water quality revealed by continuous monitoring in a salmon spawning stream. *River Research and Applications*.
- Stanford G, Dzienia S, and Vander Pol RA (1975) Effect of temperature on denitrification rate in soils. *Soil Science Society of America Journal*. 39:867-870.
- Stenstrom MK, Poduska RA (1980) The effect of dissolved oxygen concentration on nitrification. *Water Research* 14:643–649.
- Stow CA, Walker JT, Cardoch L, et al. (2005) N₂O Emissions from streams in the Neuse River watershed, North Carolina. *Environmental Science & Technology* 39:6999–7004.
- Strauss EA, Mitchell NL, Lamberti GA (2002) Factors regulating nitrification in aquatic sediments: effects of organic carbon, nitrogen availability, and pH. *Canadian Journal of Fisheries and Aquatic Sciences* 59:554–563.
- Thomann RV and Mueller JA (1987) Principles of surface water quality modeling and control: quality modeling and control. Harper & Row. New York.
- Triksa FJ, Duff JH, and Avazino RJ (1990) Influence of exchange flow between the channel and hyporheic zone on nitrate production in a small mountain stream. *Canadian Journal of Fisheries and Aquatic Science* 47: 2099–2111.
- Van Breemen N, Boyer EW, Goodale CL, et al. (2002) Where did all the nitrogen go? Fate of nitrogen inputs to large watersheds in the northeastern U.S.A. *Biogeochemistry* 57/58:267–293.
- Vidon P, Allan C, Burns D, et al. (2010) Hot spots and hot moments in riparian zones: Potential for improved water quality management. *Journal of the American Water Resources Association* 46:278–298.
- Vilain G, Garnier J, Tallec G, Tournebize J (2012) Indirect N₂O emissions from shallow groundwater in an agricultural catchment (Seine Basin, France). *Biogeochemistry* 111:253–271.
- Vitousek PM, Aber JD, Howarth RW, et al. (2012) Human Alteration of the Global Nitrogen Cycle: Sources and Consequences. *Ecological Applications* 7:737–750.
- Wanninkhof R (1992) Relationship between wind speed and gas exchange. *Journal of Geophysical Research* 97:7373–7382.

Wanninkhof R, Mulholland PJ, Elwood JW (1990) Gas exchange rates for a first-order stream determined with deliberate and natural tracers. *Water Resources Research* 26:1621–1630.

Weiss RF, Price BA (1980) Nitrous oxide solubility in water and seawater. *Marine Chemistry* 8:347–359.

Well R, Augustin J, Meyer K, and Myrold DD (2003) Comparison of field and laboratory measurement of denitrification and N₂O production in the saturated zone of hydromorphic soils. *Soil Biology and Biochemistry*. 35:783–799.

Well R, Weymann D, and Flessa H (2005) Recent research progress on the significance of aquatic systems for indirect agricultural N₂O emissions. *Environmental Science*. 2:143–151.

Werner SF, Browne BA, Driscoll CT (2010) Three-dimensional spatial patterns of trace gas concentrations in baseflow-dominated agricultural streams: implications for surface–ground water interactions and biogeochemistry. *Biogeochemistry* 107:319–338.

Weymann D, Well R, von der Heide C, et al. (2009) Recovery of groundwater N₂O at the soil surface and its contribution to total N₂O emissions. *Nutrient Cycling in Agroecosystems* 85:299–312.

Wilcock RJ, Sorrell BK (2008) Emissions of greenhouse gases CH₄ and N₂O from low-gradient streams in agriculturally developed catchments. *Water, Air, and Soil Pollution* 188:155–170.

Wilson GB, Andrews JN, Bath AH (1990) Dissolved gas evidence for denitrification in the Lincolnshire limestone groundwaters, eastern England. *Journal of Hydrology* 113:51–60.

Yan W, Laursen AE, Wang F, et al. (2004) Measurement of denitrification in the Changjiang River. *Environmental Chemistry* 1:95–98.

Chapter 2: Storm and baseflow nutrient export from agricultural and forested watersheds on the coastal plain of Maryland, USA

Abstract

Storm and baseflow nutrient dynamics and hydrology were investigated over the 2013 water year and compared with previously collected data in three Maryland (USA) coastal plain watersheds ($1.4\text{-}8.4 \text{ km}^2$) with a range of agricultural and forested land use. The forested watershed had very low inorganic nitrogen and phosphorus concentrations; NO_3^- ($1 \mu\text{M}$; 3.3% of total nitrogen), NH_4^+ ($2.4 \mu\text{M}$; 7.2% of total nitrogen), and PO_4^{3-} ($0.1 \mu\text{M}$; 26% of total phosphorus) on average during baseflow with minor increases in NO_3^- , total nitrogen, and total phosphorus during storms. In contrast, the agriculturally impacted watersheds were characterized by high NO_3^- concentrations in base ($198\text{-}325 \mu\text{M}$; 77 to 91% of total nitrogen) and stormflow ($101\text{-}216 \mu\text{M}$; 54 to 67% of total nitrogen) with notable variation in nutrient concentrations during storms. Annual export of NH_4^+ , PO_4^{3-} , and total phosphorus was overwhelmingly a result of quickflow (61 to 77% of annual export) in these agricultural watersheds.

Introduction

Anthropogenic nitrogen (N) and phosphorus (P) inputs have negatively impacted aquatic ecosystems around the world (Carpenter et al. 1998; Diaz and Rosenberg 2008). The Chesapeake Bay has suffered from hypoxic bottom waters, declining fisheries, and loss of habitat as a result of elevated N and P inputs increasing phytoplankton production, a process described as eutrophication (Nixon et al. 1995; Kemp et al. 2005).

Eutrophication also occurs in Chesapeake Bay tributaries. The Choptank River drains to the Chesapeake from the Delmarva Peninsula and has a long term trend of increasing N and P concentrations at an upstream, non-tidal USGS (01491000) gauging station in Greensboro, MD (Fisher et al. 2006; Fisher et al. 2010). Consequently, the dissolved oxygen in the bottom waters of the downstream Choptank estuary are approaching the hypoxic threshold similar to conditions observed in the Chesapeake Bay for decades (Hagy et al. 2004; Fisher et al. 2006). The Choptank is on an unsustainable trajectory, and it is critical to understand the quantities and mechanisms of nutrient export in the Chesapeake Bay region, specifically within the agriculturally dominated coastal plain.

Land use and stream discharge are important drivers of nutrient concentrations and export from watersheds (Jordan et al. 1997; Sobota et al. 2009). Agriculture and urban development are generally associated with higher N and P concentrations compared with forests and undisturbed areas (Novotny and Olem 1994; Sharpley et al. 1994; Allan 2004; Fisher et al. 2010). Stream discharge has varying effects on N and P dynamics, and investigating nutrient fluxes at the event scale can reveal

hydrologic transport mechanisms and sources. Events that generate overland or high velocity flows mobilize P, often bound to particles, from land and stream channel surfaces (Sharpley et al. 1999). Storms are typically linked to increased P fluxes in agricultural watersheds, and a large fraction of annual P export can occur during just a few events (Correll et al. 1999; Novak et al. 2003; Sharpley et al. 2008). However, this may depend on the soil characteristics, propensity of soils/sediments to erode, and whether P source areas overlap with transport pathways (Dillon and Kirchner 1975; Sharpley et al. 1999; McDowell et al. 2004).

N dynamics are complex over event and long term scales with a variety of responses depending on hydrology, land use, climate, and watershed features (Mitchell et al. 1996; Cirmo and McDonnell 1997; Norton and Fisher 2000; Poor and McDonnell 2007; Schaefer and Alber 2007; Steinburg et al. 2011; Howarth et al. 2012). In forested watersheds, many studies have found that NO_3^- concentration increase during storm events with peaks on the rising limb of the hydrograph (McHale et al. 2002; Inamdar et al. 2004, 2006; Rusjan et al. 2008; Christopher et al. 2008). The flushing hypothesis describes such observations where NO_3^- and other solutes are transported through the shallow subsurface due to the rising water table connecting streams with a larger terrestrial area (Hornberger et al. 1994; Creed and Band, 1996). In agricultural watersheds NO_3^- concentrations often decrease during storms as a result of “new” event water diluting NO_3^- rich groundwater (Petry et al. 2002; Blanco et al. 2010). Event water is composed of direct precipitation, throughfall, saturation excess overland flow, and potentially quick subsurface flow. Yet others have observed increasing NO_3^- concentrations during rain events in

agricultural watersheds or variable results within a site depending on antecedent conditions or other factors (Biron et al. 1999; Macrae et al. 2010; Koskelo 2008; Jiang et al. 2010). In all cases, NO_3^- export (Kg N day^{-1}) increases during events as a result of elevated discharge. However, the short-term patterns of NO_3^- concentrations differ, indicating variable flowpaths, timing, and sources within and across watersheds.

At the annual scale, some studies have concluded that storm events are responsible for a majority of NO_3^- export (Owens et al. 1991; Owens et al. 2008), while others suggested NO_3^- was transported primarily during baseflow (Vanni et al. 2001; Jordan et al. 1997; Zhu et al. 2012). This often depends on the fraction of the annual discharge that can be attributed to base and quickflow. Therefore, it is important to compare the percent of annual N export in baseflow with the annual Base Flow Index (BFI) to determine if export is proportional to discharge.

Studies of stormflow dynamics have largely focused on NO_3^- and P while fewer have investigated NH_4^+ , which also is an important bioavailable N species that can contribute to eutrophication. The hydrologic and biogeochemical processes controlling NH_4^+ export differ greatly from NO_3^- . NH_4^+ can adsorb to the soil matrix, is subject to nitrification, and in-stream biotic uptake rates are generally higher compared to NO_3^- (Peterson et al. 2001; Ensign and Doyle, 2006). Increasing NH_4^+ concentrations during storms has been observed in both agricultural and forested watersheds, but through different processes. In an agricultural watershed, NH_4^+ mobilization occurred due to overland flow of near stream agricultural NH_4^+ sources (Petry et al. 2002). In forested watersheds NH_4^+ peaks have been attributed to high

NH_4^+ concentrations in throughfall/litter leachate (Hill et al. 1993; Inamdar 2007), and/or wetland sources (McHale et al. 2004; Inamdar 2007). In the Choptank basin, large peaks in NH_4^+ concentrations have been observed in agricultural watersheds, and storm events may account for a significant portion of annual export (Koskelo 2008)

Given the variability in hydrochemical responses over event and annual scales, more empirical measurements are needed from a diversity of landscapes with emphasis on base and quickflow export of different N and P species. This study focuses on three small coastal plain watersheds with 0, 25 and 60% (Table 8) of the land area dedicated to agriculture, with the remaining portion largely forested. It is increasingly recognized that small headwater streams often have high NO_3^- and TP concentrations (Morgan and Kline 2011) and can supply a significant fraction of N loading to downstream systems (Alexander et al. 2007).

Table 8. Area, land use, soil properties, and mean (standard error) baseflow nitrate, total nitrogen and total phosphorus concentrations over the 2012-2013 water year for the Marshy Hope (MH), Baltimore Corner (BC), and South Forge (SF) watersheds.

Watershed	Area (km ²)	% Ag	%Forest	% Hydric Soils	NO_3^-	TN	TP
MH	1.36	1.0	99	55	1.11 (0.47)	33.3 (3.1)	0.41 (0.07)
BC	4.84	26	60	1.0	199 (21)	256 (23)	1.15 (0.14)
SF	8.49	66	28	35	325 (17)	354 (18)	1.32 (0.18)

The objectives of this study were to use three watersheds with a range of agricultural land use to 1) characterize hydrologic storm response, 2) investigate patterns of nutrient concentrations during storms and baseflow conditions to understand transport mechanisms and sources, and 3) compare base and quickflow nutrient export at the event and annual scale. Specifically, the following hypotheses

were tested: 1) Stormflow will account for a disproportionate amount of TP and TN export at the annual scale, and 2) NO_3^- will demonstrate flushing behavior (increasing concentration during storm events) in the forested watershed, but NO_3^- concentrations will decrease during rainfall events in the agricultural watersheds due to the dilution of NO_3^- rich groundwater.

Methods

Study Sites

The study watersheds are located in the Choptank and Nanticoke River Basins, which drain into the Chesapeake Bay from the Delmarva Peninsula (Figure 1). This area lies within the Atlantic coastal plain physiographic region characterized by flat topography (<30 m asl). The hydrogeomorphology typically ranges from poorly drained uplands with shallow streams to well-drained, sandy soils with incised stream channels (Hamilton et al. 1993). Land use in the Choptank Basin is dominated by agriculture (62%), followed by forest (26%) and a small impervious component (5%) (Norton and Fisher 2000; Fisher et al. 2006). The climate is humid temperate with an average annual rainfall of 112 cm evenly distributed throughout the year and stream flow largely driven by seasonal variation in evapotranspiration (Lee et al. 2000; Fisher et al. 2010).

The watersheds were selected to represent a range of land use from forest to agriculture. Marshy Hope (MH) is a small (1.36 km^2), 99% forested watershed in Nanticoke River Basin (Table 8) dominated by hydric soils (55% of area). The uplands were logged 30-40 years ago and are mostly pine species, and the floodplain

is covered by hardwood species. Baltimore Corner (BC) watershed (4.8 km^2) is located in the upper Choptank Basin with 25.6% agricultural, 59.6% forest, and 13.1% fallow, and 1.7 % impervious surfaces (Table 8). The stream network has been largely channelized to drain adjacent fields in production under a corn-wheat-soybean rotation. Soils are generally well drained sandy loams, and 67.6% of the watershed is partially hydric with only 1% of the area classified as hydric. South Forge (SF) is the largest (8.49 km^2) most agriculturally dominated watershed and is also located in the Choptank Basin. The land use is 66.5% agriculture, 28.2% forest, and 5.3% impervious surfaces (Table 8). Thirty-five percent of the watershed area contains hydric soils exclusively found in the riparian zone. The main channel of the SF stream network is not channelized and has an intact floodplain containing mature forest. Most of the SF stream network (55%) is buffered by forest, and the remaining unbuffered portion is largely ephemeral, zero order ditches.

Monitoring

Each watershed was continuously gauged (30 minute intervals) for stream depth and temperature with a Solinst Gold Levelogger pressure transducer (Model 3001, Solinst, Canada). The logger was anchored to a cinderblock at the watershed outlet, staff gauges were installed to provide stationary depth datum to compare with logger depth, and rating curves were developed to convert stage to discharge (Fisher et al. 2010). Discharge was measured over a range of conditions by measuring cross sectional area and velocity using a Flo-Mate (Model 2000, Marsh-McBirney, Loveland, CO), but a StreamPro Acoustic Doppler Current Profiler (Teledyne RD Instruments, Poway, CA) was used during extreme flows.

Baseflow samples were collected approximately monthly at the stream gauging station in 1000 mL plastic bottles from September 2012 to October 2013 and kept on ice until returning to the laboratory. Storms were sampled episodically using ISCO auto-samplers (Models 3700 and 6712, Teledyne ISCO, Lincoln, NE). ISCOs were manually initiated and programmed to sample every hour over 48 hours compositing two samples per bottle. Stream discharge and baseflow chemistry has been monitored at SF since 2003, since 2006 at MH, and BC monitoring began with this study. Data collected prior to this study at MH and SF (Koskelo et al. in prep) were analyzed for comparison.

Laboratory Analysis

All base and storm flow samples were analyzed for TN, TP, PO_4^{3-} , NO_3^- , NH_4^+ , pH, and conductivity. Upon returning to the laboratory, conductivity, temperature (Yokogawa SC82, Tokyo, Japan), and pH (VWR Symphony, Randor, USA) were measured. Samples were filtered with GFF filters for analysis of dissolved nutrients. Unfiltered aliquots were autoclaved with a persulfate reagent (Valerama 1981) for subsequent TN and TP analysis. When samples were not immediately processed, subsamples were frozen and analyzed within a few weeks. NH_4^+ , PO_4^{3-} , and TP (as PO_4^{3-} after persulfate digestion) were analyzed using colorimetric methods. TN and NO_3^- (nitrate + nitrite, but will be referred to as NO_3^-) were measured with a Technicon AutoAnalyzer II at the Horn Point Laboratory Analytical Services facility.

Data Analysis and Calculations

Daily precipitation data were acquired from eight weather stations that were within 5-55 km of the watersheds including seven NOAA National Climatic Data Center stations (<http://www.ncdc.noaa.gov/cdo-web/>) as well the University of Maryland Wye Research Center National Atmospheric Deposition Program (NADP) site (<http://agresearch.umd.edu/wye/weather-data>). No weather stations were located within the watershed boundaries; therefore, daily precipitation for each watershed was estimated using an arithmetic mean of the nearest 4-5 stations which varied depending on the watershed. Most of the stations were highly correlated ($r = 0.69$ - 0.90) with little bias (linear regression slopes 0.65-1.04) using daily data from 2007-2013 indicating relatively minor spatial variability (Table 9). Wye and Royal Oak were the exceptions since they are located the furthest west, but after applying a 1 day lag correlations improved and bias was reduced.

Table 9. Spearman-rank correlation coefficients (top right panel) between all precipitation stations using daily data from 2007 to 2013. All P-values were <0.001 . *Denotes where 1 day lag applied.

	Trappe	Easton	Seaford	Greensboro	Denton	Vienna	Wye	Royal Oak
Trappe	-	0.90	0.77	0.85	0.87	0.72	0.79*	0.66
Easton		-	0.77	0.85	0.87	0.70	0.84*	0.65
Seaford			-	0.78	0.77	0.70	0.68*	0.52
Greensboro				-	0.88	0.69	0.78*	0.59
Denton					-	0.70	0.81*	0.62
Vienna						-	0.70*	0.74*
Wye							-	0.60
Royal oak								-

Discharge was separated into base and quick flow and storm events were identified on an annual time scale using the 1-day Sliding Average with Rainfall Record (SARR) method (Koskelo et al. 2012). This method was developed for small watersheds ($<50 \text{ km}^2$) and previously applied to catchments in the Choptank Basin (Koskelo et al. 2012). SARR is based on the smoothed minima technique, or United Kingdom Institute of Hydrology (UKIH) method (Gustard et al., 1992). However, it has several mathematical modifications and empirical additions; most notably 1) a reduced time step to reflect hydrologic response in smaller catchments and 2) rainfall data input as a quality control step to verify flow increases. This method is easy to implement using a freely available MATLAB® script, requires only daily stream discharge and rainfall data, and provides output of event identification as well as daily base and quickflow. Output from SARR was incorporated into subsequent calculations and allowed partitioning of base and quickflow nutrient export.

For each event identified by SARR, the antecedent precipitation index (API) runoff coefficient, and event base flow index (BFI_{event}) were calculated. API is an indicator of the soil moisture conditions prior to storm events by weighting daily precipitation (McDonnell et al. 1991; Inamdar and Mitchell 2006). API was calculated 7 (API_7) and 14 (API_{14}) days prior to all events representing shallow and deeper aquifer conditions,

$$API_x = \sum_{i=1}^x \frac{p_i}{i} \quad (\text{Eq. 11})$$

where $x = 7$ and 14 days before an event, and p_i is the daily precipitation (mm) on the i th day preceding the event. Runoff coefficient (ROC) was calculated by dividing the event quickflow depth from SARR output (meters) by event precipitation depth (P ,

meters). Quickflow depth was estimated within the SARR program by dividing quickflow volume ($Q_{F_{event}}$, m^3) by watershed area (A , m^2). BFI_{event} was calculated with SARR output by dividing the event baseflow (m^3) by event total flow (m^3).

$$ROC = \frac{Q_{F_{event}} / A}{P} \quad (\text{Eq. 12})$$

Event volume weighted mean concentrations (EMC) of TN, TP, PO_4^{3-} , NO_3^- , NH_4^+ , H^+ , and conductivity were calculated using sampled concentrations and continuous (30 minute) discharge data. Hydrogen ion concentration (H^+) was logged following weighting to convert back to pH. Each storm flow sample represented two hours, therefore the 30-minute discharge data were averaged over the same time period (Q_i , L s^{-1}) and multiplied by concentration (C_i , $\mu\text{mol L}^{-1}$). The sum of these two hour flux rates were divided by the total discharge during the 48 hour sampling period as in equation (13).

$$EMC = \frac{\sum (C_i Q_i)}{\sum Q_i} \quad (\text{Eq. 13})$$

Storm flow often lasted longer than could be sampled in 48 hours. Hysteresis patterns were utilized to extrapolate over the unsampled portion of storms, typically the long recession tails. The midpoint between the first and last time point was interpolated and this concentration (C_{est}) was assumed to equal the volume-weighted mean concentration of the unsampled portion of the storm. Total event volume-weighted mean concentration was then calculated by summing the product of sampled and unsampled volume-weighted means and volumes and divided by total volume.

$$Total EMC = \frac{\sum (C_i Q_i)_{sampled} + (C_{est} Q_{unsampled})}{\sum Q_i + Q_{unsampled}} \quad (\text{Eq. 14})$$

Annual N and P export were separated into base and quickflow components based on daily SARR discharge output and base and stormflow chemistry. Three different approaches were used depending on observations of storm and baseflow chemistry. 1) If a significant relationship was found between EMC and event quickflow or total flow volume, then this regression was used to estimate EMC for unsampled events (e.g. TP, PO_4^{3-} , NH_4^+ in BC and SF; Figure 15). At the event scale, export was attributed to base or quickflow using separated flow data and extrapolated EMC values. Between storms, monthly baseflow concentrations and daily discharge data were used to calculate export and added to the baseflow component of event export for the annual calculation. 2) If there was no relationship between EMC and quickflow volume, but EMC and baseflow concentrations were significantly different (Kruskal-Wallis test), then the average sampled EMC was applied to all unsampled events to estimate event export separated into base and quickflow components (e.g. TN, TP, NO_3^- , NH_4^+ in MH; NO_3^- and TN in BC; NO_3^- in SF). Export between events was calculated as in approach one. 3) If there was no difference between sampled baseflow concentrations and EMC or relationships for extrapolation, baseflow concentrations and daily discharge separated into base and quickflow were used to estimate annual export (e.g. PO_4^{3-} in MH; TN in SF).

Results

Hydrology

The 2013 water year (WY) was preceded by a summer drought in 2012; however, precipitation in 2013 (136 cm, Table 10) was greater than the long-term annual mean of 112 cm (Lee et al. 2000). The water year began with little

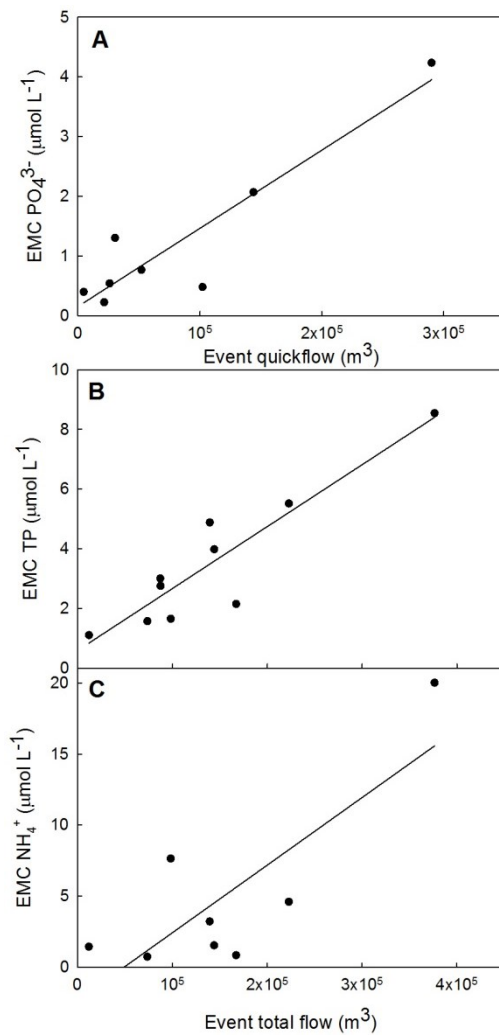


Figure 15. (A) Event volume weighted mean concentration (EMC) of PO₄³⁻ vs event quickflow ($r^2 = 0.86$, $P < 0.001$), (B) EMC of TP vs event total flow ($r^2 = 0.83$, $P < 0.001$), and (C) EMC of NH₄⁺ c vs event total flow ($r^2 = 0.64$, $P = 0.016$) using pooled data from BC and SF watersheds.

precipitation, experienced an extreme event in October, Hurricane Sandy, and had an unusually wet summer in 2013 (Figure 17-19). Thirty-eight percent of the annual precipitation occurred during Hurricane Sandy and the month of June. A majority of storm events identified by SARR were small (0-2 cm) with few large storms greater than 10 cm (Figure 19a).

The hydrology of MH, BC, and SF watersheds differed on annual and event time scales over the 2013 water year. MH had a unimodal baseflow distribution peaking in February (Figure 16), while BC and SF had bi-modal distributions in baseflow with peaks in December-January and June (Figure 17-18). Baseflow separation using SARR estimated Base Flow Indexes (BFI) of 32, 43, and 65% for MH, BC, and SF respectively (Table 10). BFI was slightly below the mean for the MH and SF sites which had flow data since 2006 and 2004 respectively (Table 10).

Table 10. Annual precipitation, Base Flow Index (BFI), water yield, and percent of precipitation lost as evapotranspiration (estimated as precipitation minus water yield) in the South Forge, Marshy Hope, and Baltimore Corner watersheds.

Water Year	Precip (cm)	<u>South Forge</u>			<u>Marshy Hope</u>			<u>Baltimore Corner</u>		
		BFI	Water Yield (cm)	ET (cm)	BFI	Water Yield (cm)	ET (cm)	BFI	Water Yield (cm)	ET (cm)
2005	104	73	42	62	-	-	-	-	-	-
2006	124	64	31	93	-	-	-	-	-	-
2007	93	71	46	47	37	69	24	-	-	-
2008	104	63	23	81	56	3	102	-	-	-
2009	129	73	44	85	-	-	-	-	-	-
2010	144	55	69	75	19	72	65	-	-	-
2011	143	48	51	92	35	18	117	-	-	-
2012	97	85	60	37	66	12	85	-	-	-
2013	135	65	74	61	32	54	84	43	85	38
Mean	120	66	49	71	41	38	79	43	85	38

SARR detected 53, 52, and 63 storm events in MH, BC, and SF respectively over the 2013 WY, but most events produced little to no quickflow. As expected, hydrologic variables (i.e. event precipitation, quickflow, peak flow, BFI_{event}) were highly correlated (Table 11 for details on all regressions). Excluding the largest event at the MH site (Hurricane Sandy), event precipitation was positively correlated with event quickflow ($r^2 = 0.60-0.93$) with a different slope for each watershed. The slopes of these regressions represent the average proportion of precipitation that became quickflow: 0.59, 0.46, and 0.30 for MH, BC, and SF respectively. MH and BC slopes were not significantly different from each other but they were different from SF (Figure 19b). Hurricane Sandy was included in a separate regression analysis of only MH data partitioned by API_7 less than and greater than 1, which resulted in drastically different slopes in the quickflow versus precipitation relationship (Figure 19c).

There was no such separation by API_7 at BC or SF. Considering only storms that had ≥ 2 cm of precipitation, API_7 and API_{14} were weakly, but significantly, correlated with the runoff coefficient in the MH ($r^2 = 0.28$ and 0.59) and BC ($r^2 = 0.30$ and 0.29) watersheds but not in SF (Table 11). Event quickflow was also significantly related to peak discharge ($r^2 = 0.88-0.99$, Table 11) with varying slopes for each watershed, but again MH and BC were not significantly different (Figure 20a). The BFI for each event (BFI_{event}) was negatively and non-linearly related to peak discharge (Figure 20b).

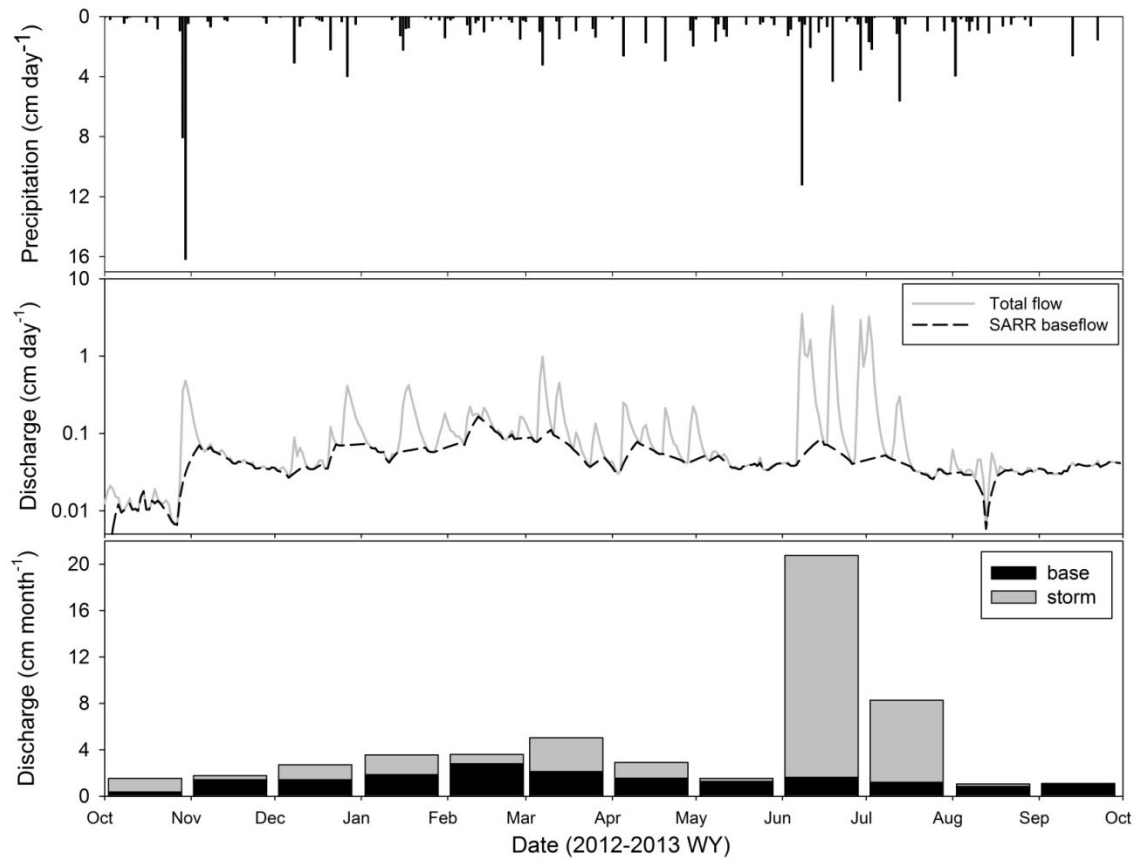


Figure 16. SARR output from the Marshy Hope watershed over the 2013 water year. Top panel is daily precipitation (cm), middle panel is the log of daily discharge (cm day^{-1}) as well as the separated baseflow represented by the dashed line. The bottom panel is the monthly base and quickflow components (cm month^{-1})

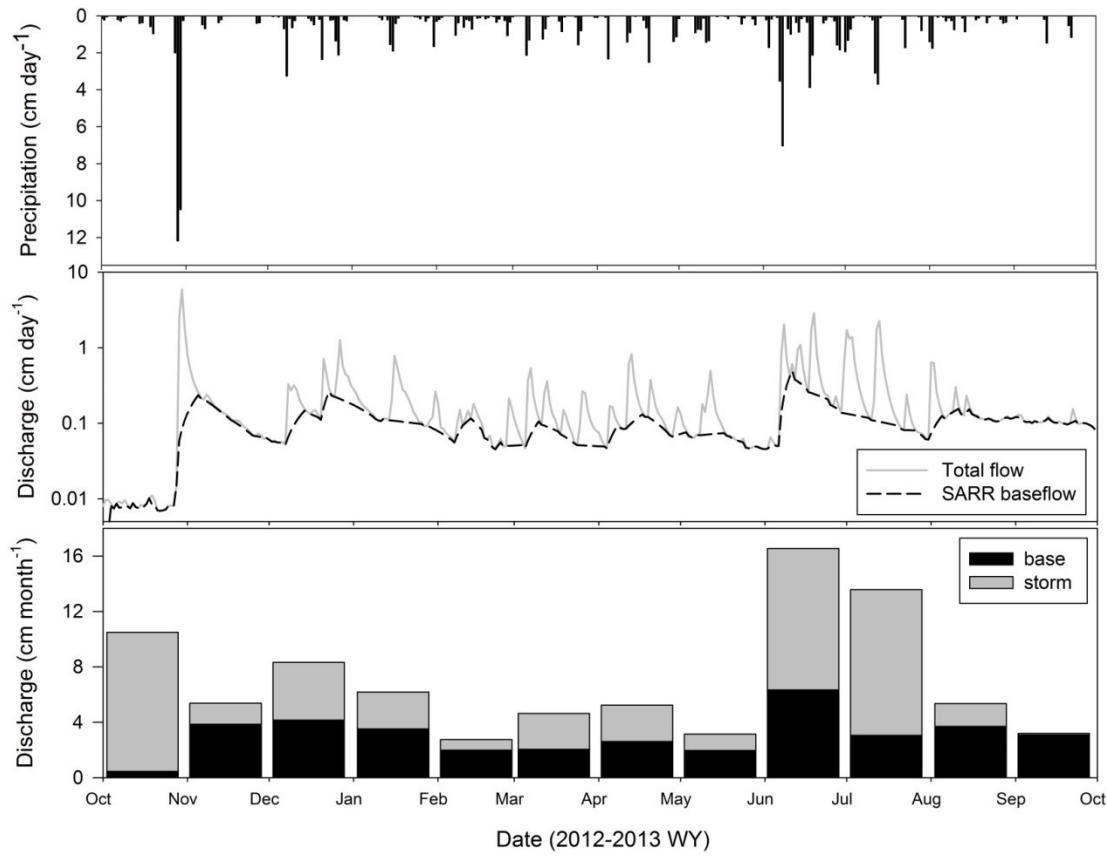


Figure 17. SARR output from the Baltimore corner watershed over the 2013 water year. Top panel is daily precipitation (cm), middle panel is the log of daily discharge (cm day^{-1}) as well as the separated baseflow represented by the dashed line. The bottom panel is the monthly base and quickflow components (cm month^{-1}).

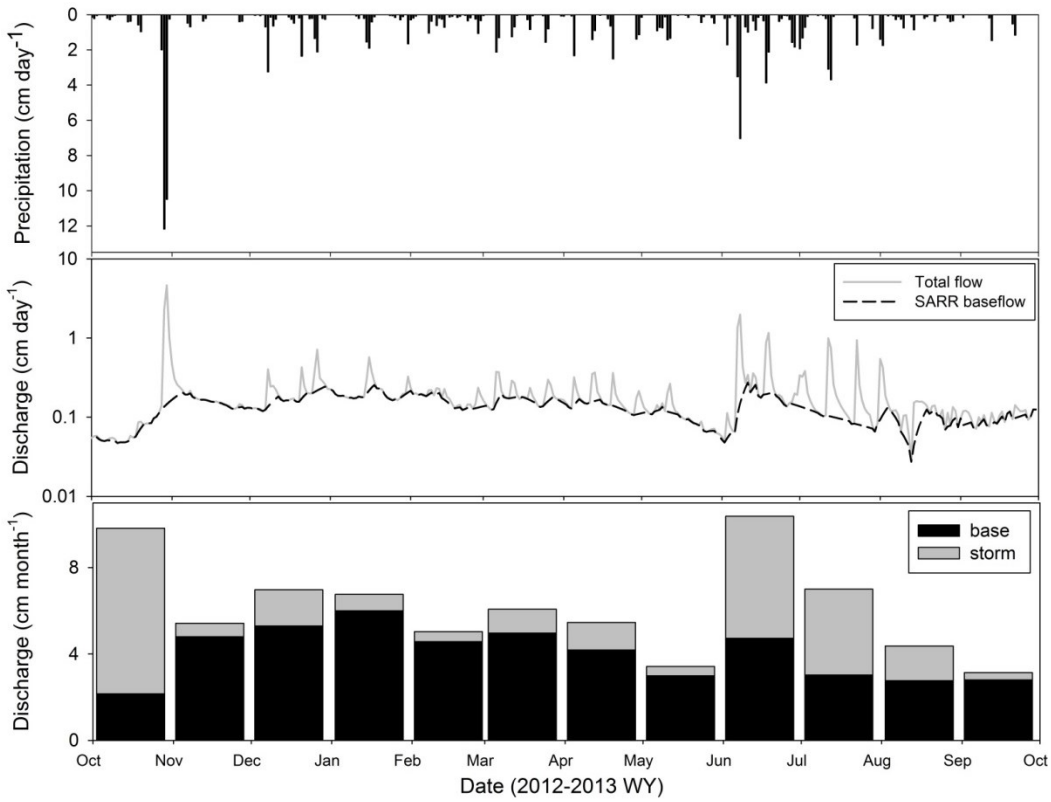


Figure 18. SARR output from the South Forge watershed over the 2013 water year. Top panel is daily precipitation (cm), middle panel is the log of daily discharge (cm day^{-1}) as well as the separated baseflow represented by the dashed line. The bottom panel is the monthly base and quickflow components (cm month^{-1}).

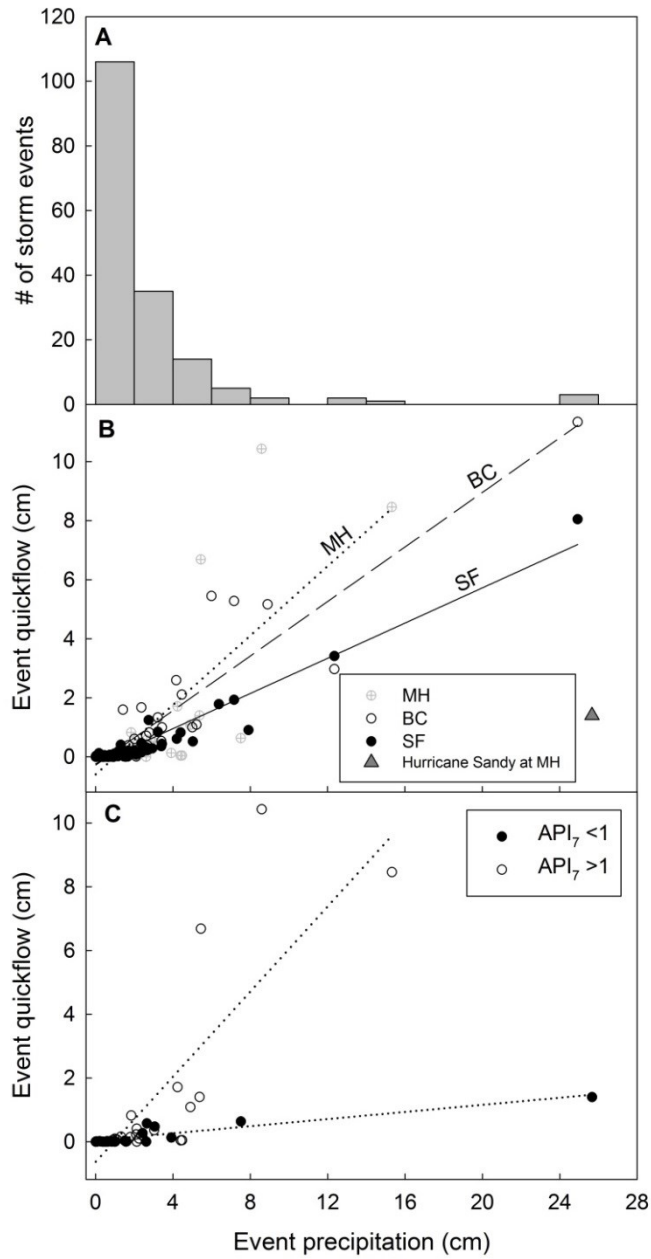


Figure 19. Top panel (A) shows histogram of event precipitation for storms in all watersheds in bins of 2 cm. (B) shows the relationship between precipitation (cm) and quickflow (cm) with linear regressions for each watershed. Only MH and BC slopes were not significantly different. Hurricane Sandy was omitted for regression in the MH watershed. The bottom panel (C) shows only MH data separated by antecedent precipitation index (API_7) less than and greater than 1 and includes Hurricane Sandy.

Table 11. Details from all regressions including x and y variables, equation, r^2 , P-value, and sample size (n). Significant relationships are noted with an asterisk*.

Sites	x	y	Equation	r^2	P	n
SF	peak discharge (cm day ⁻¹)	event quickflow (cm day ⁻¹)	y=0.84x -0.09	0.99	<0.0001*	63
BC	peak discharge (cm day ⁻¹)	event quickflow (cm day ⁻¹)	y=1.55x -0.10	0.88	<0.0001*	52
MH	peak discharge (cm day ⁻¹)	event quickflow (cm day ⁻¹)	y=1.76x -0.06	0.88	<0.0001*	53
SF	Precipitation (cm day ⁻¹)	event quickflow (cm day ⁻¹)	y=0.30x -0.24	0.93	<0.0001*	63
BC	Precipitation (cm day ⁻¹)	event quickflow (cm day ⁻¹)	y=0.46x -0.28	0.84	<0.0001*	52
MH	Precipitation (cm day ⁻¹)	event quickflow (cm day ⁻¹)	y=0.59x -0.60	0.6	<0.0001*	52
all	Precipitation (cm day ⁻¹)	peak discharge (cm day ⁻¹)	y=0.26x-0.04	0.63	<0.0001*	168
BC	baseflow discharge (L s ⁻¹)	baseflow NO ₃ ⁻ (μmol L ⁻¹)	y=550x-0.27	0.61	0.001*	14
BC	base and storm discharge (L s ⁻¹)	base and storm NO ₃ ⁻ (μmol L ⁻¹)	y=690 x-0.37	0.77	<0.0001*	116
BC	base/storm cond (μS cm ⁻¹)	base and storm NO ₃ ⁻ (μmol L ⁻¹)	y=1.33x -37.5	0.79	<0.0001*	116
SF	baseflow cond (μS cm ⁻¹)	baseflow NO ₃ ⁻ (μmol L ⁻¹)	y=0.58x+248	0.008	0.18	110
SF	stormflow cond (μS cm ⁻¹)	stormflow NO ₃ ⁻ (μmol L ⁻¹)	y=2.01x-10.9	0.34	<0.0001*	112
MH	API7	runoff coefficient	y=0.09x+0.06	0.28	0.014*	21
MH	API14	runoff coefficient	y=0.06x-0.04	0.59	<0.001*	21
BC	API7	runoff coefficient	y=0.03x+0.23	0.3	0.01*	21
BC	API14	runoff coefficient	y=0.02x+0.19	0.29	0.01*	21
SF	API7	runoff coefficient	y=0.001-0.18	0.002	0.87	21
SF	API14	runoff coefficient	y=0.004-0.15	0.05	0.34	21
MH	API7	EMC TP (μmol L ⁻¹)	y=0.07x+0.76	0.24	0.32	6
MH	API7	EMC TN (μmol L ⁻¹)	y=0.07x+0.76	0.24	0.32	6
SF	API7	EMC NO ₃ ⁻ (μmol L ⁻¹)	y=-6.81x+242	0.2	0.45	5
BC	API7	EMC NO ₃ ⁻ (μmol L ⁻¹)	y=-5.02x+119	0.66	0.09	5
BC, SF	API7	EMC TP (μmol L ⁻¹)	y=0.70x+0.96	0.6	0.008*	10
BC, SF	event quickflow volume (m ³ day ⁻¹)	EMC PO ₄ ³⁻ (μmol L ⁻¹)	y=1.3*10 ⁻⁵ x +0.16	0.86	<0.001*	8
BC, SF	event total volume (m ³ day ⁻¹)	EMC TP (μmol L ⁻¹)	y=2.1*10 ⁻⁵ x +0.59	0.83	0.0002*	10
BC, SF	event total volume (m ³ day ⁻¹)	EMC NH ₄ ⁺ (μmol L ⁻¹)	y=4.8x10 ⁻⁵ -2.33	0.64	0.016*	8
SF	water yield (cm)	TN export (Kg ha ⁻¹ yr ⁻¹)	y=0.54x+1.129	0.86	<0.001*	9
SF	water yield (cm)	TP export (Kg ha ⁻¹ yr ⁻¹)	y=0.21x-0.23	0.39	0.07	9
MH	water yield (cm)	TN export (Kg ha ⁻¹ yr ⁻¹)	y=0.072x+0.023	0.99	<0.001*	6
MH	water yield (cm)	TP export (Kg ha ⁻¹ yr ⁻¹)	y=0.0025x+0.0025	0.99	<0.001*	6
all	runoff coefficient	watershed area (km ²)	y=0.04x-0.65	0.99	.03*	3
MH	stream temperature (°C)	baseflow NH ₄ ⁺ (μmol L ⁻¹)	y=0.02x ² -0.1x	0.19	0.008*	72
SF	stream temperature (°C)	baseflow NH ₄ ⁺ (μmol L ⁻¹)	y=0.22x+0.87	0.20	< 0.001*	100

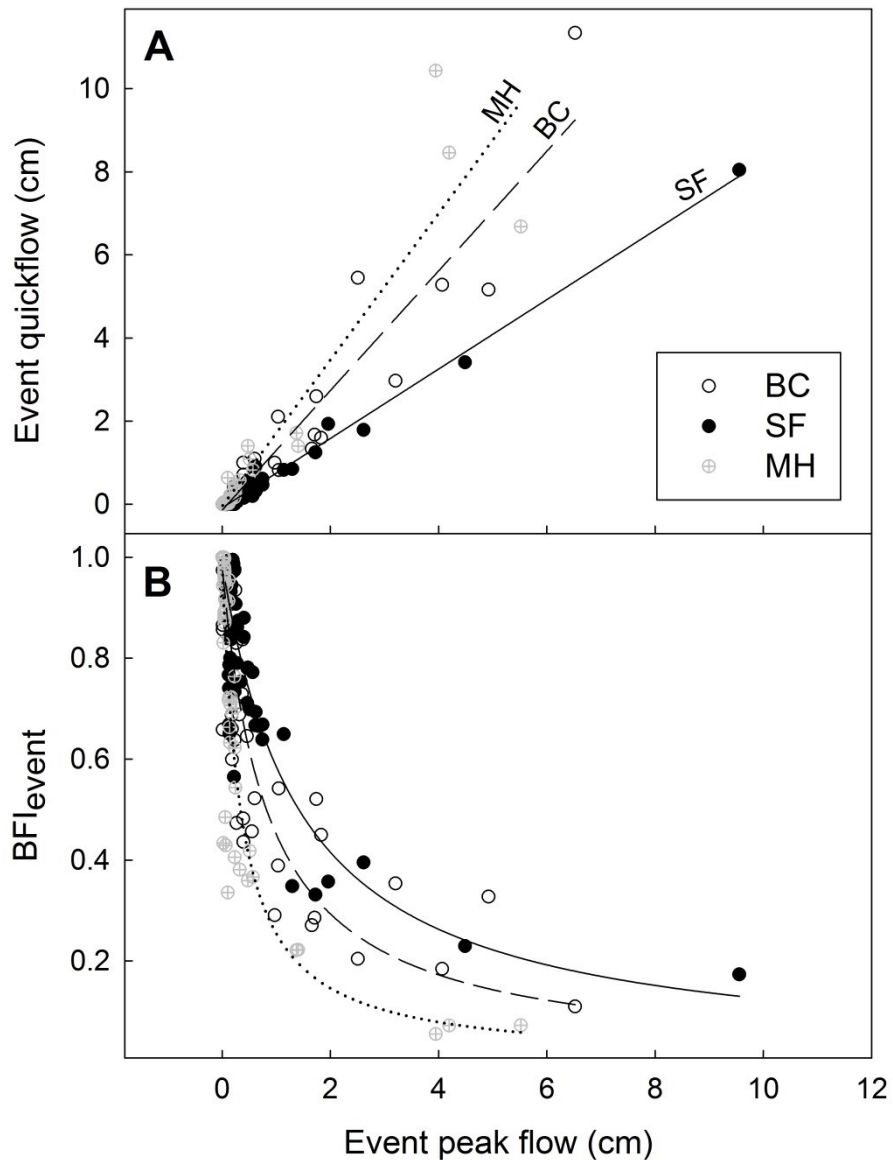


Figure 20. Top panel (A) shows the relationship between peak flow and quickflow (cm) with linear regressions for each watershed. BC and MH slopes were not significantly different, but they are both significantly greater than SF. The bottom panel (B) shows the negative non-linear relationship between peak flow and event base flow index (BFI_{event}).

Baseflow Chemistry

Monthly baseflow concentrations were variable, but some patterns emerged which were generally consistent with long term trends (Figure 21). At MH, NO_3^- was typically below 1 μM , but peaked from January to March. NH_4^+ remained low (< 2 μM) most of the year but a summer peak in concentration was observed from June to August. The observed patterns are consistent with the monthly average concentrations at MH since 2006, but TP and PO_4^{3-} were lower on average (Figure 21). In SF, NO_3^- and TN had a bimodal pattern with peaks in January and late summer (August-September). Warm season NH_4^+ peaks have also been observed at SF, but with greater variance. Patterns at SF generally agreed with long term monthly averages since 2004 (Figure 21). At both MH and SF, baseflow NH_4^+ concentrations were weakly but significantly related to stream temperature ($r^2 = 0.23$ and 0.19 respectively, $P < 0.001$) over the period of record (Figure 22, Table 11).

At BC, no patterns in monthly nutrient concentrations were observed except for NO_3^- , which was low in winter and high in summer. NO_3^- varied as an inverse power function with instantaneous streamflow during baseflow ($r^2 = 0.61$) as well as when combining all instantaneous stormflow and baseflow data ($r^2 = 0.77$, Figure 23c). NO_3^- was positively correlated with specific conductivity during baseflow ($r^2 = 0.84$) as well as all instantaneous base and stormflow measurements at BC ($r^2 = 0.79$, Figure 23b). A weak correlation between instantaneous stormflow measurements of conductivity and NO_3^- ($r^2 = 0.34$, Figure 23a) was observed at SF (Table 11); however, there were no similar baseflow relationships at SF and none at MH.

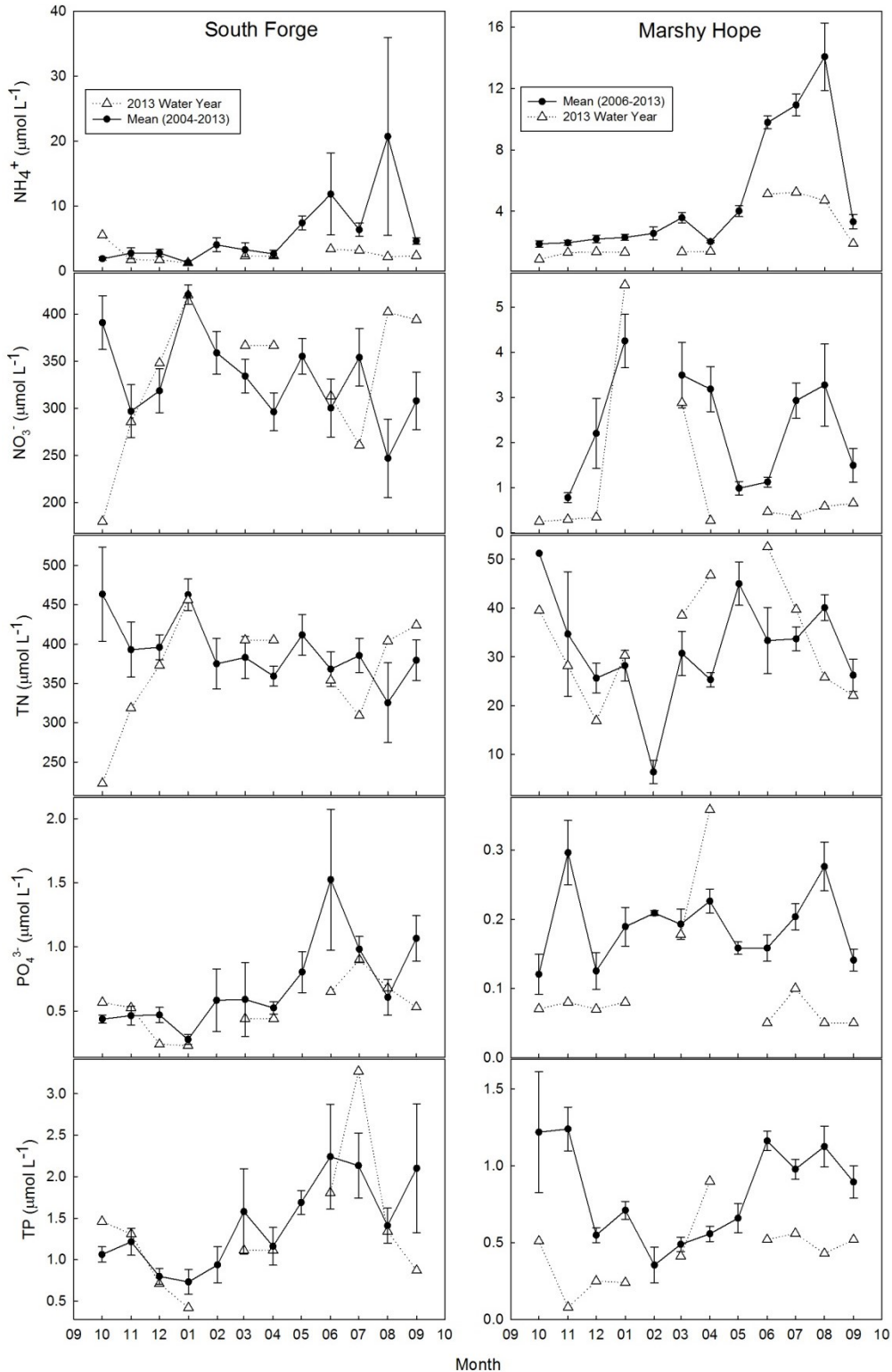


Figure 21. Left panel shows mean monthly concentrations (black circles) from 2004-2013 as well as data over the study period (white triangles) in the SF watershed. Right panel is the same but for the MH watershed and mean data is from 2006-2013

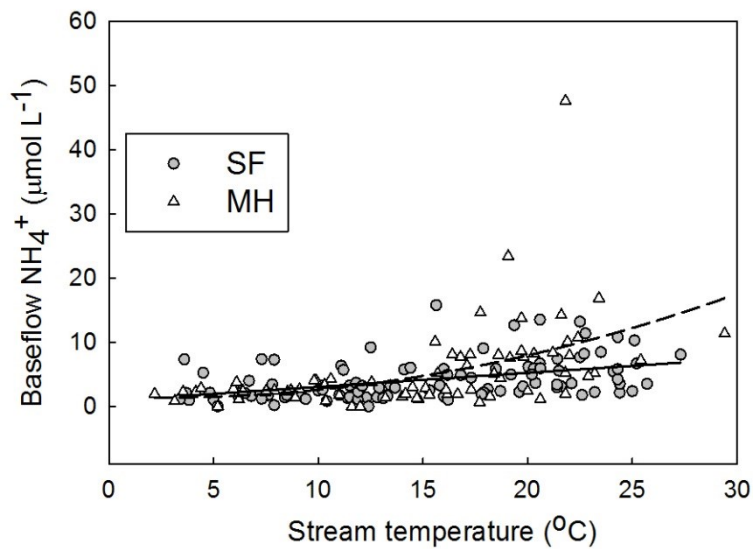


Figure 22. (A) Baseflow NH_4^+ concentration vs stream temperature at MH from 2006-2013 (quadratic-dashed line, $r^2 = 0.23$, $P = 0.008$), and SF from 2004-2013 (linear-solid line, $r^2 = 0.19$, $P < 0.001$).

Baseflow concentrations of NO_3^- , TN, PO_4^{3-} , and TP were consistent with what would be expected based on land use, and average concentrations of these constituents were significantly different between sites (Table 12, Figure 24). NH_4^+ was not different between any sites during baseflow and was a small fraction of the TN on average (7.2, 1.2, and 0.76% for MH, BC, and SF respectively). NO_3^- was small fraction of TN at MH in base (3.5%) and storm flow (4.9%), but was the dominant N species at BC and SF in base (77 and 91% of TN) and stormflow (54 and 67% of TN). PO_4^{3-} accounted for 37, 43, and 43% of TP in baseflow at MH, BC, and SF respectively. During stormflow, PO_4^{3-} was a lower proportion of TP: 12, 31, and 27% in MH, BC, and SF. Organic and/or particulates were the dominant forms of N and P at MH during all conditions.

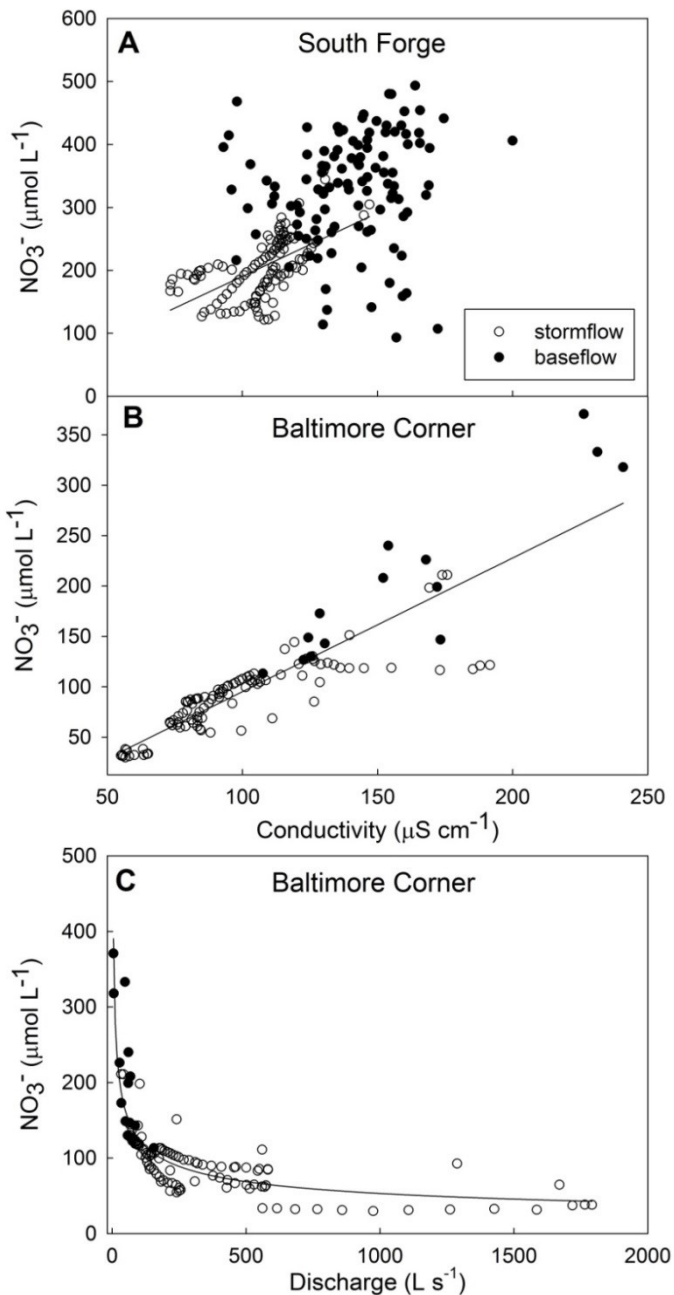


Figure 23. Top panel (A) shows instantaneous NO_3^- vs conductivity during base and stormflow, only stormflow was significant ($r^2 = 0.35, P < 0.0001$), in the SF watershed. (B) Shows the same for the BC watershed (base and storm, $r^2 = 0.79, P < 0.0001$). (C) Instantaneous NO_3^- concentration during base and stormflow vs discharge and in the BC watershed. An inverse power function was fit ($r^2 = 0.77, P < 0.0001$).

Table 12. P-values from Kruskal-Wallis tests. In the top panel, base and storm flow were compared within each site. In the bottom panel, baseflow concentrations were compared between sites. *Italics* highlight significant differences.

<u>Base vs. Storm flow</u>					
Site	PO4	TP	NH4	NO3	TN
BC	0.33	<i>0.045</i>	0.174	<i>0.0002</i>	<i>0.015</i>
MH	0.86	<i>0.002</i>	<i>0.047</i>	<i>0.02</i>	<i>0.016</i>
SF	0.17	<i>0.005</i>	0.146	<i>0.026</i>	0.126

<u>Comparison of baseflow between sites</u>					
BC-SF	0.327	0.66	0.415	<i>0.002</i>	<i>0.012</i>
BC-MH	<i>0.0002</i>	<i>0.007</i>	0.196	<i><0.0001</i>	<i><0.0001</i>
SF-MH	<i><0.0001</i>	<i>0.0002</i>	0.173	<i><0.0001</i>	<i><0.0001</i>

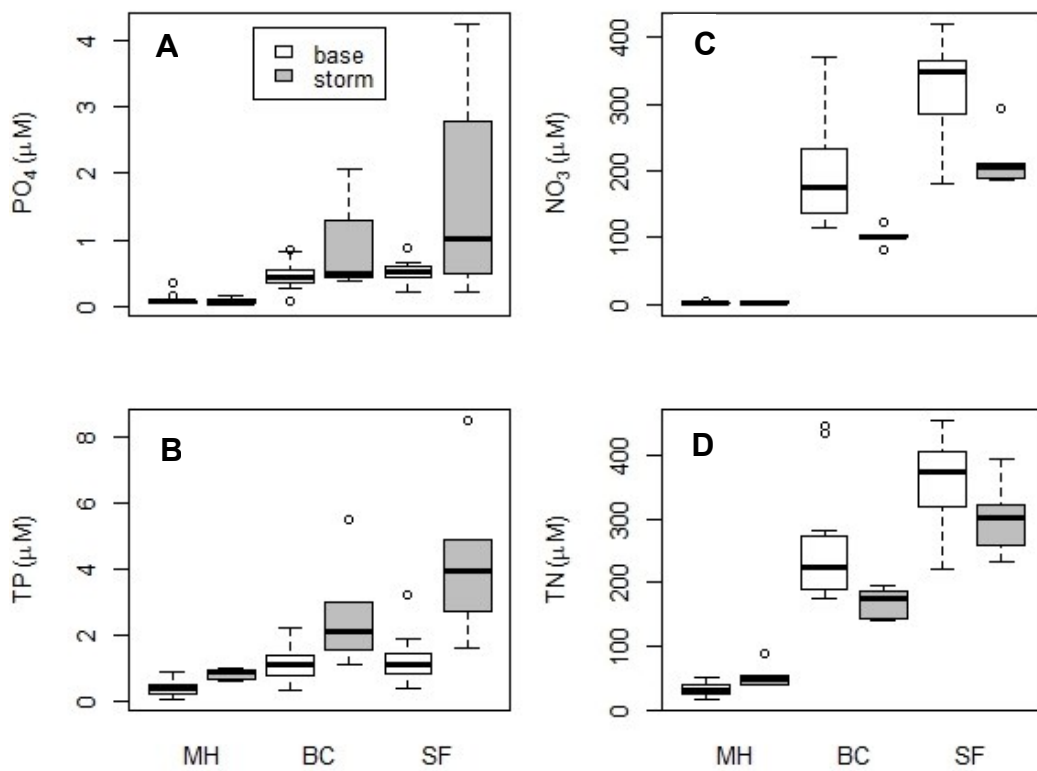


Figure 24. Comparison of baseflow and volume weighted stormflow concentrations in the MH, BC, and SF watersheds for (A) PO_4^{3-} , (B) TP, (C) NO_3^- , and (D) TN over the 2013 water year. Boxes indicate upper and lower quartiles with the mean (black line). Dashed lines indicate the variance with extremes indicated by white circles. See Table 5 for significant differences between sites as well as between base and storm flow. There is a clear land use effect on NO_3^- and TN during all conditions, but only during stormflow for PO_4^{3-} and TP.

Stormflow Chemistry

Stormflow chemistry was sampled during six events at MH and five at BC and SF from October 2012 to June 2013. The sampled storms represented a wide range of hydrologic characteristics (Table 13), but overall small sample size with bias towards the winter and spring of 2013 since there were few storms during the dry summer and fall of 2012. One fall storm (Hurricane Sandy) was captured, but only at MH due to flooded instrumentation at the other sites. Significant differences were detected between baseflow concentrations and EMC in each watershed for certain species of N and P (Figure 24; Table 12).

Examples of storm hydrographs and chemographs from each watershed are plotted in Figure 25-27. Only TP demonstrated a similar pattern, rising limb peaks, in all watersheds. The remaining nutrients exhibited different patterns depending on land use: the forested (MH) versus agricultural watersheds (BC and SF). At MH, TN had simultaneous peaks as TP, and NO_3^- sometimes demonstrated minor rising limb peaks. However, there was little to no variability in PO_4^{3-} and NH_4^+ during storms. BC and SF had similar responses. TP and PO_4^{3-} increased with discharge with rising limb peaks. NH_4^+ also generally increased with discharge, but often peaked on the falling limb in SF and the rising limb in BC. In both BC and SF, NO_3^- was diluted during all storms. Concentration was also plotted versus discharge instead of time to observe hysteresis patterns (Figure 28-30), which are discussed in more detail in the next section.

Table 13. Hydrologic characteristics of each sampled storm event, the mean of all storms detected by SARR, and mean of all storms that were greater than 2 cm over the 2013 water year. Date represents the storm start date.

Site	Sampling Start Date	Precip (cm)	Peak Q ($\text{m}^3 \text{s}^{-1}$)	API ₇	API ₁₄	Quick flow (cm)	Total flow (cm)	BFI _{event}	Runoff Coefficient
BC	12/21/12	2.5	1.05	3.60	7.94	0.82	1.80	0.54	0.32
BC	1/15/13	4.2	1.04	1.38	1.38	2.11	3.45	0.39	0.50
BC	2/8/13	1.4	0.18	0.99	3.63	0.10	0.25	0.60	0.07
BC	4/19/13	3.4	0.46	4.36	6.22	0.54	1.52	0.65	0.16
BC	6/6/13	12.4	3.21	7.10	8.36	2.97	4.60	0.35	0.24
Mean all events		2.60	0.74	3.54	6.25	0.92	1.6	0.71	0.20
mean all events >2 cm		5.27	1.57	4.01	7.11	2.13	3.17	0.46	0.35
MH	10/28/12	25.7	1.41	0.06	1.49	1.40	1.80	0.22	0.05
MH	12/21/12	2.2	0.16	1.91	5.02	0.10	0.35	0.71	0.05
MH	1/15/13	5.1	0.48	1.59	1.60	1.40	2.19	0.36	0.28
MH	2/8/13	1.8	0.25	0.75	2.94	0.27	0.91	0.70	0.15
MH	4/4/13	2.6	0.33	0.45	2.57	0.58	0.93	0.38	0.22
MH	4/19/13	3.0	0.25	3.00	4.89	0.37	0.80	0.54	0.12
Mean all events		2.6	0.42	2.82	5.72	0.68	0.94	0.72	0.14
mean all events >2 cm		5.46	0.94	2.15	4.91	2.08	1.65	0.50	0.24
SF	12/21/12	2.5	0.62	3.60	7.94	0.32	1.03	0.69	0.12
SF	1/15/13	4.2	0.75	1.38	1.38	0.61	1.70	0.64	0.15
SF	4/4/13	2.4	0.47	0.59	3.11	0.25	1.16	0.78	0.11
SF	4/19/13	3.4	0.48	6.22	4.36	0.36	1.64	0.78	0.11
SF	6/6/13	12.4	4.49	7.10	8.36	3.42	4.43	0.23	0.28
Mean all events		2.15	0.59	3.82	6.65	0.40	1.01	0.80	0.18
mean all events >2 cm		5.26	0.82	3.66	6.94	1.15	2.20	0.60	0.17

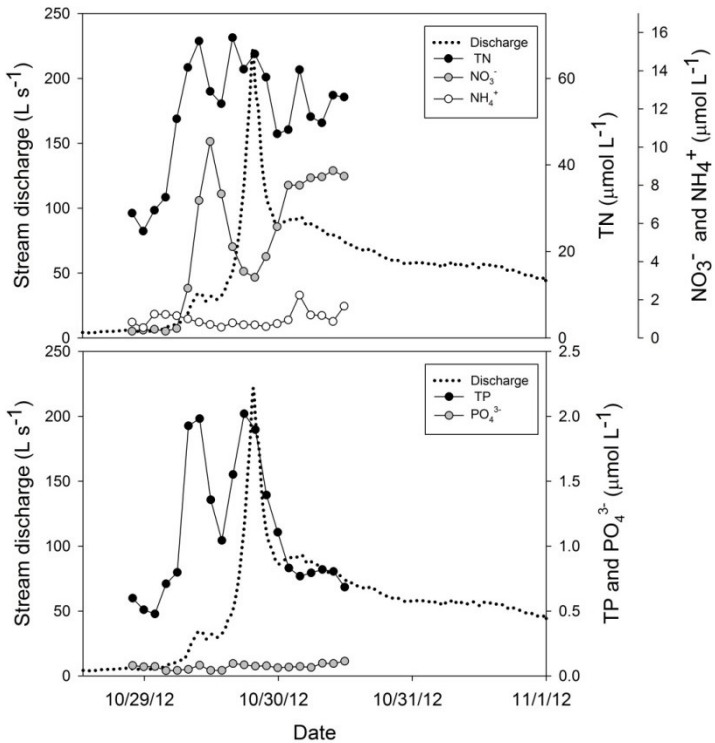


Figure 25. Hydrograph and chemographs for TN, NO_3^- , NH_4^+ (top), TP, and PO_4^{3-} (bottom) during the Hurricane Sandy (October 2012) in the MH watershed.

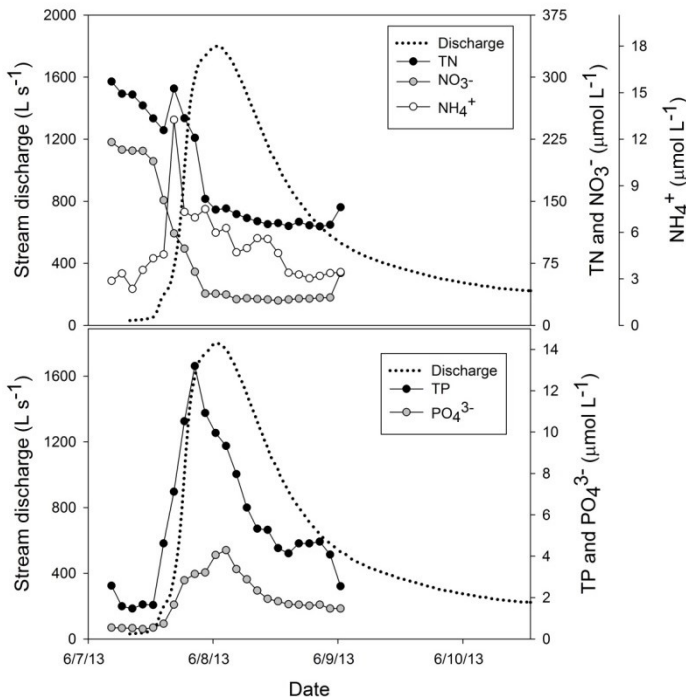


Figure 26. Hydrograph and chemographs for TN, NO_3^- , NH_4^+ (top), TP, and PO_4^{3-} (bottom) during the June 2013 storm in the BC watershed.

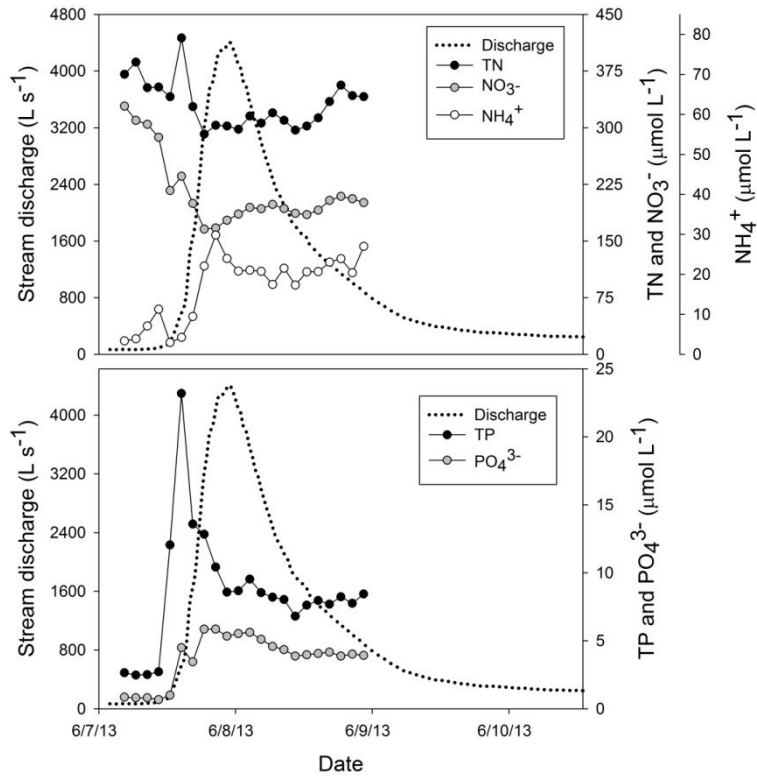


Figure 27. Hydrograph and chemographs for TN, NO₃⁻, NH₄⁺ (top), TP, and PO₄³⁻ (bottom) during the June 2013 storm in the SF watershed.

Annual Nutrient Export

Export (Kg ha⁻¹ yr⁻¹) reflected the amount of agricultural land use, and quickflow dominated annual nutrient export, except for TN and NO₃⁻ at SF (Figure 31). Over the 2013 WY, TN export was 3.9, 21, and 38 Kg N ha⁻¹ yr⁻¹ and TP was 0.10, 1.50, and 1.16 Kg P ha⁻¹ yr⁻¹ at MH, BC and SF respectively (Table 14). TN export was proportional to flow in all watersheds at the event scale (Figure 32) and also annually when comparing BFI and percent export in baseflow (Table 14). In contrast, quickflow accounted for a disproportionate fraction of the TP, PO₄³⁻, and NH₄⁺ export in BC and SF (Figure 32). However, at MH PO₄³⁻ and NH₄⁺ were more

dominated by baseflow as indicated by the % export in baseflow exceeding the annual BFI.

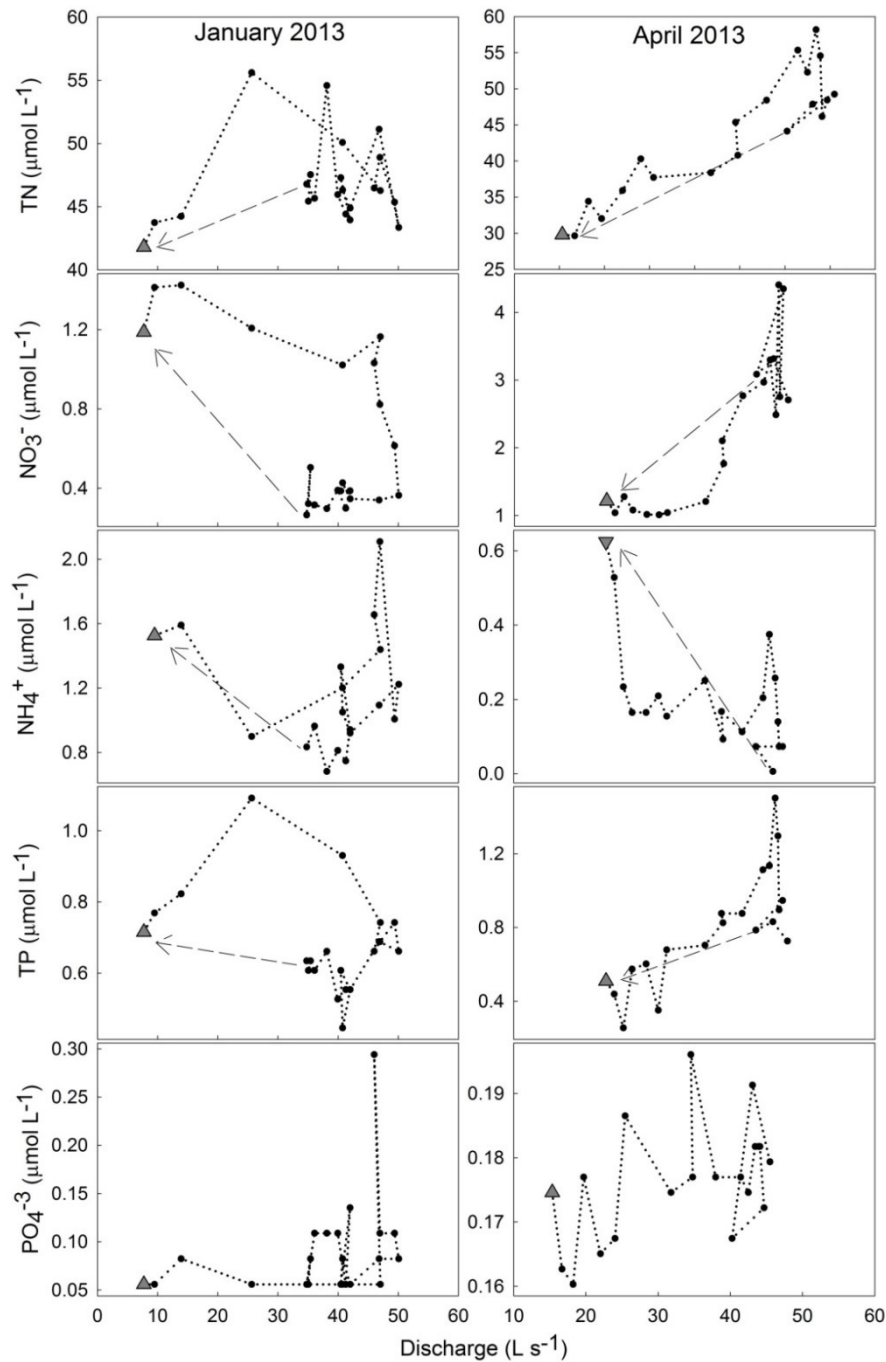


Figure 28. Concentration-Discharge plots for TN, NO₃⁻, NH₄⁺, TP, and PO₄³⁻ during a January (left) and April (right) storm in the MH watershed during 2013. Gray triangles show the starting point and indicate the initial direction (up or down). Dashed arrows connect the last measurement to the first showing extrapolation of hysteresis during recession.

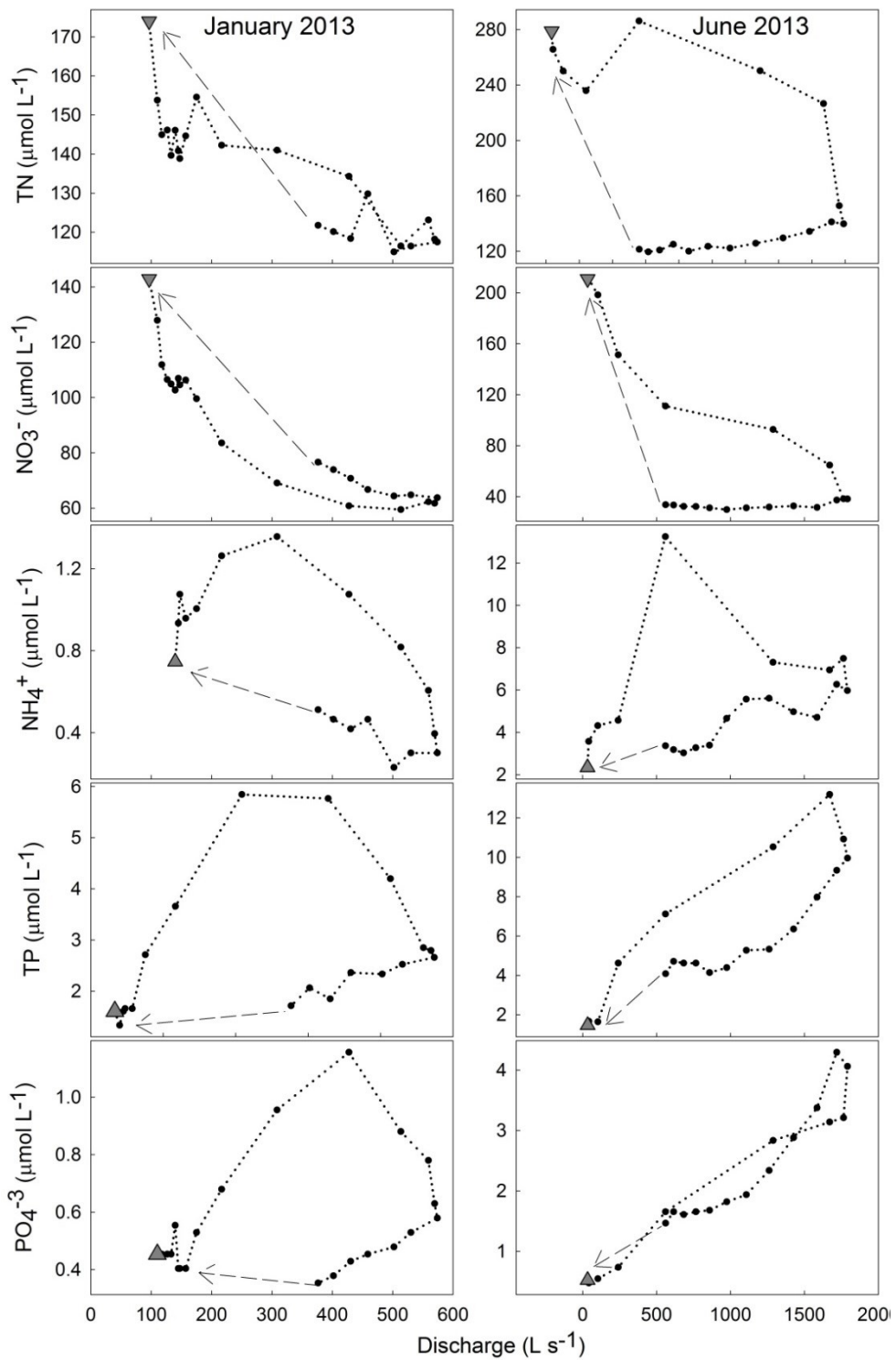


Figure 29. Concentration-Discharge plots for TN, NO_3^- , NH_4^+ , TP, and PO_4^{3-} during a January (left) and June (right) storm in the BC watershed during 2013. Gray triangles show the starting point and indicate the initial direction (up or down). Dashed arrows connect the last measurement to the first showing extrapolation of hysteresis during recession.

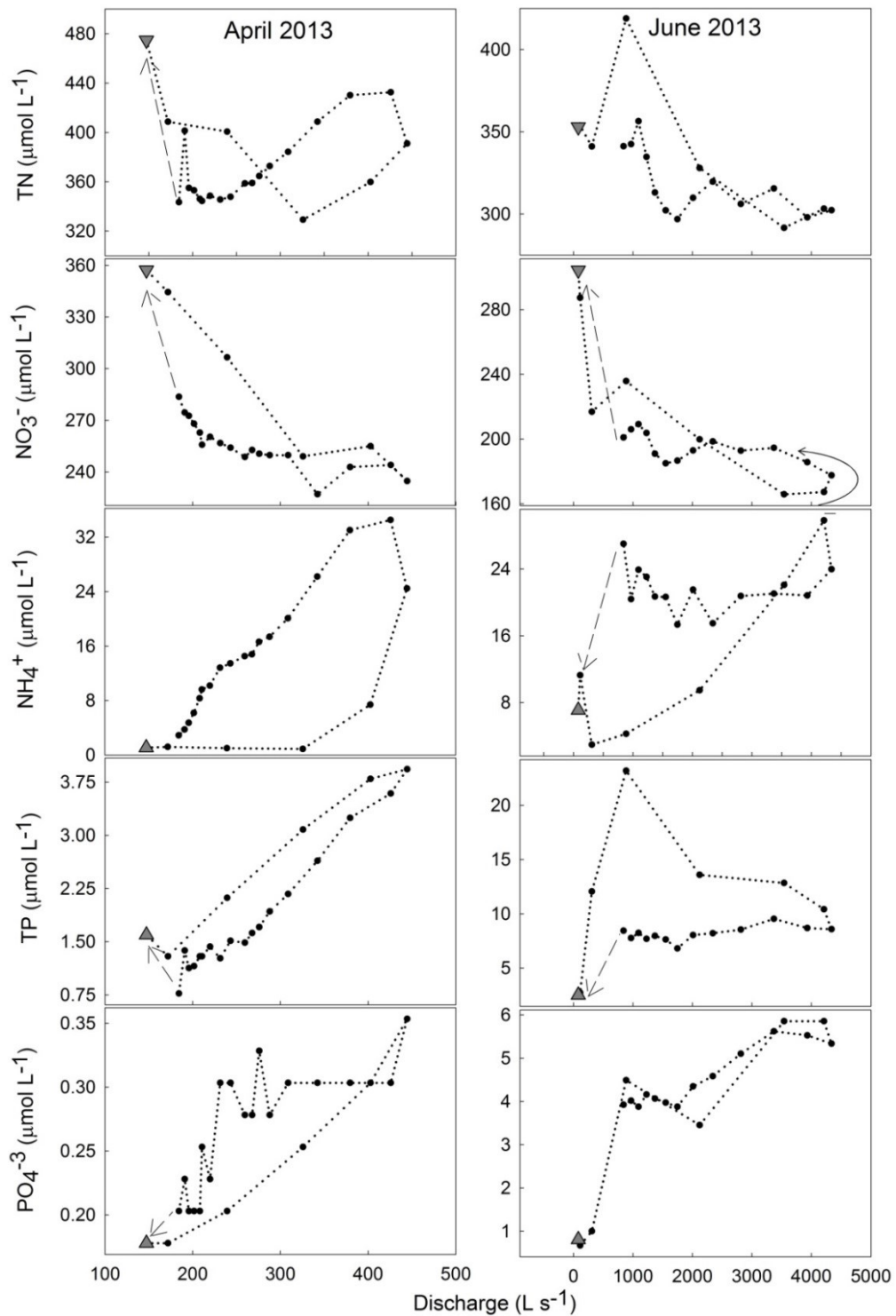


Figure 30. Concentration-Discharge plots for TN, NO₃⁻, NH₄⁺, TP, and PO₄³⁻ during an April (left) and June (right) storm in the SF watershed during 2013. Gray triangles show the starting point and indicate the initial direction (up or down). Dashed arrows connect the last measurement to the first showing extrapolation of hysteresis during recession.

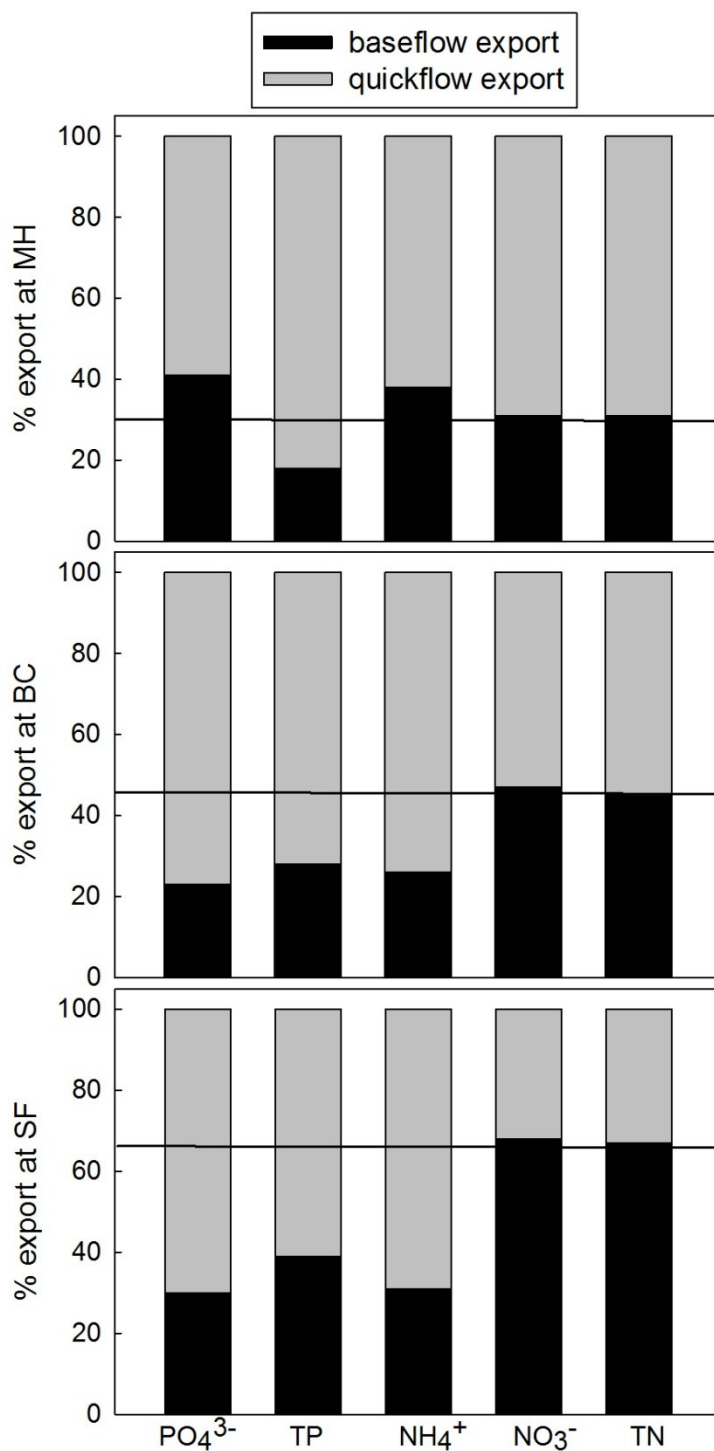


Figure 31. Proportion of annual export of PO_4^{3-} , TP, NH_4^+ , NO_3^- , and TN over the 2013 water year attributed to base (black) and quickflow (gray) in the MH (top), BC (middle), and SF (bottom) watersheds. The horizontal black line represents the annual Baseflow Index (BFI).

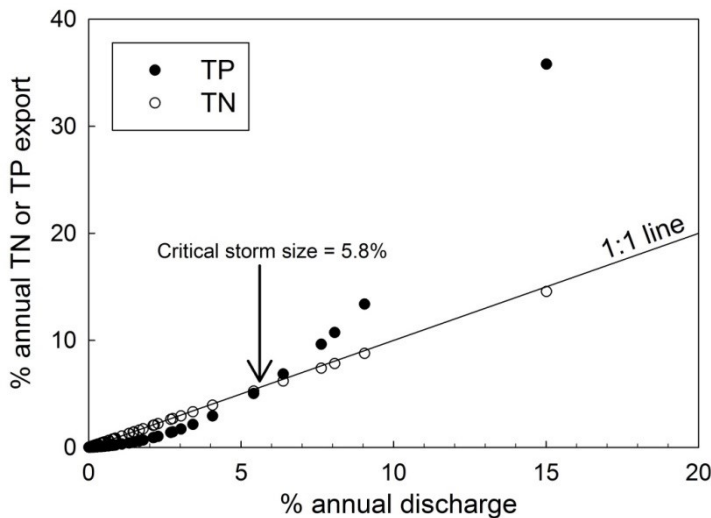


Figure 32. Relationship between % annual discharge and % annual export of TP and TN from individual storm events in the BC watershed. Sampled storm data was extrapolated to all unsampled events to estimate export. TP reaches a threshold storm size (5.8% of annual flow or $2.7 \text{ m}^3 \text{ s}^{-1}$), and export rapidly increases above the 1 to 1 line.

Table 14. Nutrient export ($\text{Kg ha}^{-1} \text{ yr}^{-1}$), annual BFI, and percent of annual export attributed to base and quickflow for the MH, BC, and SF watersheds as well as export ranges from the literature.

	PO_4^{3-}	NH_4^+	NO_3^-	TN	TP	annual BFI
<i><u>Marshy Hope</u></i>						
Export coefficients	0.02	0.10	0.16	3.89	0.12	0.32
% export in baseflow	41	38	31	31	18	
% export in quickflow	59	62	69	69	82	
<i><u>Baltimore Corner</u></i>						
Export coefficients ($\text{Kg ha}^{-1} \text{ yr}^{-1}$)	0.66	1.18	12.8	20.7	1.48	0.43
% export in baseflow	23	26	47	45	28	
% export in quickflow	77	74	53	55	72	
<i><u>South Forge</u></i>						
Export coefficients	0.46	1.02	24.4	38.1	1.16	0.65
% export in baseflow	30	31	68	67	39	
% export in quickflow	70	69	32	33	61	
Beaulac and Reckhow (1980)						
Forest				1.4-6.3	0.02-0.83	
Row crops				0.26-79	2.1-18	
Jordan et al. (1997)				0.86-15	0.083-1.3	

Data collected prior to 2012 at MH and SF demonstrated inter-annual variation in TN and TP export, as well as the proportion attributed to baseflow and quickflow. At MH, export was highly variable with TN ranging from 0.18 to 5.1 (mean = 2.8) and TP from 0.0007 to 0.18 (mean = 0.1) Kg ha⁻¹ yr⁻¹ (Figure 33). The proportions of TN and TP export attributed to baseflow were approximately equal each year, but varied inter-annually from 15 to 66% (Figure 33). At SF, TN and TP export varied from 15 to 42 (mean = 27.5) and 0.37 to 2.0 (mean = 0.80) Kg ha⁻¹ yr⁻¹ respectively (Figure 34). The proportion of TN exported by baseflow ranged from 52 to 83% and TP from 25 to 66% (Figure 34). As expected because of the autocorrelation of discharge and export, water yield and TN export were positively related at MH ($r^2 = 0.99$) and SF ($r^2 = 0.85$) TP was significantly correlated with water yield at MH ($r^2 = 0.99$, Table 11), but not at SF. Export during the 2013 WY was above average as a result of the above average water yield.

Discussion

Hydrology

Hydrologic response varied between the watersheds likely as a result of land use, watershed size, and soil properties. At the MH forested watershed, streamflow decreased during the growing season, ceased flowing during the summer of 2012 due to drought conditions, and peaked in late winter (Figure 16). This pattern is indicative of evapotranspiration (ET) and the poorly drained soils. At the BC and SF sites, large storms could recharge shallow groundwater, sustaining baseflow during periods of

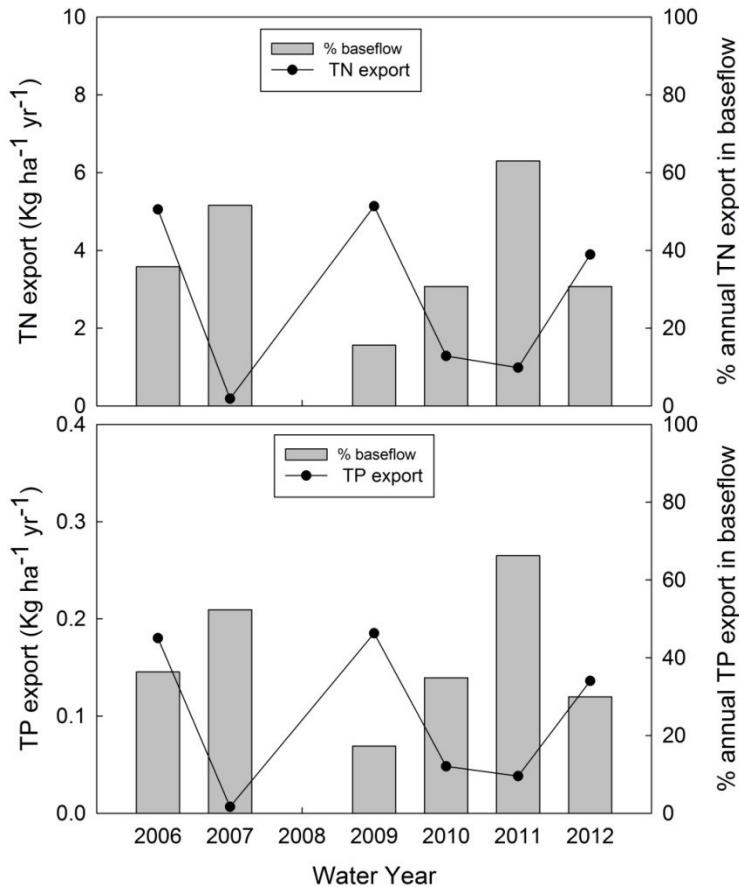


Figure 33. TN (top) and TP (bottom) annual export over water years 2006 to 2012 in the MH watershed as indicated by the line graph and left y-axis. Bar graphs (right y-axis) show the percent exported in baseflow, the remaining percent was due to stormflow. The 2008-2009 water year is not shown due to missing discharge data from instrument failure.

high ET (e.g. summer 2013; Figure 17-18). On average, water yields were higher in the agriculturally dominated watershed (SF) and ET was higher in the forested watershed (MH) (Table 10). This is consistent with the well-established link between decreasing forest cover and increasing water yields as a result of lower evapotranspiration (Bosch and Hewlett 1982; Farley et al. 2005).

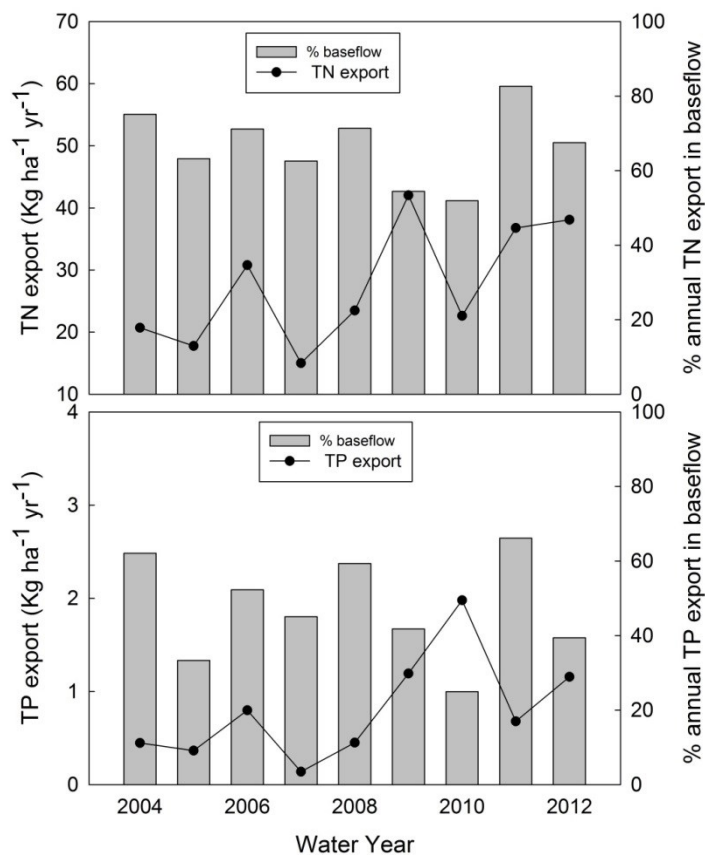


Figure 34. TN (top) and TP (bottom) annual export over water years 2005 to 2013 in the SF watershed as indicated by the line graph and left y-axis. Bar graphs (right y-axis) show the percent exported in baseflow, the remaining percent was due to stormflow.

Comparing annual BFI (SF > BC > MH) between the watersheds seems counter intuitive from a land use perspective, but is likely an effect of watershed size. As watershed size increases, streams generally become less “flashy” (Baker et al. 2004); therefore, baseflow conditions are dominant in streams draining larger areas. Applying the Richards-Baker flashiness Index (Baker et al. 2004) to these watersheds (0.68 for MH, 0.53 for BC, and 0.38 for SF), the smallest watershed (MH) was the flashiest following the same pattern as BFI and proportion of rainfall that becomes quickflow. Hydric soils may also play a role when comparing BC and SF. The SF watershed contains 34% hydric soils mostly in the floodplain as opposed to only 1%

in BC. Koskelo et al. (2012) demonstrated that annual BFI increased with percent hydric soils in adjacent agricultural watersheds as a result of increased ponding.

On an event basis, response also differed between the watersheds despite receiving similar precipitation inputs. The average fraction of precipitation became quickflow was greatest in MH and least in SF (Figure 19b), again likely an effect of watershed size. Smaller watersheds have shorter flowpaths before entering the stream network and converging at the outlet; therefore, MH generally exported a greater proportion of the rainfall as quickflow except under dry conditions. However, a sample size of three is too small to generalize beyond these data. Furthermore, there are drastic differences in the soil properties (i.e. % hydric) and their spatial arrangement which may have an impact on stormflow response.

Antecedent soil moisture conditions are often a strong control on hydrologic response (Dunne and Black 1970). The relationship between precipitation and quickflow appears to be influenced by antecedent soil moisture conditions in the MH watershed, but there is less evidence for this at BC and SF. When API₇ was less than one, the slope of quickflow versus precipitation regression dramatically decreased compared to events with API₇ greater than one (Figure 19c). However, this was driven by the largest precipitation event (Hurricane Sandy) which had a minor quickflow response. Hurricane Sandy far exceeded any precipitation event in the 2013 WY, but was only the 6th largest event by discharge at MH. This may reflect the ability of this forested watershed to retain large amounts of storm water under dry conditions. In the BC and SF watersheds, Hurricane Sandy was the largest discharge event, accounting for 15 and 13% of annual flow respectively.

Further evidence of the effect of antecedent soil moisture on storm response was provided by the significant positive correlation between runoff coefficient and API₇ and API₁₄ for storms with precipitation ≥ 2 cm or greater in the MH and BC watersheds, but not SF (Table 11). In the MH and BC watersheds, as antecedent soil moisture increased the proportion of the precipitation that became quickflow (runoff coefficient) increased. However, these correlations were not strong ($r^2 = 0.3\text{--}0.6$) and did not exist at SF. The API calculation used in this study is a simple proxy for soil moisture conditions that is useful in the absence of measurements, but it is not a comprehensive index that takes into account evapotranspiration or antecedent hydrologic conditions such as streamflow and water table elevation. Therefore, it is unlikely to be a strong predictor of stormflow response. Some studies have found antecedent hydrologic conditions and precipitation to be strongly related to runoff response (Heppel et al. 2002; James and Roulet 2007). In coastal plain watersheds of southern USA, Epps et al. (2013) did not find a correlation between API and runoff coefficients. However, they did find water table elevation and initial streamflow, both likely influenced by soil moisture conditions, to be important runoff controls. Macrae et al. (2010) found similar correlations as Epps et al. (2013), but no predictive relationships over a large number of storms and attributed this to the variability and non-linearity of hydrologic response to storm events.

The relationship between peak discharge and event quickflow (Figure 20a) suggests SARR accurately identified events and that both event quickflow and peak discharge describe event size. The difference in slopes between the watersheds implies that for a given peak discharge (i.e. storm size) more quickflow was produced

in MH and BC compared to SF. This effect can also be observed by the more rapid decrease in BFI_{event} as peak discharge increases at MH compared to SF (Figure 20b). Watershed size and perhaps soil properties likely play a role as previously discussed. Also, stream morphology may have an effect at BC which is 3.5 times larger than MH, yet the storm response was not significantly different between these watersheds. The BC stream network is mostly channelized, lacking riparian buffers, and is therefore by design routing floods more efficiently. In contrast, much of the SF network is buffered and has maintained its natural sinuosity and floodplain connectivity which is of course true at MH as well since it is relatively undisturbed.

At the event scale, SARR may have overestimated quickflow compared to hydrochemical baseflow separation methods (Koskelo et al. 2012). In a coastal plain watershed using hydrochemical methods, Eshleman et al. (1994) demonstrated that “old” water often dominated stream flow during events except during peak flow where “new” water could be significant. It should be noted that quickflow and baseflow are not necessarily synonymous with new and old water and different methods of baseflow separation yield variable results. SARR is best suited for flow separation at the annual scale; however, it is sensitive to baseflow increases during events and estimated a higher annual BFI than the UKIH smoothed minima approach (Koskelo et al. 2012). For the purpose of annual flow separation and analysis of many events, SARR is a practical and appropriate method for these small watersheds.

Phosphorus Sources and Transport Mechanisms

Event chemographs (Figure 25-27) and hysteresis patterns (Figure 28-30) indicate TP and PO_4^{3-} transport resulted from the erosive power of stream discharge

and overland flows. TP and PO_4^{3-} increased with discharge during all events in the three watersheds (except for MH storms with little change in PO_4^{3-}) and peaked on the rising limb indicating a first flush from near or in-stream sources. Sharpley and Syers (1979) demonstrated that 77% of the TP export was a result of streambank erosion and resuspension of material from the streambed, and that 29% of PO_4^{3-} was from *in-situ* desorption from particles. However, there were two storms in BC and one in SF where PO_4^{3-} peaked during the falling limb, perhaps indicating sources of desorption from a saturated soil matrix (Gatcher et al. 2004). Given the low topographic relief and less frequent overland flows in the coastal plain region, much of the P in stormflow likely originated from in-stream/riparian sources or overland flows intercepted by ephemeral upstream tributaries. The ultimate source of P in streams is overland flow pulses from agricultural fields that over time accumulate P in and near streams. Surficial soil P concentrations are known to be high in agricultural areas across the Delmarva Peninsula due to the legacy of poultry manure amendments (Sims 1998).

Organic P (PP + DOP) was the dominant form during storms as inferred from the difference between TP and PO_4^{3-} . Previous studies in adjacent Choptank catchments (Koskelo 2008) and elsewhere (Correll 1999; Jordan et al. 1997a) have demonstrated the importance of organic and/or particulate P during storms and found a strong correlation between TP and total suspended sediments (TSS). Sharpley et al. (2008) found storm size, as defined by return period (i.e. inverse probability a storm of a given size will occur), was related to storm P concentration. This is similar to the relationship found in this study between event flow and EMC of TP and PO_4^{3-} (Figure

15). To visualize the effect of storm size, Figure 32 shows the percent of annual TP export plotted versus percent of annual discharge accounted for by individual storms. This is not a predictive relationship given the autocorrelation of discharge and export, and TP export was empirically extrapolated to unsampled events. However, this plot may demonstrate the nature of P export in these agricultural watersheds. During small events, TP export is below the one to one line meaning less TP is exported proportional to discharge. A critical storm size is reached when the TP export curve exceeds the 1 to 1 line (~5.8% of annual discharge or $2.7 \text{ m}^3 \text{ s}^{-1}$), and TP export rapidly increases disproportionate to flow.

This critical storm size represents flows that suspend PP in the water column and/or the expansion of the stream network to include a larger source area. Variable source area hydrology (VSA, Dunne and Black 1970) is considered to play an important role in P transport (Pionke 1998; Grubek et al. 2002). As the water table rises the near stream zone becomes connected with the stream and saturation excess overland flow provides a pathway for surficial nutrients to enter the stream. Large storms in watersheds subject to VSA may have a compounding effect on TP transport due to increasing channel velocities as well as expanding source areas.

Antecedent soil moisture conditions are important to VSA hydrology and runoff generation. API₇ was directly related to EMC of TP from BC and SF watersheds ($r^2 = 0.60$, Table 11, Figure 35). Based on the positive correlations between API₇ and runoff coefficients as well as EMC of TP concentration, VSA is likely an important mechanism for P mobilization in these watersheds as well as much of the coastal plain given the low relief and typical concave hill slopes.

Management should focus on minimizing inputs and retaining P on the landscape as far away from streams and even riparian areas as possible.

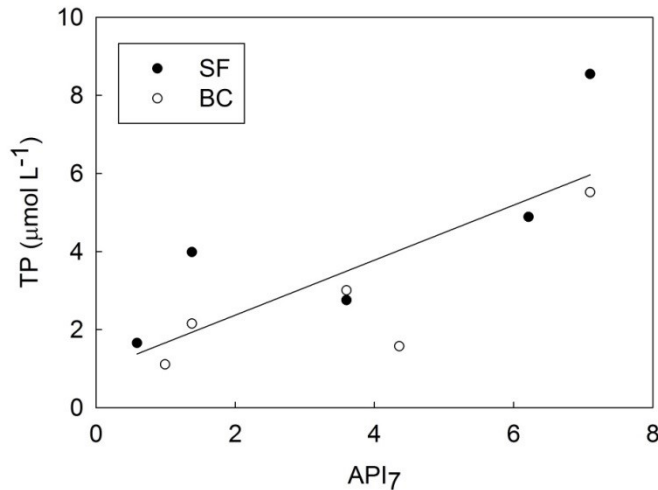


Figure 35. Relationship between event volume-weighted mean TP concentration and antecedent precipitation index (API_7) for the BC and SF watersheds ($r^2 = 0.60$, $P = 0.008$).

Nitrate Sources and Transport Mechanisms

Baseflow was the main supplier of NO_3^- to the agriculturally impacted streams, BC and SF. The consistent pattern of decreasing NO_3^- during storm events at SF and BC indicated a groundwater NO_3^- source that was diluted by new event water. This is consistent with the high groundwater NO_3^- concentrations observed in agricultural watersheds across the Choptank Basin (Fox et al. 2014; Fisher et al. 2010). According to the nearest NADP site (Wye Research Center, MD013), the mean volume weighted NO_3^- concentration in precipitation over the study period was 53 μM , which was 16 and 26% of the mean baseflow concentration at SF and BC respectively.

During storm events, the conflicting hysteresis trends at BC and SF suggest different hydrologic flowpaths or timing of NO_3^- transport. It is impossible to discern exactly why these contrasting patterns emerged given the small sample size of storms and lack of observations from other end members. However, hysteresis patterns in concentration-discharge plots may provide an explanation for the relative contributions of NO_3^- from ground, soil, and event water (Evans and Davies 1996; Chanat et al. 2002).

Only the two largest storms in BC exhibited hysteresis in NO_3^- (Figure 29). The large winter storm's counter clockwise pattern suggests that soil water contributed more NO_3^- relative to event water with high concentrations along the falling limb. NO_3^- may have accumulated in the vadose zone during the winter. Additionally, the water table was higher in January, and this storm was sufficiently large to activate subsurface flowpaths to the stream. Baseflow recession can supply a large N load to streams during such storms where soil NO_3^- is flushed (Jiang et al. 2010). The June 2013 storm's clockwise hysteresis suggests event water contributed more NO_3^- than soil water. This is unlikely, but possible if NO_3^- accumulated in surficial soils as a result of fertilization, and was transported to the stream via overland or quick subsurface flow. The BC (and SF) storms where no hysteresis was observed (i.e. NO_3^- was curvilinearly related to discharge) were likely not large enough to sufficiently raise the water table inducing additional flowpaths. This reflects a two end member mixing of high NO_3^- groundwater and low NO_3^- event water where NO_3^- behaves relatively conservatively.

In contrast to BC, the typical counter-clockwise or slight figure-eight hysteresis at SF (Figure 30) suggests soil water generally contributed more NO_3^- than event water, but only briefly during the falling limb when a figure-eight pattern was observed (Chanat et al. 2002). This could be a result of a slower subsurface quickflow response at SF given the prevalence of riparian hydric soils (Rusjan et al. 2008; Weiler and McDonnell 2006).

Clockwise hysteresis at BC and SF may also reflect the transition from hydrologic to biogeochemically controlled NO_3^- export as the hydrograph progresses. Clockwise hysteresis was only observed during the June 2013 storm at BC when biological rate processes (i.e. denitrification and uptake) are probably greater relative to the cool season. Clockwise patterns were observed during most events at SF which has an extensive and hydric riparian zone that could facilitate N removal. Ocampo et al. (2006) demonstrated that in low-relief hill slopes NO_3^- export during baseflow recession can shift from hydrologic to biogeochemical control, most likely as a result of riparian denitrification. Therefore, NO_3^- concentrations are slow to recover to baseflow levels following a storm. Other studies have explained similar mechanisms of biogeochemical control of NO_3^- in riparian zones associated with high flows and stream stage fluctuations (Gu et al. 2008; 2012). Data from a companion study (Gardner et al. in prep), reported high NO_3^- concentration in emerging groundwater in three BC stream reaches (mean = 226 μM , range = 0-1138 μM) compared to one SF reach (mean = 0.47 μM , range = 0.27-0.67 μM). This suggests the riparian zone of SF is actively removing agricultural NO_3^- , but in BC removal is relatively less efficient and spatially variable.

The relationship between discharge and NO_3^- may also point to hydrologic versus biogeochemical control of NO_3^- export or sources at the catchment scale. BC seems to be dominated by hydrology given the inverse power relationship between discharge and NO_3^- during base and stormflow (Figure 23c). NO_3^- concentrations were greatest during low flow indicating deep groundwater flowpaths may be an important NO_3^- source. Additionally, the contributing area contracts during low flow. Therefore, at the watershed outlet the stream water is fed almost exclusively by groundwater from adjacent agricultural fields, but this source is diluted by water from upland forested areas when the contributing area expands during the cool season. The conductivity and NO_3^- correlation at BC may support this idea of the water mixing from different source areas. Mixing occurs between the presumably low NO_3^- /conductivity water from forested areas and high NO_3^- /conductivity water from agricultural fields producing this linear relationship (Figure 23b). However, at SF (and MH) no relationships were observed between NO_3^- and discharge or conductivity. This may reflect the lack of upstream forest at SF (which are exclusively riparian) and/or a stronger biogeochemical control of NO_3^- export at both SF and MH.

Stormflow NO_3^- response at the forested MH differed greatly from the two agricultural watersheds and suggests an atmospheric NO_3^- source. The mean NO_3^- concentration in precipitation ($53 \mu\text{M}$, NADP) was much greater compared to baseflow ($1.1 \mu\text{M}$) and shallow riparian groundwater ($0.4 \mu\text{M}$, Bunnell-Young unpublished data). Direct precipitation and throughfall likely contributed to the minor NO_3^- peaks ($1-10 \mu\text{M}$) occurring on the rising limb. However, there were no

consistent hysteresis patterns. During Hurricane Sandy, the highest NO_3^- concentration at MH was recorded (10 μM) which peaked along the rising limb, was diluted by peak flow, and then increased again (Figure 25). The second NO_3^- peak was the only potential evidence of flushing soil NO_3^- since this event occurred following a severe summer drought when soil NO_3^- could accumulate and hydrologic transport could be delayed until after peak flow. Therefore, the hypothesis that MH would exhibit NO_3^- flushing behavior was not supported since when trivial increases in NO_3^- during storms were observed, it was likely a result of direct atmospheric inputs and throughfall with little to no flushing from soils.

Atmospheric N deposition has caused N saturation in many forests resulting in leaching of dissolved N during storm events (Aber et al. 1989; Aber et al. 2003). There is no sign of nitrogen saturation at MH, unlike many of the forested systems that have been studied in the eastern US (Stoddard 1994; Peterjohn et al. 1996; Driscoll et al. 2003). However, recent evidence indicates N export from forested watersheds is decreasing as a result of decreasing N deposition (Eshleman et al. 2013). MH has been monitored since 2006 with consistently low baseflow NO_3^- concentrations around 1 μM and often below the detection limit (<0.05 μM).

As opposed to the competing hydrologic/biogeochemical control of N export in the agricultural watersheds, MH seems to be tightly biologically controlled through biotic uptake as well as the frequently saturated, reducing terrestrial environment. In a forested watershed in Canada, Hill et al. (1999) proposed stream N chemistry could be controlled through biological utilization of limited terrestrial N even during storm

events. Entirely forested watersheds are rare on the Delmarva Peninsula, but those that exist may be an important sink for atmospheric N inputs.

Ammonium Sources and Transport Mechanisms

The similar long term seasonal patterns in NH_4^+ baseflow concentrations in the MH and SF streams suggest a biological control and wetland source (Inmadar 2007). Most of the upstream MH watershed is a forested wetland, and at SF the riparian zone contains many pockets of wetlands. During the warm season, NH_4^+ production across the watershed likely increases as a result of suppressed in-stream nitrification, due to low dissolved oxygen concentrations and flow, as well as enhanced N mineralization (Devito and Dillon 1993; McHale et al. 2004).

Consistent with baseflow patterns, storm events occurring under warmer conditions produced the largest NH_4^+ peaks compared to winter storms. In all cases, NH_4^+ increased during storms in BC and SF. However, contrasting hysteresis patterns suggested different sources or transport mechanisms. At SF, hysteresis was generally counter-clockwise, but clockwise or no hysteresis at BC (Figure 29). For BC this suggests NH_4^+ was primarily transported via overland flow, re-suspension of in-stream material, and/or desorption from streambanks similar to PO_4^{3-} (Gatcher et al. 2004). These processes also likely contributed to NH_4^+ mobilization at SF, but elevated falling limb concentrations and counter-clockwise hysteresis (Figure 30) indicated a subsurface flowpath (i.e. soil water source) or a delayed hydrologic pathway. Petry (2002) found rising limb peaks in NH_4^+ in agricultural catchments and attributed this to compacted riparian soils and animal production sources. SF does not

have compacted riparian soils, but small dairy operations are present near the headwaters.

Inamdar (2007) also found similar NH_4^+ patterns during storm events but in a forested watershed. Using detailed end member measurements, Inamdar (2007) concluded NH_4^+ in throughfall and litter leachate was an important source during storms and adjacent wetlands were the primary NH_4^+ source during baseflow. Average volume-weighted NH_4^+ concentration in precipitation over the 2013 WY was 17.0 μM (+/- 1.6). Therefore, throughfall may have been an important end member at BC and SF during cool season storms with small NH_4^+ peaks (1.4-8.1 μM), but additional sources would be necessary to produce the peaks observed during the warmer months (13- 34 μM). Spring fertilizer applications may have contributed to the June storm NH_4^+ export but would not have influenced sampling during earlier storm events.

The lack of NH_4^+ patterns during storms at MH and generally lower concentrations suggests atmospheric inputs may explain instances when minor peaks were observed on the rising limb (Figure 28). This result, as well as the on average higher baseflow concentrations compared to event volume weighted mean concentrations of NH_4^+ , does not agree with previous studies in forested systems. However, no summer storms were sampled, perhaps biasing this result. NH_4^+ concentrations in streams draining forested watersheds typically increase during storms compared to baseflow (Hill et al. 1999; Inamdar 2007). This may suggest there was little saturation excess overland flow mobilizing NH_4^+ from litter

leachate/throughfall and/or NH_4^+ was adsorbed within the soil matrix and perhaps biologically utilized during events.

Annual Base and Stormflow Export

Nutrient export ($\text{Kg ha}^{-1} \text{ yr}^{-1}$) from the study watersheds was comparable with previous studies in agricultural and forested systems. In row crop catchments, Beaulac and Reckhow (1980) reported TP and TN export ranges of 2.10-18.6 and 0.26-79.6 $\text{Kg ha}^{-1} \text{ yr}^{-1}$ with means of 4.46 and 16.09 $\text{Kg ha}^{-1} \text{ yr}^{-1}$ respectively. Forested systems had a TP export range of 0.02-0.83 $\text{Kg ha}^{-1} \text{ yr}^{-1}$ (mean = 0.24) and a TN range of 1.38 - 6.26 $\text{Kg ha}^{-1} \text{ yr}^{-1}$ (mean = 2.86). In Maryland Coastal Plain watersheds of comparable land use and size, Jordan et al. (1997a) reported TN and TP export ranges of 0.86-15.0 and 0.093-1.30 respectively, and observed an increase in TP export moving from outer to inner coastal plain. In SF and BC, TN export exceeded the range reported by Jordan et al. (1997a). This is likely a result of the greater than average precipitation and water yield occurring over the study period. TN and NO_3^- export scaled with land use as expected considering the correlation between land use and N concentration (Jordan et al. 1997b; Fisher et al. 2010); however, PO_4^{3-} , TP, and NH_4^+ did not scale with land use (Table 14). Despite having 2.5 times greater agricultural land use in the SF watershed compared to BC, export of PO_4^{3-} , TP, and NH_4^+ was higher in BC. This was likely an artifact of how event export was extrapolated with pooled SF and BC data. Also, event NH_4^+ export may be overestimated during the cool season since the temperature effect on NH_4^+ concentration could not be accounted for when extrapolating to unsampled storms. Putting these limitations aside, greater PO_4^{3-} , TP, and NH_4^+ export in BC compared to

SF may also reflect the differences between these watersheds. The lack of riparian buffers and extensive channelization of the BC stream network could enhance nutrient transport. Yarbro et al. (1984) demonstrated a channelized catchment exported more PP and NO_3^- compared to an un-channelized agricultural catchment in the southern coastal plain of North Carolina.

Quickflow dominated annual nutrient export with the exception of NO_3^- and TN in the SF watershed (Figure 31). However, when comparing the annual BFI to fraction exported in baseflow, TN and NO_3^- export were proportional to flow in all watersheds (Table 14). NO_3^- is primarily transported via groundwater flow, and therefore is often correlated with the amount of baseflow (Jordan et al. 1997b). TP, PO_4^{3-} and NH_4^+ export were disproportionate to discharge, meaning the percent exported during baseflow was lower than the BFI. Export was therefore truly dominated by quickflow. This is consistent with studies that have observed NO_3^- export proportional to flow and PO_4^{3-} and TP export primarily a result of quickflow (Vanni et al. 2001; Koskelo et al. 2008; Zhu et al. 2010).

When considering total event export for individual events not separated into base and quickflow components, the largest events were responsible for a substantial portion of P and NH_4^+ export at BC and SF. At SF, Hurricane Sandy was estimated to account for 46%, 60%, and 54% of the annual TP, PO_4^{3-} , and NH_4^+ export respectively. The second largest storm (6% annual flow) at SF was sampled and accounted for 10, 11.8, and 10.5% of the annual TP, PO_4^{3-} , and NH_4^+ export respectively. In BC, Hurricane Sandy supplied 35, 41, and 41% of the annual TP, PO_4^{3-} , and NH_4^+ export respectively. At MH, event export was approximately

proportional to discharge for all N and P forms. Hurricane Sandy was the largest sampled storm at MH which accounted for 3.3% of the annual discharge and 2.9 and 3.6% of the annual TN and TP export respectively.

Conclusions

- Large storm events were very important for transport of TP, PO_4^{3-} , and NH_4^+ in coastal plain agricultural watersheds, accounting for a disproportionate amount of annual export supporting our hypothesis. However, this hypothesis was only partially supported since TN was proportional to flow in all watersheds, and at the MH forested watershed quickflow had a relatively small impact on nutrient export.
- Annual TN and TP export the BC and SF watersheds was relatively high given their percent agriculture (26 and 65% respectively), indicating that small streams can be important nutrient sources. However, there was substantial inter-annual variation in export due to discharge variability.
- In agricultural watersheds, NO_3^- was the dominant N species during base and stormflow and groundwater was the source. Organic P (PP and DOP) was dominant during storms and was likely mobilized from in and near stream sources. NH_4^+ was a small portion of TN and largely from in and near stream sources. However, conflicting hysteresis patterns at BC and SF indicated subsurface flowpaths may be supplying NH_4^+ during baseflow recession at SF but not at BC.

- In the MH stream, N and P occurred predominantly in their organic forms during both base and stormflow. The NO_3^- source during storms was likely atmospheric. Warm season NH_4^+ peaks in baseflow were observed suggesting a wetland source due to depressed in-stream nitrification and enhanced mineralization.
- NO_3^- export in the BC watershed was largely hydrologically controlled. However, at SF there could be competing hydrologic and biogeochemical control. MH had a very limited N supply that is tightly controlled by biotic uptake and reducing conditions.
- Antecedent hydrologic conditions are important for quickflow generation and TP export. API₇, as a proxy for soil moisture conditions, was weakly but significantly correlated with runoff coefficient in two of the three watersheds as well as TP export in the agricultural watersheds.
- The recently developed SARR method (Koskelo et al. 2012) of baseflow separation provided accurate event identification and reliable separation at the annual scale for all watersheds.

References

- Aber JD, Goodale CL, Ollinger SV, et al. (2003) Is nitrogen deposition altering the nitrogen status of northeastern forests? *BioScience* 53:375–389.
- Aber JD, Nadelhoffer KJ, Steudler P, Melillo JM (1989) Nitrogen saturation in forest ecosystems. *BioScience* 39:378–386.
- Alexander RB, Boyer EW, Smith RA., et al. (2007) The role of headwater streams in downstream water quality. *Journal of the American Water Resources Association* 43:41–59. x
- Allan DJ (2004) Landscapes and riverscapes: The influence of land use on stream ecosystems. *Annual Review of Ecology, Evolution, and Systematics* 35:257–284.
- Baker DB, Richards RP, Loftus TT, Kramer JW (2004) A new flashiness index: Characteristics and applications to midwestern rivers and streams. *Journal of The American Water Resources Association* 40:503–522.
- Beaulac MN, Reckhow KH (1982) An examination of land use-nutrient export relationships. *Water Resources Bulletin* 18:1013–1024.
- Biron PM, Roy AG, Courschesne F, et al. (1999) The effects of antecedent moisture conditions on the relationship of hydrology to hydrochemistry in a small forested watershed. *Hydrological Processes* 13:1541–1555.
- Blanco AC, Nadaoka K, Yamamoto T, Kinjo K (2010) Dynamic evolution of nutrient discharge under stormflow and baseflow conditions in a coastal agricultural watershed in Ishigaki Island, Okinawa, Japan. *Hydrological Processes* 24:2601–2616.
- Bosch J and Hewlett J (1982) A review of catchment experiments to determine the effect of vegetation changes on water yield and evapotranspiration. *Hydrology* 55:2-23.
- Carpenter SR, Carcao NF, Correll DL, et al. (1998) Nonpoint pollution of surface waters with phosphorus and nitrogen. *Ecological Applications* 8:559–568.
- Chanat JG, Rice KC, Hornberger GM (2002) Consistency of patterns in concentration-discharge plots. *Water Resources Research* 38: WR000971.
- Christopher SF, Mitchell MJ, Mchale MR, et al. (2008) Factors controlling nitrogen release from two forested catchments with contrasting hydrochemical responses. *Hydrological Processes* 22:46–62.

- Cirmo, C.P., McDonnell JJ (1997) Linking the hydrologic and biogeochemical controls of nitrogen transport in near-stream zones of temperate-forested catchments: a review. *Journal of Hydrology* 199:88–120.
- Correll DL, Jordan TE, Weller DE (1999) Transport of nitrogen and phosphorus from Rhode River watersheds during storm events. *Water Resources* 35:2513–2521.
- Creed IF, Band LE, Foster NW, et al. (1996) Regulation of Nitrate-N Release from Temperate Forests: A Test of the N Flushing Hypothesis. *Water Resources Research* 32:3337–3354.
- Devito KJ and Dillon PJ (1993) The influence of hydrologic condition and Peat oxia on the phosphorus and nitrogen dynamics of a conifer swamp. *Water Resources Research* 2:2675–2685.
- Diaz RJ, Rosenberg R (2008) Spreading Dead Zones and Consequences for Marine Ecosystems. *Science* 321:926–929.
- Dillon PJ and Kirchner WB (1975) The effects of geology and land use on the export of phosphorus from watersheds. *Water Resources* 9:135–148.
- Driscoll CT, Whitall D, Aber J, et al. (2003) Nitrogen pollution in the Northeastern United States: sources, effects, and management options. *BioScience* 53:357–374.
- Dunne T, Black RD (1970) Partial area contributions to storm runoff in a small New England watershed. *Water Resources Research* 6:1296–1311.
- Epps TH, Hitchcock DR, Jayakaran AD, et al. (2013) Characterization of storm flow dynamics of headwater streams in the South Carolina lower coastal plain. *Journal of the American Water Resources Association* 49:76–89.
- Eshleman KN, Pollard JS, O'Brien AK (1994) Interactions between groundwater and surface water in a Virginia coastal plain watershed. 1. Hydrological flowpaths. *Hydrological Processes* 8:389–410.
- Eshleman KN, Sabo RD, Kline KM (2013) Surface water quality is improving due to declining atmospheric N deposition. *Environmental Science and Technology* 47:12193–12200.
- Evans C, Davies TD (1998) Causes of concentration/discharge hysteresis and its potential as a tool for analysis of episode hydrochemistry. *Water Resources Research* 34:129–137.

Fisher TR, Benitez JA, Lee K-Y, Sutton AJ (2006a) History of land cover change and biogeochemical impacts in the Choptank River basin in the mid Atlantic region of the US. *International Journal of Remote Sensing* 27:3683–3703.

Fisher TR, Gustafson AB, Koskelo AI, et al. (2010) The Choptank Basin in transition: intensifying agriculture, slow urbanization, and estuarine eutrophication. In *Coastal Lagoons: Systems of Natural and Anthropogenic Change* 137–168.

Fisher TR, Hagy III JD, Boynton WR, Williamns MR (2006b) Cultural eutrophication in the Choptank and Patuxent estuaries of Chesapeake Bay. *Limnology and Oceanography* 51:435–447.

Gachter R, Steingrubler SM, Reinhardt M, Wehrli B (2004) Nutrient transfer from soil to surface waters: Differences between nitrate and phosphate. *Aquatic Sciences* 66:117–122.

Gburek WJ, Drungil C, Srinivasan MS, et al. (2002) Variable-source area controls on phosphorus transport: Bridging the gap between research and design. *Journal of Soil and Water Conservation* 57:534–543.

Gu C, Anderson W, Maggi F (2012) Riparian biogeochemical hot moments induced by stream fluctuations. *Water Resources Research* WR011720.

Gu C, Hornberger GM, Herman JS, Mills AL (2008) Influence of stream-groundwater interactions in the streambed sediments on NO_3^- flux to a low-relief coastal stream. *Water Resources Research* WR006739.

Gustard A, Bullock A, Dixon JM, (1992) Low Flow Estimation in the United Kingdom. Report No. 108. Inst. of Hydrology, Wallingford, England, pp. 19–25.

Hagy JD, Boynton WR, Keefe CW, and Wood KV (2004) Hypoxia in the Chesapeake Bay, 1950–2001: Long-term changes in relation to nutrient loading and river flows. *Estuaries*. 27: 634– 658.

Hamilton PA, Denver JM, Phillips PJ, and Shedlock RJ (1993) Water-quality assessment of the Delmarva Peninsula, Delaware, Maryland, and Virginia: Effects of agricultural activities on, and distribution of, nitrate and other inorganic constituents in the surficial aquifer. USGS Open File Report 93-40.

Heppell CM, Worrall F, Burt TP, Williams RJ (2002) A classification of drainage and macropore flow in an agricultural catchment. *Hydrological Processes* 16:27–46.

Hill A (1993) Nitrogen dynamics of storm runoff in the riparian zone of a forested watershed. *Biogeochemistry* 20:19–44.

Hill AR, Kemp WA, Buttle JM, Goodyear D (1999) Nitrogen chemistry of subsurface storm runoff on forested Canadian Shield hillslopes. *Water Resources Research* 35:811–821.

Hornberger GM, Bencala KE, McKnight DM (1994) Hydrological controls on dissolved organic carbon during snowmelt in the Snake River near Montezuma, Colorado. *Biogeochemistry* 25:147–165.

Howarth R, Swaney D, Billen G, et al. (2012) Nitrogen fluxes from the landscape are controlled by net anthropogenic nitrogen inputs and by climate. *Frontiers in Ecology and the Environment* 10:37–43.

Inamdar SP, Christopher SF, Mitchell MJ (2004) Export mechanisms for dissolved organic carbon and nitrate during summer storm events in a glaciated forested catchment in New York, USA. *Hydrological Processes* 18:2651–2661.

Inamdar SP, Mitchell MJ (2006) Hydrologic and topographic controls on storm-event exports of dissolved organic carbon (DOC) and nitrate across catchment scales. *Water Resources Research* 42:W03421.

James AL, Roulet NT (2007) Investigating hydrologic connectivity and its association with threshold change in runoff response in a temperate forested watershed. *Hydrological Processes* 21:3391–3408.

Jiang R, Woli KP, Kuramochi K, et al. (2010) Hydrological process controls on nitrogen export during storm events in an agricultural watershed. *Soil Science and Plant Nutrition* 56:72–85.

Jordan TE, Correll DL, Weller DE (1997a) Effects of agriculture on discharges of nutrients from coastal plain watersheds of Chesapeake Bay. *Journal of Environment Quality* 26:836–848.

Jordan TE, Correll DL, Weller DE (1997b) Relating nutrient discharges from watersheds to land use and streamflow variability. *Water Resources* 33:2579–2590.

Kemp WM, Boynton WR, Adolf JE, et al. (2005) Eutrophication of Chesapeake Bay: historical trends and ecological interactions. *Marine Ecology Progress Series* 303:1–29.

Koskelo AI (2008) Hydrologic and biogeochemical storm response in the Choptank Basin headwaters. MS Thesis, University of Maryland.

Koskelo AI, Fisher TR, Utz RM, Jordan TE (2012) A new precipitation-based method of baseflow separation and event identification for small watersheds ($<50\text{km}^2$). *Journal of Hydrology* 450-451:267–278.

Lee K, Fisher TR, Jordan TE, et al. (2000) Modeling the hydrochemistry of the Choptank River Basin using GWLF and Arc/Info:1. Model calibration and validation. *Biogeochemistry* 49:143–173.

Macrae ML, English MC, Schiff SL, Stone M (2010) Influence of antecedent hydrologic conditions on patterns of hydrochemical export from a first-order agricultural watershed in Southern Ontario, Canada. *Journal of Hydrology* 389:101–110.

McDonnell JJ, Owens IF, Stewart MK (1991) A case study of shallow flow paths in a steep zero-order basin. *Water Resources Bulletin* 27:679–685.

Mcdowell RW, Biggs BJF, Sharpley AN, Nguyen L (2004) Connecting phosphorus loss from agricultural landscapes to water quality. *Chemistry and Ecology* 20:1–40.

McHale MR, Cirmo CP, Mitchell MJ, McDonnell JJ (2004) Wetland nitrogen dynamics in an Adirondack forested watershed. *Hydrological Processes* 18:1853–1870.

McHale MR, McDonnell JJ, Mitchell MJ, Cirmo CP (2002) A field-based study of soil water and groundwater nitrate release in an Adirondack forested watershed. *Water Resources Research*. 38:WR000102.

Mitchell MJ, Driscoll CT, Kahl JS, et al. (1996) Climatic control of nitrate loss from forested watersheds in the Northeast United States. *Environmental science & technology* 30:2609–2612.

Morgan RP, Kline KM (2011) Nutrient concentrations in Maryland non-tidal streams. *Environmental monitoring and assessment* 178:221–235.

Nixon SW (1995) Coastal marine eutrophication: A definition, social causes, and future concerns. *Ophelia* 41:199–219.

Norton MM, Fisher TR (2000) The effects of forest on stream water quality in two coastal plain watersheds of the Chesapeake Bay. *Ecological Engineering* 14:337–362.

Novak JM, Stone KC, Watts DW, Johnson MH (2003) Dissolved phosphorus transport during storm and baseflow conditions from an agriculturally intensive southeastern coastal plain watershed. *American Society of Agricultural Engineers* 46:1355–1363.

Novotny V and Olem H (1994) Water Quality: Prevention, Identification, and Management of Diffuse Pollution. New York: Van Nostrand Reinhold.

Ocampo CJ, Oldham CE, Sivapalan M, Turner J V (2006) Hydrological versus biogeochemical controls on catchment nitrate export: a test of the flushing mechanism. *Hydrological Processes* 20:4269–4286.

Owens LB, Edwards WM, Keuren RW (1991) Baseflow and stormflow transport of nutrients from mixed agricultural watersheds. *Journal of Environment Quality* 20:407–414.

Owens LB, Shipitalo MJ, Bonta JV (2008) Water quality response times to pasture management changes in small and large watersheds. *Journal of Soil and Water Conservation* 63:292–299.

Peterjohn WT, Adams M, Gilliam F (1996) Symptoms of nitrogen saturation in two central Appalachian hardwood forest ecosystems. *Biogeochemistry* 35:507–522.

Petry J, Soulsby C, Malcolm IA, Youngson AF (2002) Hydrological controls on nutrient concentrations and fluxes in agricultural catchments. *The Science of the Total Environment* 294:95–110.

Pionke HB, Gburek WJ, Sharpley AN, Zollweg JA (1998) Chapter 10: Hydrological and chemical controls on phosphorus loss from catchments. In *Phosphorus loss from soil to water*, pp 225–242. CAB International.

Poor CJ, McDonnell JJ (2007) The effects of land use on stream nitrate dynamics. *Journal of Hydrology* 332:54–68.

Rusjan S, Brilly M, Mikoš M (2008) Flushing of nitrate from a forested watershed: An insight into hydrological nitrate mobilization mechanisms through seasonal high-frequency stream nitrate dynamics. *Journal of Hydrology* 354:187–202.

Schaefer SC, Alber M (2007) Temperature controls a latitudinal gradient in the proportion of watershed nitrogen exported to coastal ecosystems. *Biogeochemistry* 85:333–346.

Sharpley AN, Chapra SC, Wedepohl R, et al. (1994) Managing agricultural phosphorus for protection of surface waters: Issues and options. *Journal of Environmental Quality* 23:437–451.

Sharpley AN, Gburek WJ, Folmar G, Pionke HB (1999) Sources of phosphorus exported from an agricultural watershed in Pennsylvania. *Agricultural Water Management* 41:77–89.

Sharpley AN, Syers JK (1979) Phosphorus inputs into a stream draining an agricultural watershed II: Amounts contributed and relative significance of runoff types. *Water, Air, and Soil Pollution* 11:417–428.

- Sharpley, Andrew N Kleinman PJA, Heathwaite LA, Gburek WJ, et al. (2008) Phosphorus Loss from an Agricultural Watershed as a Function of Storm Size. *Journal of Environmental Quality* 37:362–368.
- Sims JT, Simard RR, Joern BC (1998) Phosphorus loss in agricultural drainage: Historical perspective and current research. *Journal of Environment Quality* 27:277–293.
- Sobota DJ, Harrison JA, Dahlgren RA (2009) Influences of climate, hydrology, and land use on input and export of nitrogen in California watersheds. *Biogeochemistry* 94:43–62.
- Steinberg PD, Brett MT, Bechtold JS, et al. (2010) The influence of watershed characteristics on nitrogen export to and marine fate in Hood Canal, Washington, USA. *Biogeochemistry*.
- Stoddard JL (1994) Long-term changes in watershed retention of nitrogen. In *Environmental Chemistry of Lakes and Reservoirs*; Baker, L. A., Ed.; Advances in Chemistry Series 237; American Chemical Society: Washington, DC, pp 223–284.
- Valderrama (1981) The simultaneous analysis of total nitrogen and total phosphorus on natural waters. *Marine Chemistry*. 10:109-122.
- Vanni MJ, Renwick WH, Jenifer L, et al. (2001) Dissolved and particulate nutrient flux from three adjacent agricultural watersheds: A five-year study. *Biogeochemistry* 54:85–114.
- Weiler M, McDonnell JJ (2006) Testing nutrient flushing hypotheses at the hillslope scale: A virtual experiment approach. *Journal of Hydrology* 319:339–356. d
- Yarbro LA, Kuenzler EJ, Mulholland PJ, Sniffen RP (1984) Effects of stream channelization on exports of nitrogen and phosphorus from North Carolina coastal plain watersheds. *Environmental Management* 8:151–160.
- Zhu Q, Schmidt JP, Bryant RB (2012) Hot moments and hot spots of nutrient losses from a mixed land use watershed. *Journal of Hydrology* 414-415:393–404.
- Zhu Q, Schmidt JP, Buda AR, et al. (2011) Nitrogen loss from a mixed land use watershed as influenced by hydrology and seasons. *Journal of Hydrology* 405:307–315.

Overall Bibliography

- Aber JD, Goodale CL, Ollinger SV, et al. (2003) Is nitrogen deposition altering the nitrogen status of northeastern forests? *BioScience* 53:375–389.
- Aber JD, Nadelhoffer KJ, Steudler P, Melillo JM (1989) Nitrogen saturation in forest ecosystems. *BioScience* 39:378–386.
- Alexander RB, Boyer EW, Smith RA., et al. (2007) The role of headwater streams in downstream water quality. *Journal of the American Water Resources Association* 43:41–59. x
- Allan DJ (2004) Landscapes and riverscapes: The influence of land use on stream ecosystems. *Annual Review of Ecology, Evolution, and Systematics* 35:257–284.
- Andersen JM (1977) Rates of denitrification of undisturbed sediment from six lakes as a function of nitrate concentration, oxygen and temperature. *Archives Hydrobiologia* 80:147-159.
- Baker DB, Richards RP, Loftus TT, Kramer JW (2004) A new flashiness index: Characteristics and applications to midwestern rivers and streams. *Journal of The American Water Resources Association* 40:503–522.
- Baulch HM, Schiff SL, Maranger R, Dillon PJ (2011) Nitrogen enrichment and the emission of nitrous oxide from streams. *Global Biogeochemical Cycles* GB004047.
- Baulch HM, Venkiteswaran JJ, Dillon PJ, Maranger R (2010) Revisiting the application of open-channel estimates of denitrification. *Limnology and Oceanography: Methods* 8:4–6.
- Beaulac MN, Reckhow KH (1982) An examination of land use-nutrient export relationships. *Water Resources Bulletin* 18:1013–1024.
- Beaulieu JJ, Arango CP, Hamilton SK, Tank JL (2008) The production and emission of nitrous oxide from headwater streams in the Midwestern United States. *Global Change Biology* 14:878–894.
- Beaulieu JJ, Tank JL, Hamilton SK, et al. (2011) Nitrous oxide emission from denitrification in stream and river networks. *Proceedings of the National Academy of Sciences of the United States of America* 108:214–9.
- Benitez JA, Fisher TR (2004) Historical land-cover conversion (1665-1820) in the Choptank watershed, eastern United States. *Ecosystems* 7:219–232.

Biron PM, Roy AG, Courschesne F, et al. (1999) The effects of antecedent moisture conditions on the relationship of hydrology to hydrochemistry in a small forested watershed. *Hydrological Processes* 13:1541–1555.

Blanco AC, Nadaoka K, Yamamoto T, Kinjo K (2010) Dynamic evolution of nutrient discharge under stormflow and baseflow conditions in a coastal agricultural watershed in Ishigaki Island, Okinawa, Japan. *Hydrological Processes* 24:2601–2616.

Bohlke JK, Denver JM (1995) Combined use of groundwater dating, chemical, and isotopic analyses to resolve the history and fate of nitrate contamination in two agricultural watersheds, Atlantic coastal plain, Maryland. *Water Resources Research* 31:2319–2339.

Bosch J and Hewlett J (1982) A review of catchment experiments to determine the effect of vegetation changes on water yield and evapotranspiration. *Hydrology* 55:2-23.

Burnett WC, Dulaiova H (2003) Estimating the dynamics of groundwater input into the coastal zone via continuous radon-222 measurements. *Journal of Environmental Radioactivity* 69:21–35.

Cable JE, Bugna GC, Burnett WC, Chanton JP (2014) Application of ^{222}Rn of and CH^4 for assessment of groundwater discharge to the coastal ocean. *Limnology and Oceanography* 41:1347–1353.

Canion A, Kostka JE, Gihring TM, et al. (2014) Temperature response of denitrification and anammox reveals the adaptation of microbial communities to in situ temperatures in permeable marine sediments that span 50° in latitude. *Biogeosciences* 11:309–320.

Carpenter SR, Caraco NF, Correll DL, et al. (1998) Nonpoint pollution of surface waters with phosphorus and nitrogen. *Ecological Applications* 8:559–568.

Chanat JG, Rice KC, Hornberger GM (2002) Consistency of patterns in concentration-discharge plots. *Water Resources Research* 38: WR000971.

Christopher SF, Mitchell MJ, McHale MR, et al. (2008) Factors controlling nitrogen release from two forested catchments with contrasting hydrochemical responses. *Hydrological Processes* 22:46–62.

Cirino, C.P., McDonnell JJ (1997) Linking the hydrologic and biogeochemical controls of nitrogen transport in near-stream zones of temperate-forested catchments: a review. *Journal of Hydrology* 199:88–120.

Colt J (1984) Computation of dissolved gas concentrations in water as functions of temperature, salinity, and pressure. Special publication No. 14 of the American Fisheries Society.

Cook PG, Favreau G, Dighton JC, Tickell S (2003) Determining natural groundwater influx to a tropical river using radon, chlorofluorocarbons and ionic environmental tracers. *Journal of Hydrology* 277:74–88.

Correll DL, Jordan TE, Weller DE (1999) Transport of nitrogen and phosphorus from Rhode River watersheds during storm events. *Water Resources* 35:2513–2521.

Creed IF, Band LE, Foster NW, et al. (1996) Regulation of Nitrate-N Release from Temperate Forests: A Test of the N Flushing Hypothesis. *Water Resources Research* 32:3337–3354.

Davidson EA, Seitzinger S (2006) The enigma of progress in denitrification research. *Ecological applications: a publication of the Ecological Society of America* 16:2057–63.

Devito KJ and Dillon PJ (1993) The influence of hydrologic condition and Peat oxia on the phosphorus and nitrogen dynamics of a conifer swamp. *Water Resources Research* 2:2675–2685.

Diaz RJ (2001) Overview of hypoxia around the world. *Journal of Environmental Quality* 30:275–81.

Diaz RJ, Rosenberg R (2008) Spreading Dead Zones and Consequences for Marine Ecosystems. *Science* 321:926–929.

Dillon PJ and Kirchnr WB (1975) The effects of geology and land use on the export of phosphorus from watersheds. *Water Resources* 9:135–148.

Dimova NT, Burnett WC (2011) Evaluation of groundwater discharge into small lakes based on the temporal distribution of radon-222. *Limnology and Oceanography* 56:486–494.

Driscoll CT, Whitall D, Aber J, et al. (2003) Nitrogen pollution in the Northeastern United States: sources, effects, and management options. *BioScience* 53:357–374.

Duff H, Triska F (1990) Denitrification in sediments from the hyporheic zone adjacent to a forested stream. *Canadian Journal of Fisheries and Aquatic Sciences* 47:1140–1147.

Dulaiova H, Camilli R, Henderson PB, Charette MA (2010) Coupled radon, methane and nitrate sensors for large-scale assessment of groundwater discharge and non-point source pollution to coastal waters. *Journal of environmental radioactivity* 101:553–63.

Dunkle SA, Plummer LN, Busenberg E, Phillips PJ, Denver JM, Hamilton PA, Michel RL, and Coplen TB (1993) Chlorofluorocarbons (CCl_3F and CCl_2F_2) as dating tools and hydrologic tracers in shallow groundwater of the Delmarva Peninsula, Atlantic Coastal Plain, United States. *Water Resources Research*. 29: 3837–3860.

Dunne T, Black RD (1970) Partial area contributions to storm runoff in a small New England watershed. *Water Resources Research* 6:1296–1311.

Ellins KK, Roman-Mas A, Lee R (1990) Using ^{222}Rn to examine groundwater/surface discharge interaction in the rio Grande de Mantai, Puerto Rico. *Journal of Hydrology* 115:319–341.

Epps TH, Hitchcock DR, Jayakaran AD, et al. (2013) Characterization of storm flow dynamics of headwater streams in the South Carolina lower coastal plain. *Journal of the American Water Resources Association* 49:76–89.

Eshleman KN, Pollard JS, O'brien AK (1994) Interactions between groundwater and surface water in a Virginia coastal plain watershed. 1. Hydrological flowpaths. *Hydrological Processes* 8:389–410.

Eshleman KN, Sabo RD, Kline KM (2013) Surface water quality is improving due to declining atmospheric N deposition. *Environmental Science and Technology* 47:12193–12200.

Evans C, Davies TD (1998) Causes of concentration/discharge hysteresis and its potential as a tool for analysis of episode hydrochemistry. *Water Resources Research* 34:129–137.

Fisher DC, Oppenheimer M (1991) Atmospheric nitrogen deposition and the Chesapeake Bay. *Ambio* 20:102–108.

Fisher TR, Benitez JA, Lee K-Y, Sutton AJ (2006a) History of land cover change and biogeochemical impacts in the Choptank River basin in the mid Atlantic region of the US. *International Journal of Remote Sensing* 27:3683–3703.

Fisher TR, Gustafson AB, Koskelo AI, et al. (2010) The Choptank Basin in transition: intensifying agriculture, slow urbanization, and estuarine eutrophication. In *Coastal Lagoons: Systems of Natural and Anthropogenic Change* 137–168.

Fisher TR, Hagy III JD, Boynton WR, Williamns MR (2006b) Cultural eutrophication in the Choptank and Patuxent estuaries of Chesapeake Bay. *Limnology and Oceanography* 51:435–447.

Forster P, Ramaswamy V, Artaxo P, Berntsen T, Betts R, Fahey DW, Haywood J, Lean J, Lowe DC, Myhre G, Nganga J, Prinn R, Raga G, Schulz M, Van Dorland R (2007) Changes in Atmospheric Constituents and in Radiative Forcing. In: *Climate Change 2007. The Physical Science Basis. Contribution of Working Group I to the Fourth Assessment Report of the Intergovernmental Panel on Climate Change* [Solomon, S., D. Qin, M. Manning, Z. Chen, M. Marquis, K.B. Averyt, M.Tignor and H.L. Miller (eds.)]. Cambridge University Press, Cambridge, United Kingdom and New York, NY, USA.

Fox RJ, Fisher TR, Gustafson AB, et al. (2014) Searching for the missing nitrogen: biogenic nitrogen gases in groundwater and streams. *The Journal of Agricultural Science*.

Gachter R, Steingruber SM, Reinhardt M, Wehrli B (2004) Nutrient transfer from soil to surface waters: Differences between nitrate and phosphate. *Aquatic Sciences* 66:117–122.

Garcia HE, Gordon LI (1992) Oxygen solubility in seawater: Better fitting equations. *Limnology and Oceanography* 37:1307–1312.

Garcia-Ruiz R, Pattinson SN, Whitton BA (1998) Denitrification in river sediments: relationship between process rate and properties of water and sediment. *Freshwater Biology* 39:467–476.

Gburek WJ, Drungil C, Srinivasan MS, et al. (2002) Variable-source area controls on phosphorus transport: Bridging the gap between research and design. *Journal of Soil and Water Conservation* 57:534–543.

Genereux DP, Hemond HF, Mulholland PJ (1993) Use of radon-222 and calcium as tracers in a three-end-member mixing model for streamflow generation on the West Fork of Walker Branch Watershed. *Journal of Hydrology* 142:167–211.

Golterman HL (2004) *The Chemistry of Phosphate and Nitrogen Compounds in Sediments*. Kluwer Academic Publishers , Dorsrecht.

Groffman PM, Altabet MA, Böhlke JK, et al. (2006) Methods for measuring denitrification: diverse approaches to a difficult problem. *Ecological Applications* 16:2091–2122.

Gu C, Anderson W, Maggi F (2012) Riparian biogeochemical hot moments induced by stream fluctuations. Water Resources Research WR011720.

Gu C, Hornberger GM, Herman JS, Mills AL (2008) Influence of stream-groundwater interactions in the streambed sediments on NO_3^- flux to a low-relief coastal stream. Water Resources Research WR006739

Gustard A, Bullock A, Dixon JM, (1992) Low Flow Estimation in the United Kingdom. Report No. 108. Inst. of Hydrology, Wallingford, England, pp. 19–25.

Hagy JD, Boynton WR, Keefe CW, and Wood KV (2004) Hypoxia in the Chesapeake Bay, 1950–2001: Long-term changes in relation to nutrient loading and river flows. *Estuaries*. 27: 634– 658.

Hamilton PA, Denver JM, Phillips PJ, and Shedlock RJ (1993) Water-quality assessment of the Delmarva Peninsula, Delaware, Maryland, and Virginia: Effects of agricultural activities on, and distribution of, nitrate and other inorganic constituents in the surficial aquifer. USGS Open File Report 93-40.

Hamme RC, Emerson SR (2004) The solubility of neon, nitrogen and argon in distilled water and seawater. *Deep Sea Research Part I* 51:1517–1528.

Harrison J, Matson P (2003) Patterns and controls of nitrous oxide emissions from waters draining a subtropical agricultural valley. *Global Biogeochemical Cycles* 17:1080.

Harrison JA, Matson PA, Fendorf SE (2005) Effects of a diel oxygen cycle on nitrogen transformations and greenhouse gas emissions in a eutrophied subtropical stream. *Aquatic Sciences* 67:308–315.

Hasegawa K, Hanaki K, Matsuo T, Hidaka S (2000) Nitrous oxide from the agricultural water system contaminated with high nitrogen. *Chemosphere - Global Change Science* 2:335–345.

Heaton TH., Vogel JC (1981) “Excess air” in groundwater. *Journal of Hydrology* 50:201–216.

Hemond HF, Duran AP (1989) Fluxes of N_2O at the sediment-water and water-atmosphere boundaries of a nitrogen-rich river. *Water Resources Research* 25:839–846.

Heppell CM, Worrall F, Burt TP, Williams RJ (2002) A classification of drainage and macropore flow in an agricultural catchment. *Hydrological Processes* 16:27–46.

Higgins TM, McCutchan JH, Lewis WM (2008) Nitrogen ebullition in a Colorado plains river. *Biogeochemistry* 89:367–377.

Hill A (1993) Nitrogen dynamics of storm runoff in the riparian zone of a forested watershed. *Biogeochemistry* 20:19–44.

Hill AR (1983) Denitrification: its importance in a river draining an intensively cropped watershed. *Agriculture, Ecosystems & Environment*. 10:47-62.

Hill AR, Devito KJ, Campagnolo S, Sanmugadas K (2000) Subsurface denitrification in a forest riparian zone : Interactions between hydrology and supplies of nitrate and organic carbon. *Biogeochemistry* 51:193–223.

Hill AR, Kemp WA, Buttle JM, Goodyear D (1999) Nitrogen chemistry of subsurface storm runoff on forested Canadian Shield hillslopes. *Water Resources Research* 35:811–821.

Hornberger GM, Bencala KE, McKnight DM (1994) Hydrological controls on dissolved organic carbon during snowmelt in the Snake River near Montezuma, Colorado. *Biogeochemistry* 25:147–165.

Howarth R, Swaney D, Billen G, et al. (2012) Nitrogen fluxes from the landscape are controlled by net anthropogenic nitrogen inputs and by climate. *Frontiers in Ecology and the Environment* 10:37–43.

Howarth RW, Elmgren R, Caraco N, et al. (1996) Regional nitrogen budgets and riverine N & P fluxes for the drainages to the North Atlantic Ocean : Natural and human influences. *Biogeochemistry* 35:75–139.

Inamdar SP, Christopher SF, Mitchell MJ (2004) Export mechanisms for dissolved organic carbon and nitrate during summer storm events in a glaciated forested catchment in New York, USA. *Hydrological Processes* 18:2651–2661.

Inamdar SP, Mitchell MJ (2006) Hydrologic and topographic controls on storm-event exports of dissolved organic carbon (DOC) and nitrate across catchment scales. *Water Resources Research* 42:W03421.

Jahne B, Heinz G, Dietrich W (1987) Measurement of the diffusion coefficients of sparingly soluble gases in water. *Journal of Geophysical Research* 92:10767–10776.

James AL, Roulet NT (2007) Investigating hydrologic connectivity and its association with threshold change in runoff response in a temperate forested watershed. *Hydrological Processes* 21:3391–3408.

Jiang R, Woli KP, Kuramochi K, et al. (2010) Hydrological process controls on nitrogen export during storm events in an agricultural watershed. *Soil Science and Plant Nutrition* 56:72–85.

Jordan TE, Correll DL, Weller DE (1997a) Effects of agriculture on discharges of nutrients from coastal plain watersheds of Chesapeake Bay. *Journal of Environment Quality* 26:836–848.

Jordan TE, Correll DL, Weller DE (1997b) Relating nutrient discharges from watersheds to land use and streamflow variability. *Water Resources* 33:2579–2590.

Jordan TE, Weller DE (1996) Human contributions to terrestrial nitrogen flux. *Bioscience* 46:655–664.

Kana TM, Darkangelo C, Hunt MD, et al. (1994) Membrane inlet mass spectrometer for rapid environmental water samples. *Analytical Chemistry* 66:4166–4170.

Kemp WM, Boynton WR, Adolf JE, et al. (2005) Eutrophication of Chesapeake Bay: historical trends and ecological interactions. *Marine Ecology Progress Series* 303:1–29.

Kies A, Hofmann H, Tosheva Z, et al. (2005) Using ^{222}Rn for hydrograph separation in a micro basin (Luxembourg). *Annals of Geophysics* 48:101–107.

Knee KL, Jordan TE (2013) Spatial distribution of dissolved radon in the Choptank River and its tributaries: Implications for groundwater discharge and nitrate inputs. *Estuaries and Coasts* 36:1237–1252.

Knowles R (1982) Denitrification. *Microbiology Reviews*. 46:43-70.

Koskelo AI (2008) Hydrologic and biogeochemical storm response in the Choptank Basin headwaters. MS Thesis, University of Maryland.

Koskelo AI, Fisher TR, Utz RM, Jordan TE (2012) A new precipitation-based method of baseflow separation and event identification for small watersheds ($<50\text{km}^2$). *Journal of Hydrology* 450-451:267–278.

Kroeze C, Seitzinger SP (1998) Nitrogen inputs to rivers, estuaries and continental shelves and related nitrous oxide emissions in 1990 and 2050: a global model. *Nutrient Cycling in Agroecosystems* 52:195–212.

Kroeze C, Seitzinger SP, Domingues R (2001) Future trends in worldwide river nitrogen transport and related nitrous oxide emissions: a scenario analysis. *The Scientific World Journal* 1:328–35.

Kulkarni M V, Groffman PM, Yavitt JB (2008) Solving the global nitrogen problem: it's a gas! *Frontiers in Ecology and the Environment* 6:199–206.

LaMontagne MG, Duran R, Valiela I (2003) Nitrous oxide sources and sinks in coastal aquifers and coupled estuarine receiving waters. *The Science of the total environment* 309:139–49.

Lamontagne S, Cook PG (2007) Estimation of hyporheic water residence time in situ using ^{222}Rn disequilibrium. *Limnology and Oceanography: Methods* 5:407–416.

Laursen A, Seitzinger S (2005) Limitations to measuring riverine denitrification at the whole reach scale: effects of channel geometry, wind velocity, sampling interval, and temperature inputs of N_2 -enriched groundwater. *Hydrobiologia* 545:225–236.

Laursen AE, Seitzinger SP (2002) Measurement of denitrification in rivers: an integrated, whole reach approach. *Hydrobiologia* 67–81.

Laursen AE, Seitzinger SP (2004) Diurnal patterns of denitrification, oxygen consumption and nitrous oxide production in rivers measured at the whole-reach scale. *Freshwater Biology* 49:1448–1458.

Lee K, Fisher TR, Jordan TE, et al. (2000) Modeling the hydrochemistry of the Choptank River Basin using GWLF and Arc/Info:1. Model calibration and validation. *Biogeochemistry* 49:143–173.

Lee RW and Hollyday EF (1993) Use of radon measurements in Carters Creek, Maury County, Tennessee, to determine location and magnitude of ground-water seepage, in *Field Studies of Radon in Rocks, Soils, and Water*, edited by L. C. S. Gundersen and R. B. Wanty. 237–242, C. K. Smoley, Boca Raton, Fl.

Liss PS and Slater PG (1974) Flux of gases across the air-sea interface. *Nature*. 247:181–184.

Lowrance R, Altier L, Newbold J, et al. (1997) Water Quality Functions of Riparian Forest Buffers in Chesapeake Bay Watersheds. *Environmental management* 21:687–712.

Macrae ML, English MC, Schiff SL, Stone M (2010) Influence of antecedent hydrologic conditions on patterns of hydrochemical export from a first-order agricultural watershed in Southern Ontario, Canada. *Journal of Hydrology* 389:101–110.

Malard F, Hervant F (1999) Oxygen supply and the adaptations of animals in groundwater. *Freshwater Biology* 41:1–30.

Marzolf ER, Mulholland PJ, and Steinman AD (1994) Improvements to the diurnal upstream-downstream dissolved-oxygen change technique for determining whole-stream metabolism in small streams. Canadian Journal of Fisheries and Aquatic Science. 51:1591–1599.

McCutchan JH, Lewis WM (2008) Spatial and temporal patterns of denitrification in an effluent-dominated plains river. Verh Internat Verein Limnol. 30:323–328.

McCutchan JH, Lewis WM, Saunders JF (1998) Uncertainty in the estimation of stream metabolism from open-channel oxygen concentrations. Journal North American Benthological Society 17:155–164.

McCutchan JH, Saunders JF, Pribyl AL, Lewis WM (2003) Open-channel estimation of denitrification. Limnology and Oceanography: Methods 1:74–81.

McDonnell JJ, Owens IF, Stewart MK (1991) A case study of shallow flow paths in a steep zero-order basin. Water Resources Bulletin 27:679–685.

Mcdowell RW, Biggs BJF, Sharpley AN, Nguyen L (2004) Connecting phosphorus loss from agricultural landscapes to water quality. Chemistry and Ecology 20:1–40.

McHale MR, Cirmo CP, Mitchell MJ, McDonnell JJ (2004) Wetland nitrogen dynamics in an Adirondack forested watershed. Hydrological Processes 18:1853–1870.

McHale MR, McDonnell JJ, Mitchell MJ, Cirmo CP (2002) A field-based study of soil water and groundwater nitrate release in an Adirondack forested watershed. Water Resources Research. 38:WR000102.

McMahon PB, Dennehy KF (1999) N₂O emissions from a nitrogen-enriched river. Environmental science & technology 33:21–25.

Mitchell MJ, Driscoll CT, Kahl JS, et al. (1996) Climatic control of nitrate loss from forested watersheds in the Northeast United States. Environmental science & technology 30:2609–2612.

Morgan RP, Kline KM (2011) Nutrient concentrations in Maryland non-tidal streams. Environmental monitoring and assessment 178:221–235.

Mosier A, Kroeze C, Nevison C, et al. (1998) Closing the global N₂O budget: nitrous oxide emissions through the agricultural nitrogen cycle inventory methodology. Nutrient Cycling in Agroecosystems 52:225–248.

Nixon SW (1995) Coastal marine eutrophication: A definition, social causes, and future concerns. Ophelia 41:199–219.

Nixon SW (1995) Coastal marine eutrophication: A definition, social causes, and future concerns. *Ophelia* 41:199–219.

Norton MM, Fisher TR (2000) The effects of forest on stream water quality in two coastal plain watersheds of the Chesapeake Bay. *Ecological Engineering* 14:337–362.

Novak JM, Stone KC, Watts DW, Johnson MH (2003) Dissolved phosphorus transport during storm and baseflow conditions from an agriculturally intensive southeastern coastal plain watershed. *American Society of Agricultural Engineers* 46:1355–1363.

Novotny V and Olem H (1994) Water Quality: Prevention, Identification, and Management of Diffuse Pollution. New York: Van Nostrand Reinhold.

O'Connor BL, Harvey JW, McPhillips LE (2012) Thresholds of flow-induced bed disturbances and their effects on stream metabolism in an agricultural river. *Water Resources Research* 48:W08504.

Ocampo CJ, Oldham CE, Sivapalan M (2006) Nitrate attenuation in agricultural catchments: Shifting balances between transport and reaction. *Water Resources Research* WR003773.

Ocampo CJ, Oldham CE, Sivapalan M, Turner J V (2006) Hydrological versus biogeochemical controls on catchment nitrate export: a test of the flushing mechanism. *Hydrological Processes* 20:4269–4286.

Owens LB, Edwards WM, Keuren RW (1991) Baseflow and stormflow transport of nutrients from mixed agricultural watersheds. *Journal of Environment Quality* 20:407–414.

Owens LB, Shipitalo MJ, Bonta JV (2008) Water quality response times to pasture management changes in small and large watersheds. *Journal of Soil and Water Conservation*. 63:292-299.

Paul EA and Clark FE (1989) Soil microbiology and biochemistry. Academic Press. New York.

Payn RA, Gooseff MN, McGlynn BL, et al. (2009) Channel water balance and exchange with subsurface flow along a mountain headwater stream in Montana, United States. *Water Resources Research* WR007644.

Peng TH, Broecker WS, Mathieu GG, et al. (1979) Radon evasion rates in the atlantic and pacific oceans as determined during the geosecs program. *Journal of Geophysical Research* 84:2471–2486.

- Peterjohn WT, Adams M, Gilliam F (1996) Symptoms of nitrogen saturation in two central Appalachian hardwood forest ecosystems. *Biogeochemistry* 35:507–522.
- Petry J, Soulsby C, Malcolm IA, Youngson AF (2002) Hydrological controls on nutrient concentrations and fluxes in agricultural catchments. *The Science of the Total Environment* 294:95–110.
- Pfenning KS, McMahon PB (1996) Effect of nitrate, organic carbon, and temperature on potential denitrification rates in nitrate-rich riverbed sediments. *Journal of Hydrology* 187:283–295.
- Piña-Ochoa E, Álvarez-Cobelas M (2006) Denitrification in aquatic environments: A Cross-system analysis. *Biogeochemistry* 81:111–130.
- Pionke HB, Gburek WJ, Sharpley AN, Zollweg JA (1998) Chapter 10: Hydrological and chemical controls on phosphorus loss from catchments. In *Phosphorus loss from soil to water*, pp 225–242. CAB International.
- Poor CJ, McDonnell JJ (2007) The effects of land use on stream nitrate dynamics. *Journal of Hydrology* 332:54–68.
- Pribyl AL, McCutchan JH, Lewis WM, Saunders JF (2005) Whole-system estimation of denitrification in a plains river: A comparison of two methods. *Biogeochemistry* 73:439–455.
- Puckett LJ, Zamora C, Essaid H, Wilson JT, Johnson HM, Brayton M, and Vogel JR (2008) Transport and Fate of Nitrate at the Ground-Water/Surface-Water Interface. USGS Staff Published Research Paper 4. <http://digitalcommons.unl.edu/usgsstaffpub/4>.
- Ravishankara AR, Daniel JS, Portmann RW (2009) Nitrous oxide (N_2O): the dominant ozone-depleting substance emitted in the 21st century. *Science* 326:123–125.
- Raymond PA, Zappa CJ, Butman D, et al. (2012) Scaling the gas transfer velocity and hydraulic geometry in streams and small rivers. *Limnology & Oceanography: Fluids & Environments* 2:41–53.
- Roley SS, Tank JL, Williams MA (2012) Hydrologic connectivity increases denitrification in the hyporheic zone and restored floodplains of an agricultural stream. *Journal of Geophysical Research* JG001950.
- Rusjan S, Brilly M, Mikoš M (2008) Flushing of nitrate from a forested watershed: An insight into hydrological nitrate mobilization mechanisms through seasonal high-frequency stream nitrate dynamics. *Journal of Hydrology* 354:187–202.

- Saleh-Lakha S, Shannon KE, Henderson SL, et al. (2009) Effect of pH and temperature on denitrification gene expression and activity in *Pseudomonas mandelii*. *Applied and environmental microbiology* 75:3903–3911.
- Savoy L, Surbeck H, Hunkeler D (2011) Radon and CO₂ as natural tracers to investigate the recharge dynamics of karst aquifers. *Journal of Hydrology* 406:148–157.
- Schaefer SC, Alber M (2007) Temperature controls a latitudinal gradient in the proportion of watershed nitrogen exported to coastal ecosystems. *Biogeochemistry* 85:333–346.
- Seitzinger S, Harrison JA, Böhlke JK, et al. (2006) Denitrification across landscapes and waterscapes: a synthesis. *Ecological Applications* 16:2064–2090.
- Seitzinger SP (1988) Denitrification in freshwater and coastal marine ecosystems: Ecological and geochemical significance. *Limnology* 33:702–724.
- Sharpley AN, Chapra SC, Wedepohl R, et al. (1994) Managing agricultural phosphorus for protection of surface waters: Issues and options. *Journal of Environmental Quality* 23:437–451.
- Sharpley AN, Gburek WJ, Folmar G, Pionke HB (1999) Sources of phosphorus exported from an agricultural watershed in Pennsylvania. *Agricultural Water Management* 41:77-89.
- Sharpley AN, Syers JK (1979) Phosphorus inputs into a stream draining an agricultural watershed II: Amounts contributed and relative significance of runoff types. *Water, Air, and Soil Pollution* 11:417–428.
- Sharpley, Andrew N Kleinman PJA, Heathwaite LA, Gburek WJ, et al. (2008) Phosphorus Loss from an Agricultural Watershed as a Function of Storm Size. *Journal of Environmental Quality* 37:362–368.
- Shine KP, Fuglestvedt JS, Hailemariam K, Stuber N (2005) Alternatives to the global warming potential for comparing climate impacts of emissions of greenhouse gases. *Climate Change* 68:281–302.
- Sims JT, Simard RR, Joern BC (1998) Phosphorus loss in agricultural drainage: Historical perspective and current research. *Journal of Environment Quality* 27:277–293.
- Sjodin AL, Lewis WM, Saunders JF (1997) Denitrification as a component of the nitrogen budget for a large plains river. *Biogeochemistry* 39:327–342.

Smethie WMJ, Takahashi T, Chipman DW, Ledwell JR (1985) Gas exchange and CO₂ flux in the tropical Atlantic ocean determined from ²²²Rn and pCO₂ measurements. *Journal of Geophysical Research* 90:7005–7022.

Smith TE, Laursen AE, Deacon JR (2008) Nitrogen attenuation in the Connecticut River, northeastern USA; a comparison of mass balance and N₂ production modeling approaches. *Biogeochemistry* 87:311–323.

Sobota DJ, Harrison JA, Dahlgren RA (2009) Influences of climate, hydrology, and land use on input and export of nitrogen in California watersheds. *Biogeochemistry* 94:43–62.

Soulsby C, Malcolm IA, Tetzlaff D, Youngson AF (2009) Seasonal and inter-annual variability in the hyporheic water quality revealed by continuous monitoring in a salmon spawning stream. *River Research and Applications*.

Stanford G, Dzienia S, and Vander Pol RA (1975) Effect of temperature on denitrification rate in soils. *Soil Science Society of America Journal*. 39:867-870.

Steinberg PD, Brett MT, Bechtold JS, et al. (2010) The influence of watershed characteristics on nitrogen export to and marine fate in Hood Canal, Washington, USA. *Biogeochemistry*.

Stenstrom MK, Poduska RA (1980) The effect of dissolved oxygen concentration on nitrification. *Water Research* 14:643–649.

Stoddard JL (1994) Long-term changes in watershed retention of nitrogen. In Environmental Chemistry of Lakes and Reservoirs; Baker, L. A., Ed.; Advances in Chemistry Series 237; American Chemical Society: Washington, DC, pp 223–284.

Stow CA, Walker JT, Cardoch L, et al. (2005) N₂O Emissions from streams in the Neuse River watershed, North Carolina. *Environmental Science & Technology* 39:6999–7004.

Strauss EA, Mitchell NL, Lamberti GA (2002) Factors regulating nitrification in aquatic sediments: effects of organic carbon, nitrogen availability, and pH. *Canadian Journal of Fisheries and Aquatic Sciences* 59:554–563.

Thomann RV and Mueller JA (1987) Principles of surface water quality modeling and control: quality modeling and control. Harper & Row. New York.

Triksa FJ, Duff JH, and Avazino RJ (1990) Influence of exchange flow between the channel and hyporheic zone on nitrate production in a small mountain stream. *Canadian Journal of Fisheries and Aquatic Science* 47: 2099–2111.

Valderrama (1981) The simultaneous analysis of total nitrogen and total phosphorus on natural waters. *Marine Chemistry*. 10:109–122.

Van Breemen N, Boyer EW, Goodale CL, et al. (2002) Where did all the nitrogen go? Fate of nitrogen inputs to large watersheds in the northeastern U.S.A. *Biogeochemistry* 57/58:267–293.

Vanni MJ, Renwick WH, Jenifer L, et al. (2001) Dissolved and particulate nutrient flux from three adjacent agricultural watersheds: A five-year study. *Biogeochemistry* 54:85–114.

Vidon P, Allan C, Burns D, et al. (2010) Hot spots and hot moments in riparian zones: Potential for improved water quality management. *Journal of the American Water Resources Association* 46:278–298.

Vilain G, Garnier J, Tallec G, Tournebize J (2012) Indirect N_2O emissions from shallow groundwater in an agricultural catchment (Seine Basin, France). *Biogeochemistry* 111:253–271.

Vitousek PM, Aber JD, Howarth RW, et al. (2012) Human Alteration of the Global Nitrogen Cycle: Sources and Consequences. *Ecological Applications* 7:737–750.

Wanninkhof R (1992) Relationship between wind speed and gas exchange. *Journal of Geophysical Research* 97:7373–7382.

Wanninkhof R, Mulholland PJ, Elwood JW (1990) Gas exchange rates for a first-order stream determined with deliberate and natural tracers. *Water Resources Research* 26:1621–1630.

Weiler M, McDonnell JJ (2006) Testing nutrient flushing hypotheses at the hillslope scale: A virtual experiment approach. *Journal of Hydrology* 319:339–356. d

Weiss RF, Price BA (1980) Nitrous oxide solubility in water and seawater. *Marine Chemistry* 8:347–359.

Well R, Augustin J, Meyer K, and Myrold DD (2003) Comparison of field and laboratory measurement of denitrification and N_2O production in the saturated zone of hydromorphic soils. *Soil Biology and Biochemistry*. 35:783–799.

Well R, Weymann D, and Flessa H (2005) Recent research progress on the significance of aquatic systems for indirect agricultural N_2O emissions. *Environmental Science*. 2:143–151.

Werner SF, Browne BA, Driscoll CT (2010) Three-dimensional spatial patterns of trace gas concentrations in baseflow-dominated agricultural streams: implications for surface–ground water interactions and biogeochemistry. *Biogeochemistry* 107:319–338.

Weymann D, Well R, von der Heide C, et al. (2009) Recovery of groundwater N₂O at the soil surface and its contribution to total N₂O emissions. *Nutrient Cycling in Agroecosystems* 85:299–312.

Wilcock RJ, Sorrell BK (2008) Emissions of greenhouse gases CH₄ and N₂O from low-gradient streams in agriculturally developed catchments. *Water, Air, and Soil Pollution* 188:155–170.

Wilson GB, Andrews JN, Bath AH (1990) Dissolved gas evidence for denitrification in the Lincolnshire limestone groundwaters, eastern England. *Journal of Hydrology* 113:51–60.

Yan W, Laursen AE, Wang F, et al. (2004) Measurement of denitrification in the Changjiang River. *Environmental Chemistry* 1:95–98.

Yarbro LA, Kuenzler EJ, Mulholland PJ, Sniffen RP (1984) Effects of stream channelization on exports of nitrogen and phosphorus from North Carolina coastal plain watersheds. *Environmental Management* 8:151–160.

Zhu Q, Schmidt JP, Bryant RB (2012) Hot moments and hot spots of nutrient losses from a mixed land use watershed. *Journal of Hydrology* 414-415:393–404.

Zhu Q, Schmidt JP, Buda AR, et al. (2011) Nitrogen loss from a mixed land use watershed as influenced by hydrology and seasons. *Journal of Hydrology* 405:307–315.